

# **Drugs that thwart antibiotic resistance**

A dissertation presented

by

Laura Kathryn Stone

to

The Committee on Higher Degrees in Chemical Biology

in partial fulfillment of the requirements

for the degree of

Doctor of Philosophy

in the subject of

Chemical Biology

Harvard University Cambridge, Massachusetts

April 2015

© 2015 Laura Kathryn Stone

All rights reserved.

## **Drugs that thwart antibiotic resistance**

### **Abstract**

Antibiotics are often credited with being one of the major forces behind the expansion of human life expectancy in the past 60 years. Yet at the root of this advancement lies its potential undoing: using antibiotics promotes the emergence and spread of resistant strains, reducing the efficacy of the drugs. Now, rising antibiotic resistance threatens to undo much of the progress of modern medicine. To halt the rise of resistance and preserve the activity of antibiotics, we must find ways to neutralize, modulate, or even invert the evolutionary advantage of resistant strains. Chapter 1 reviews three strategies to overcome antibiotic resistance through the sequential or concurrent use of multiple drugs: resistance mechanism inhibitors, synergistic, antagonistic, and suppressive drug interactions, and collateral sensitivity.

Collateral sensitivity occurs when a bacterium acquires a mutation or gene that provides resistance to one drug, but makes them more susceptible to others. This new vulnerability can therefore be exploited to select against resistance mechanisms. Chapter 2 describes a screening strategy, based on direct competition between antibiotic resistant and susceptible strains, for identifying compounds that select against antibiotic resistance genes and cassettes. Using this approach we identified two compounds— $\beta$ -thujaplicin and disulfiram—that select against the TetA tetracycline resistance pump in *E. coli*. Furthermore, we demonstrate a two-phase treatment

paradigm in which  $\beta$ -thujaplicin drives a tetracycline resistant population back to susceptibility, allowing successful second-phase treatment with tetracycline.

Chapter 3 examines the consequences of linking two antibiotics—ciprofloxacin and neomycin—into one hybrid compound. We compared the cross-resistance and genotypic profiles of strains evolved in the hybrid to those evolved in mixtures of its two components. We find that the hybrid inhibits bacterial growth through its ciprofloxacin moiety, but prevents resistance through its neomycin moiety by avoiding a common multiple antibiotic resistance pathway. As a result, strains evolved in the hybrid gain less resistance than those evolved in an unlinked mixture. This indicates that linking two drugs can surpass traditional unlinked combination therapy in its ability to prevent resistance.

Finally, Chapter 4 discusses the implications of this work and possible directions for future research in treating antibiotic resistance.

# Table of Contents

Abstract.....	<i>iii</i>
Table of Contents.....	<i>v</i>
Acknowledgements.....	<i>viii</i>

## **Chapter 1: Chemical strategies to overcome antibiotic resistance**

Abstract.....	1
Introduction.....	2
Resistance mechanism inhibitors.....	3
Synergistic, antagonistic, and suppressive drug interactions.....	5
Collateral sensitivity.....	12
Future Directions.....	15
References.....	16

## **Chapter 2: New compounds that select against the tetracycline resistance efflux pump**

Abstract.....	23
Introduction.....	24
Results.....	24
Discussion.....	34
Methods.....	36
Contributions.....	44
Acknowledgements.....	45
References.....	45

**Chapter 3: A hybrid antibiotic restricts evolutionary paths to resistance by evading activation of the multiple antibiotic resistance operon**

Abstract.....	49
Introduction.....	50
Results.....	51
Discussion.....	62
Methods.....	64
Contributions.....	67
Acknowledgements.....	67
References.....	68
<b>Chapter 4: Concluding Remarks.....</b>	<b>72</b>
<b>Appendix 1: Supplementary Materials for Chapter 2: New compounds that select against the tetracycline resistance efflux pump (S1) .....</b>	<b>75</b>
Supplementary Figures.....	76
Supplementary Tables.....	92
<b>Appendix 2: Supplementary Materials for Chapter 3: A hybrid antibiotic restricts evolutionary paths to resistance by evading activation of the multiple antibiotic resistance operon (S2) .....</b>	<b>95</b>
Supplementary Figures.....	96

Supplementary Table.....100

## Acknowledgements

I would not have made it to or through graduate school without the help and support of my friends, family, and colleagues. In particular, I would like to thank:

My thesis advisor, Roy Kishony, for taking on an inexperienced chemist and teaching me to program, to do biology, and to view antibiotic resistance in unorthodox ways;

Past and present members of the Kishony lab: Tami Lieberman for inspiring me to join the lab; Remy Chait for inspiring me to take up this project; Michael Baym for always encouraging me to take the first step whether in learning to code, repairing electronics, or writing my thesis; Ylaine Gerardin for being my comrade in arms in the war of attrition that is the PhD; and Daniel Schultz, Justin Meyer, Joy Jiao, Hattie Chung, Eric Kelsic, Adrián Grenada, Joel Yao, Erdal Toprak, Ilan Wapinski, Seungsoo Kim, Kalin Vetsigian, Nick Moore, Adrian Veres, Tobias Bollenbach, Morten Ernebjerg, Jean-Baptiste Michel, and Vadim Baidin for their help, their humor, and their camaraderie;

Jon Clardy for his guidance and the Clardy lab for welcoming me into their midst and meetings and teaching me natural product isolation, especially Alexandra Cantley, Clarissa Sit, Thomas Böttcher, Elissa Hobert, Mohammad Seyedsayamdost, and Ethan Van Arnam;

My co-author and mentee, Kathy Wang, who has been the ideal collaborator: smart, organized, responsive, and super fun to work with;

The members of my dissertation advisory committee: Ralph Mazitscheck and David Rudner for their great advice, and the late Robert Moellering for his unfailing enthusiasm and support; Suzanne Walker for her suggestions on this thesis;

Sam Reed, Jason Millberg, and KeyAnna Schmiedl for administering the Chemical Biology Program, expertly cutting through red tape, navigating Harvard bureaucracy, and making



the entire program possible; Barb Grant, Tenzin Pulchung, Sam Keough, and the rest of the Systems Biology support staff for making the department such an efficient and friendly place to work;

Eric Rubin and Suzanne Walker who hosted me as a rotation student when I was still getting my feet wet in microbiology; and Kathrin Schirner who mentored me in the Walker lab and taught me *Bacillus* genetics;

My mentors at the University of Chicago: Sergey Kozmin, Steve Kron, and the late Greg Hillhouse for guiding me through undergrad and onto my PhD;

My friends from Dearborn and Chicago: Katie Okonowski, Lori Bologna Bloom, Catherine Stolar, Katie Bologna, Kawanjit Sekhon, Lauren Mickiewicz Maynard, and Christine Krizmanich, for keeping in touch over the years and across the miles. My fellow Chemical Biology classmates: Laura Strittmatter, Katharin Shaw, Michael McKeown, Ilana Goldowitz, and Justin Tan who have made graduate school fun. And the friends who make Boston home: Anna Turetsky, Tami Lieberman, Geoff Fudenberg, Winston Anthony, Nick Stroustrup, Evi Van Italie, Nour Kteilly, and especially the brave souls who roomed with me and endured many houseplants and the resultant flies: Laura Strittmatter, Ylaine Gerardin, and Tarek Anous;

Finally I would like to thank my family: the extended Stone and Huetteman families for always being full of love and fun and my brother, Peter, for keeping me grounded. Most of all, I would like to thank my parents, Mary and Chad Stone, for continuing to expose me to science and medicine even after that disastrous Body Wars ride in 1991, for enduring a basement full of Wisconsin Fast Plants® in the summer of 2002, for supporting me at the University of Chicago from 2005 to 2009, and for always encouraging me to learn for the love of it, tough it out when necessary, and get enough sleep from 1987 and beyond.

# Chapter 1: Chemical strategies to overcome antibiotic resistance<sup>1</sup>

Antibiotic treatment has two tightly linked effects: the desired, immediate effect of inhibiting bacterial growth and the undesired, long-term effect of promoting the evolution of resistance. These two effects seem inextricably linked, and indeed they cannot be decoupled with any single drug treatment. However, recent work suggests three strategies in which drugs can be combined to inhibit bacteria without selecting for long-term resistance. Resistance mechanism inhibitors can be used to bypass common resistance genes. Synergistic, antagonistic, and suppressive drug interactions can be used to modulate and even invert the selection for resistance. Finally, collateral sensitivity can be used to restrict the spontaneous evolution of resistance and exploited to cure a population of its resistance gene or cassette, allowing successful follow-up treatment with antibiotics.

---

<sup>1</sup> Parts of this work will lead to a review article in collaboration with Michael Baym and Roy Kishony.

## Introduction

Antibiotics have been one of the most important advances in modern medicine, both for curing infectious disease and allowing advances in surgery and immunotherapy. However, since the advent of antibiotic therapies, resistance has threatened this progress<sup>1</sup>. In the intervening decades resistance has become widespread and today many first-generation antibiotics are all but ineffective<sup>2,3</sup>. We have thus far avoided a crisis through the continued discovery of new antibiotic compounds and the improvement of existing scaffolds. However, resistance rates continue to grow even as the rate of antibiotic discovery drops substantially<sup>4</sup>. In order to prevent or delay the loss of all antibiotics, new treatment strategies are urgently needed. Specifically, we need treatment strategies that limit or redirect the course of resistance evolution.

Resistance evolves as a direct consequence of the defining feature of antibiotics: the inhibition of bacterial growth. By using antibiotics, we not only treat the infection, but also select for resistant strains. These mutants are less affected by the drug and thus rapidly spread throughout a population, eventually rendering the drug ineffective. These two effects—the short-term inhibition of growth and the long-term evolution of resistance—are inherently linked and cannot be decoupled by any single drug treatment. However, there is evidence that with particular combinations of compounds the conflicting effects of antibiotic therapy can be decoupled. Recent work suggests ways in which bacteria can be inhibited without selecting for resistance.

The enabling observation is that drug target inhibition and drug resistance can have pleiotropic effects. A bacterium's response to a drug can therefore have secondary consequences that change its response to other compounds. The ability to evolve resistance seems vast, but recent evidence suggests that the space of possible spontaneous resistance mutations is limited.

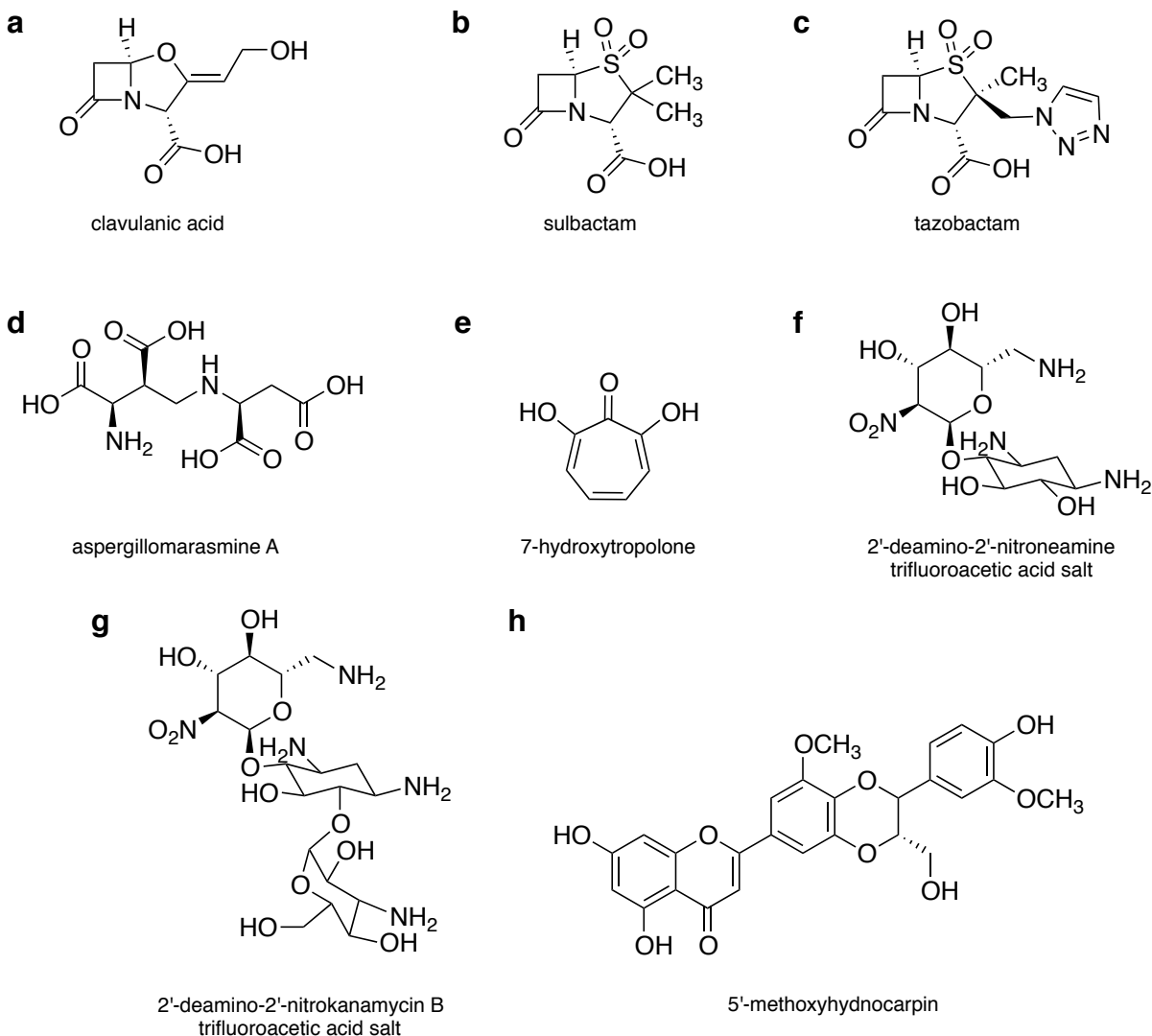
This, in turn, would suggest that evolutionary channels may exist through which resistance can be suppressed or even reversed.

Three primary mechanisms have been studied as possible ways of decoupling the evolutionary chain that leads to resistance. First, specific adjunct compounds have been used to directly inhibit resistance mechanisms. Second, combinations of drugs that interact to have different effects in combination than alone can be used to alter the evolution of resistance. Third, much recent work has focused on the evolutionary interactions between compounds, where a specific treatment may force the evolution of higher sensitivity to subsequent therapies.

## **Resistance mechanism inhibitors**

One obvious way to bypass resistance is to inhibit the resistance mechanism, thus neutralizing the advantage of resistant strains. In this strategy, an antibiotic is delivered concurrently with a resistance mechanism inhibitor. This allows the antibiotic to kill both resistant and susceptible strains and can even extend the antibiotic's spectrum to include species considered intrinsically resistant<sup>5</sup>.

Many compounds have been discovered that inhibit horizontally transferred and intrinsic resistance mechanisms<sup>6</sup>. This strategy has been deployed most successfully against serine  $\beta$ -lactamases with the combination of a  $\beta$ -lactam and a  $\beta$ -lactamase inhibitor, such as amoxicillin and clavulanic acid, ampicillin and sulbactam, and piperacillin and tazobactam, all of which are used clinically<sup>5,7</sup> (**Fig. 1.1a-c**). Recently, this work has been expanded to metallo- $\beta$ -lactamases with the discovery of aspergillomarasmine A, which inhibits NDM-1 and VIM-2<sup>8</sup> (**Fig. 1.1d**). Similarly, inhibitors of aminoglycoside-modifying enzymes have been synthesized to restore aminoglycoside activity to resistant strains<sup>9,10</sup> (**Fig. 1.1e-g**). High throughput screening<sup>11</sup> and



**Figure 1.1. Resistance mechanism inhibitors.** (a-c) Clavulanic acid, sulbactam, and tazobactam inhibit serine  $\beta$ -lactamases. (d) Aspergillomarasmine A inhibits metallo- $\beta$ -lactamases, NDM-1 and VIM-2. (e-g) Inhibitors for aminoglycoside-modifying resistance enzymes: 7-hydroxytropolone inhibits aminoglycoside-2''-O-adenylyltransferase, while 2'-deamino-2'-nitroeamine trifluoroacetic acid salt and 2'-deamino-2'-nitrokanamycin B trifluoroacetic acid salt inhibit aminoglycoside 3'-phosphotransferases. (h) The natural product 5' methoxyhydnocarpin inhibits the NorA efflux pump in *Staphylococcus aureus*.

SAR by NMR<sup>12</sup> have yielded leads for inhibitors of ErmC methyltransferase, which confers macrolide resistance. Lastly, several groups have identified inhibitors of efflux pumps, a major mode of resistance across antibiotic classes<sup>13-18</sup>.

Notably, two of these resistance mechanism inhibitor and antibiotic pairs are naturally occurring drug combinations. Clavulanic acid is produced by *Streptomyces clavuligerus*, which also produces several  $\beta$ -lactam antibiotics<sup>19</sup>. Similarly, *Berberis fremontii* makes both berberine and the efflux pump inhibitor, 5'-methoxyhydrnocarpin, that blocks berberine export and that has been repurposed to block quinolone export from *Staphylococcus aureus*<sup>17</sup> (**Fig. 1.1h**). These discoveries suggest that known antibiotic producers may be fruitful sources of resistance mechanism inhibitors.

Unfortunately, the clinical success of resistance mechanism inhibitors has so far been limited to the  $\beta$ -lactams<sup>5,7</sup>. Moreover, resistance mechanism inhibitors are themselves subject to resistance. For example, the  $\beta$ -lactamase inhibitors clavulanic acid, sulbactam, and tazobactam are ineffective against AmpC  $\beta$ -lactamases, metallo- $\beta$ -lactamases, and inhibitor resistant variants of TEM  $\beta$ -lactamases<sup>5,20</sup>. Most importantly, resistance mechanism inhibitors do not reduce resistance rates. A resistance inhibitor merely neutralizes the selective advantage of resistance; it does not inflict a cost. Without a substantial cost to resistance, the resistant strain will remain in the population, even if the patient stops taking the antibiotic for years<sup>21-24</sup>.

## **Synergistic, antagonistic, and suppressive drug interactions**

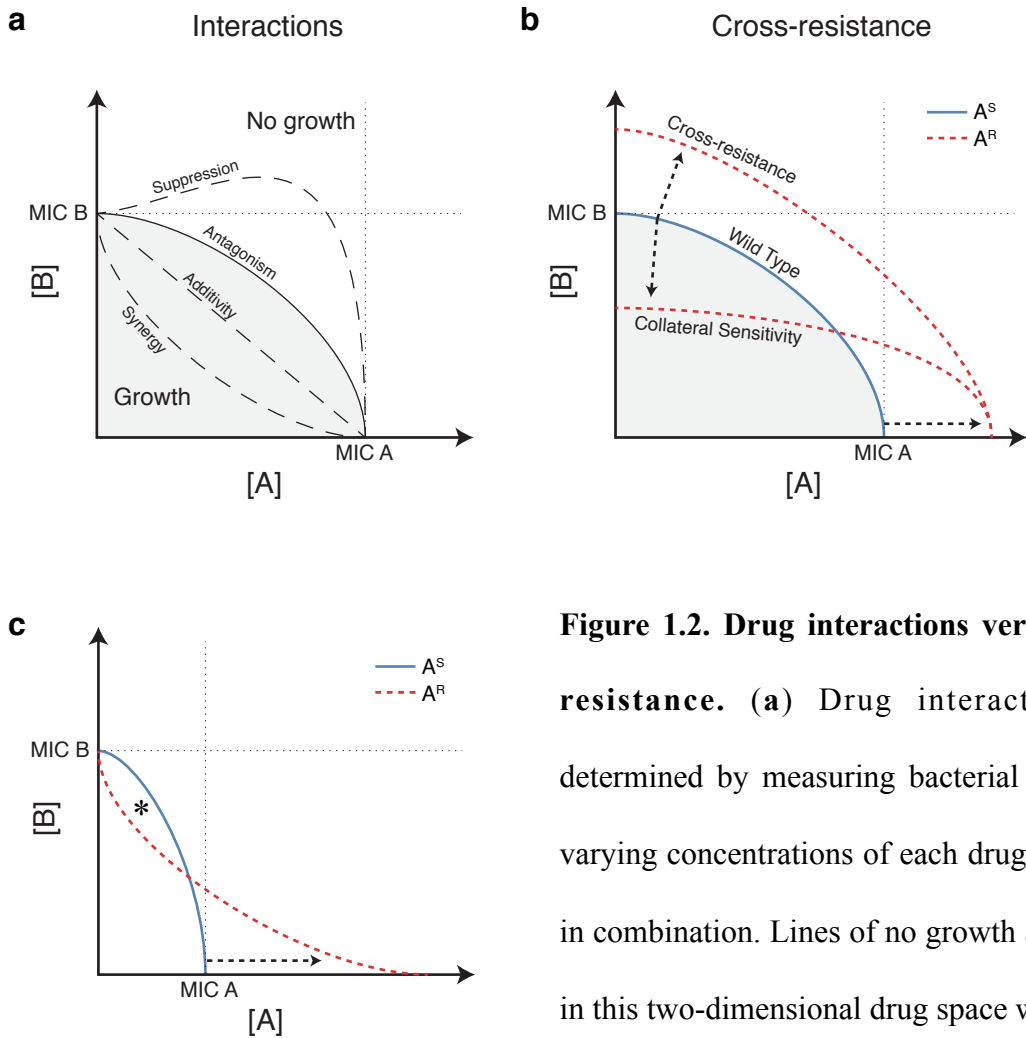
An alternative strategy that can be used to alter resistance evolution and in some cases impose a cost to resistance is using two or more antibiotics concurrently. Antibiotics are often used in combination in the clinic to hasten clearance of the infection or prevent the emergence of

resistance. However, antibiotics used in combination can interact to increase or decrease their mutual effect and can even change the rate at which resistance arises<sup>25-28</sup>. Drug interactions are defined as antagonistic, additive, or synergistic when their effect in combination is less than, equal to, or more than expected from the effect of each drug alone<sup>29,30</sup> (**Fig. 1.2a**). Drug interactions are defined as suppressive when their effect in combination is less than one or either of the drugs alone<sup>28</sup> (**Fig. 1.2a**).

Recent technical developments have enabled broad, systematic identification of such drug interactions and have revealed that they are relatively common<sup>28,31,32</sup>. Furthermore, these pairwise interaction networks reveal that drugs that have the same mode of action have the same interaction profile<sup>28</sup>, suggesting these interactions operate through the core physiology of the cell. The principles underlying these interactions, however, remain largely unknown. Two recent studies detail the mechanisms behind a synergistic interaction between two drugs hitting the same pathway<sup>33</sup> and an antagonistic interaction between two drugs that compensate for each other's effect on the cell<sup>34</sup>. These findings provide new insights into how antibiotics affect the bacterial cell and expose new principles of bacterial physiology.

In addition to interactions between antibiotics, recent work has illuminated synergistic and antagonistic interactions between antibiotics and compounds possessing little or no antibiotic activity. Simple metabolites have been found that potentiate or antagonize killing by antibiotics<sup>35-37</sup>. Screens for antibiotic adjuvants have identified compounds that act synergistically with known antibiotics against susceptible<sup>38,39</sup> and resistant strains<sup>8,40</sup>.

***Synergy and antagonism can speed up or slow down the evolution of resistance.***



**Figure 1.2. Drug interactions versus cross-resistance.**

(a) Drug interactions are determined by measuring bacterial growth in varying concentrations of each drug alone and in combination. Lines of no growth are plotted in this two-dimensional drug space with

concentrations below the line allowing growth and concentrations above the line fully inhibiting growth. The lines intersect the axes at the minimum inhibitory concentration (MIC) for each drug. (b) Resistance to drug A can increase (cross-resistance) or decrease (collateral sensitivity) resistance to drug B. (c) Drug interactions can change with the acquisition of resistance. A drug pair that interacts antagonistically in susceptible bacteria and synergistically in resistant bacteria may have a concentration regime (\*) where the susceptible strain can grow and the resistant one cannot and can therefore be used to select against resistance.



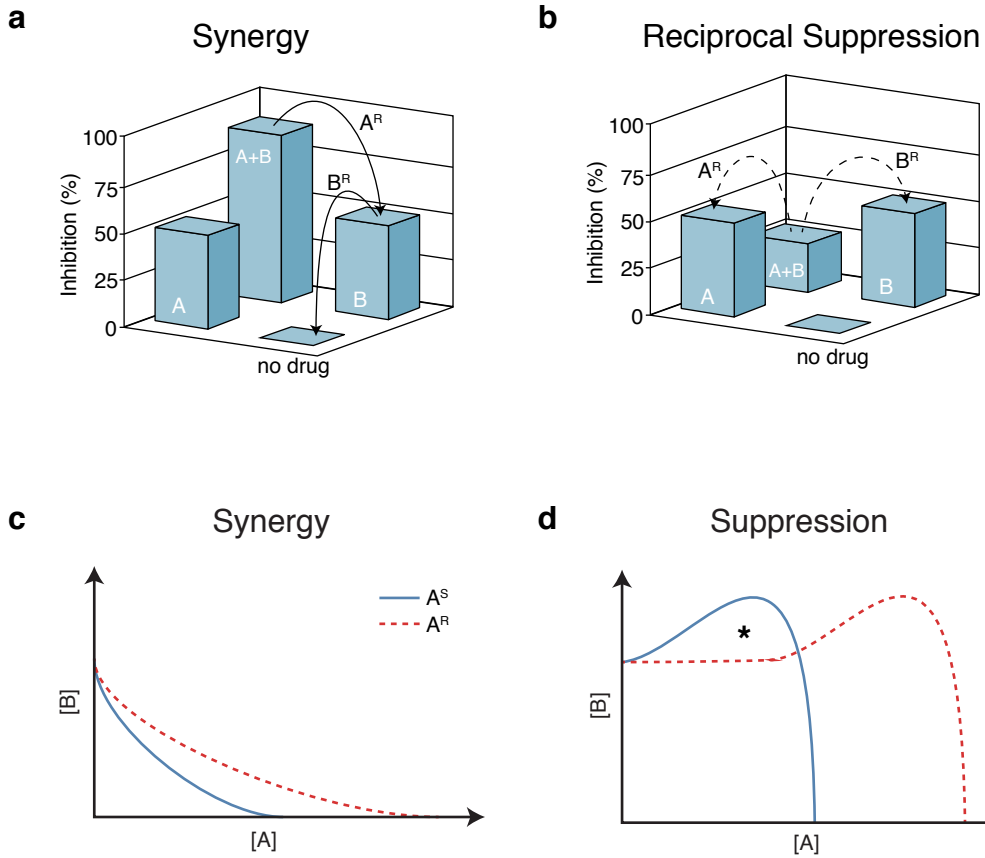
With synergistic combinations, each single drug resistance mutation is a pronounced step up in fitness (**Fig. 1.3a,c**). Perhaps as a result, synergistic combinations have been shown to speed up the evolution of resistance<sup>25,26,41</sup>. However, synergistic combinations can also clear infections faster, reducing the time in which resistance can arise<sup>42</sup>. Thus, there is an optimal level of drug synergy, depending on the context of the infection, that balances these two outcomes<sup>42</sup>.

In comparison, antagonistic interactions can shrink the mutant selection window and slow down the evolution of resistance<sup>26</sup>. Similarly, a single drug resistance mutation in a suppressive combination removes the effect of one drug, but also removes the suppression masking the effect of the other drug (**Fig. 1.3b**). The bacteria now face the full effect of the other drug and are actually *less* fit than when they were fully susceptible (**Fig. 1.3b**). Therefore, suppressive combinations can actually select *against* drug resistance within certain concentration regimes<sup>43</sup> (**Fig. 1.3d**). However, both antagonistic and suppressive combinations require larger amounts of each antibiotic to achieve the same killing effect as an additive or synergistic combination, potentially posing toxicity issues<sup>44-46</sup>, and require longer treatment times with a higher bacterial load, allowing the bacteria to undergo more generations during which they can develop resistance<sup>41,42</sup>. The need to cure the patient as quickly as possible and the difficulty of precisely controlling drug concentrations within the human body are important difficulties in the possible clinical application of antagonistic and suppressive interactions.

***The nature of drug interactions can change with the acquisition of resistance.***

In some cases, the nature of the drug interaction is preserved when the organism acquires resistance to one of the drugs<sup>43</sup> (**Fig. 1.3c-d**). In other cases, the interaction changes as resistance arises<sup>47,48</sup> (**Fig. 1.2c**). For example, Wood *et al.* studied multiple drug combinations in *E. coli*, *S.*

**Figure 1.3. Synergistic and suppressive interactions can increase or decrease the selection for resistance, respectively.** (a) In synergistic drug combinations, two antibiotics inhibit more effectively together than alone. Therefore, single-drug resistance is favorable, allowing step-wise acquisition of multi-drug resistance. (b) In suppressive drug combinations, two antibiotics cancel out each other's effect so that they are more effective alone than together. When the suppressive interaction is reciprocal between two drugs (as shown), single-drug resistance is unfavorable and multi-drug resistance requires simultaneous acquisition of resistance to both drugs, making it much less likely to occur. When the suppressive interaction is directional (one drug suppresses the other's effect, but not vice versa) then one single-drug resistance pathway is still possible (not shown). (c) If a drug pair interacts synergistically in both the susceptible and resistant strain, then the resistant strain can grow at all concentration regimes that the susceptible strain can grow. (d) If one drug suppresses the activity of another drug (directional suppression) in both susceptible and resistant strains, then there is a concentration regime (\*) where the susceptible strain can grow and the resistant one cannot. This concentration regime can therefore be used to select against the resistant strain.



**Figure 1.3 (Continued). Synergistic and suppressive interactions can increase or decrease the selection for resistance, respectively.**

*aureus*, *E. faecalis*, and a non-small-cell lung cancer line and found that many drug interactions became closer to additive when the bacteria gained single drug resistance<sup>47</sup>. In contrast, the weak synergistic interaction between doxycycline and erythromycin became more synergistic in some mutants resistant to both drugs<sup>47</sup>. Most surprisingly, gefitinib and 17-AAG interact antagonistically in EGFR mutant non-small-cell lung cancer lines, but interact synergistically when the cells gain gefitinib resistance, suggesting that this combination could reduce the emergence of gefitinib resistance<sup>47</sup>.

### ***Inverting selection for resistance with drug interactions.***

These results highlight ways in which we might use drug interactions in the fight against antibiotic resistance. Compounds that interact synergistically with antibiotics in resistant strains can restore those antibiotics' activity<sup>8,49</sup>. As the gefitinib and 17-AAG example illustrates, drug interactions that become more synergistic with resistance can lessen the selection for drug resistance<sup>47</sup>. Finally, suppressive interactions, such as that between ciprofloxacin and doxycycline, can even invert selection for resistance<sup>43</sup>.

Looking forward, we must evaluate if combination therapies are effective in clearing the infection and preventing resistance or if they only further the march towards multi-drug resistance. While we are aided in that evaluation by our increased understanding of the mechanisms behind these interactions, many interactions remain unexplained. Elucidating the physiology behind antibiotic interactions will increase our understanding of the connections between the essential pathways targeted by antibiotics and help predict the emergence of resistance. In addition, a systematic documentation of how drug interactions change upon the

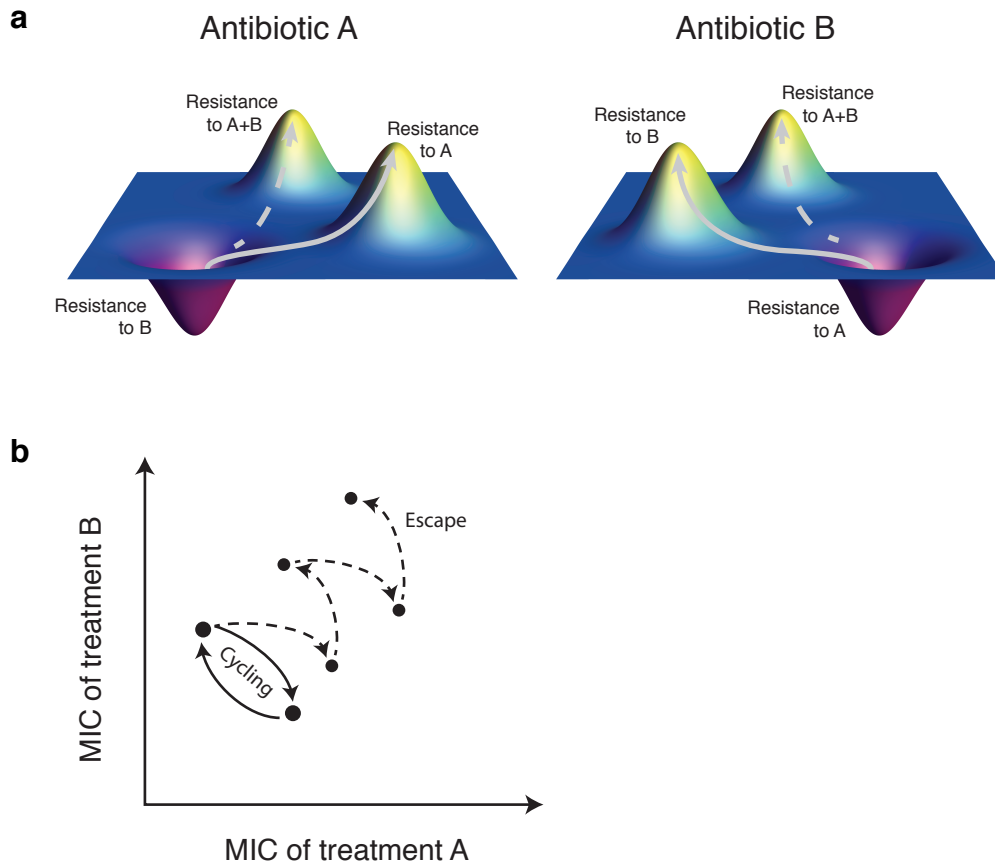
acquisition of resistance mutations would establish how combination treatment alters, and possibly restricts, the paths to resistance.

## Collateral sensitivity

Resistance can have pleiotropic effects including greater susceptibility to other drugs (Fig. 1.2b, 1.4a). This has been termed collateral sensitivity<sup>50</sup> and drugs that the resistant strain has become more susceptible to are called selection-inverting compounds<sup>51</sup>. Collateral sensitivity imposes a cost on resistant strains and a resistant strain can grow orders of magnitude slower than the susceptible strain in the presence of selection-inverting compounds<sup>50</sup>.

Most of the collateral sensitivity work to date has focused on finding selection inverters for spontaneous resistant mutants<sup>50,52-58</sup>. In fact, many well-known antibiotics work as selection inverting compounds for SNP or indel based resistance<sup>50,52-58</sup>. For example, several recent studies have highlighted the prevalent collateral sensitivity between aminoglycosides and other antibiotic classes<sup>54,55,59,60</sup>. Both the import of aminoglycosides and the export of multiple antibiotics through intrinsic efflux pumps, such as the AcrAB-TolC pump in *E. coli*, require the proton motive force<sup>61,62</sup>. Therefore, when a strain evolves resistance to aminoglycosides by diminishing the proton motive force, it becomes more susceptible to antibiotics that are normally exported through the AcrAB-TolC pump, such as  $\beta$ -lactams, quinolones, and tetracyclines<sup>54,60,63</sup>. This well-studied example illustrates the evolutionary trade-offs behind collateral sensitivity.

Using collateral sensitivity networks, we can exploit these trade-offs to suppress the evolution of resistance. A long-term evolution experiment showed that alternating daily between two drugs displaying unidirectional collateral sensitivity slowed the rate of spontaneous resistance evolution and reduced final resistance levels compared to single drug treatment<sup>64</sup>.



**Figure 1.4. Collateral sensitivity can be used to select against antibiotic resistance. (a)** Fitness landscapes of bacteria in two drugs displaying reciprocal collateral sensitivity. When bacteria are switched between the two environments, strains that had gained single-drug resistance and acquired a fitness peak are now in a fitness valley. Multi-drug resistance is a fitness peak in both drug environments. The success of using collateral sensitivity to limit resistance requires that the path to single-drug resistance (solid line) be much more probable than the path to multi-drug resistance (dashed line). **(b)** Cycling between two drugs displaying reciprocal collateral sensitivity may be used to keep resistance in check and maintain the efficacy of both drugs. However, it may be possible for bacteria to escape cycling through rare mutations or horizontally transferred genes that do not confer collateral sensitivity (dashed line).

Moreover, cycling between two drugs that show reciprocal collateral sensitivity may be used to keep resistance entirely in check<sup>55</sup> (**Fig. 1.4b**), though has not yet been demonstrated. Lastly, the evolution of spontaneous resistance can be reduced by concurrent application of drugs that display collateral sensitivity, compared to either of the drugs alone<sup>48</sup>.

There are fewer examples of collateral sensitivity caused by resistance genes and cassettes spread by horizontal gene transfer<sup>51,65-70</sup>. These examples all center on the *tet* efflux pumps, which confer tetracycline resistance, but also make bacteria more susceptible to aminoglycosides, fusaric acid, and salt stress<sup>65-69</sup>. In addition, soil bacteria produce natural products that select against the *tetA* pump<sup>51</sup>. Using fusaric acid as a positive control, we were able to develop a high-throughput competition-based screen for compounds that select against the *tetA* efflux pump, identifying two new selection-inverters (**Chapter 2**). This screen could be adapted to other resistance genes to discover novel selection-inverting compounds. However, the relatively low incidence (2 in 20,529 compounds screened) of collateral sensitivity in this screen compared to spontaneous mutation studies (35%<sup>54</sup> or 74%<sup>55</sup> of antibiotic pairs) suggests that collateral sensitivity may be less common for these specialized resistance genes and cassettes, possibly because they have been improved over many generations to reduce vulnerabilities.

Novel selection-inverting compounds could be used in a two-phase treatment strategy to first cure the strain of resistance, allowing successful treatment with a traditional antibiotic. Many resistance genes and cassettes are on mobile elements, which allow them to spread quickly to new strains and species<sup>62,71,72</sup>. However, because of the genetic instability that allows them to move around, the spontaneous loss of a mobile element occurs much more frequently than a SNP resistance mutation (**Chapter 2**)<sup>71,73</sup>. Therefore, selection-inverting compounds not only favor

susceptibility in a mixed population of resistant and susceptible bacteria, these compounds can actually convert a resistant population to antibiotic susceptibility, enabling successful follow-up treatment (**Chapter 2**). To demonstrate this, we evolved a tetracycline resistant population in  $\beta$ -thujaplicin, a selection-inverter, for seven days, and then transferred the populations to doxycycline. Seven of eight replicates had irreversibly lost their tetracycline resistance and were successfully treated with doxycycline (**Chapter 2**). A two-phase treatment strategy beginning with selection-inverting compounds followed by the corresponding traditional antibiotics may offer new non-traditional therapies for resistant infections.

## Future Directions

These strategies—resistance mechanism inhibitors, drug interactions, and collateral sensitivity—provide opportunities to decouple growth inhibition and the selection for resistance. Furthermore, these strategies can be combined to restrict the evolution of resistance while speeding infection clearance. For example, a drug pair that interacts synergistically and also displays reciprocal collateral sensitivity should provide fast clearance, while also preventing the accelerated emergence of resistance that comes with synergistic pairings. Aminoglycosides and  $\beta$ -lactams share such a relationship. Aminoglycosides and  $\beta$ -lactams have long been known to interact synergistically<sup>74,75</sup> and recent studies have highlighted the collateral sensitivity between these two classes<sup>54,60</sup>.

However, of these three strategies, only resistance mechanism inhibitors have been tested across a broad range of species and vetted in the clinic. Much of the drug interactions and collateral sensitivity work has been done *in vitro* with *E. coli* and needs to be expanded to other organisms and infection models to see if these principles apply across species and *in vivo*. For



example, meta-analysis of clinical trials for the ideal combination of aminoglycoside and  $\beta$ -lactams predicted above from *in vitro* drug interaction and collateral sensitivity data show no significant improvement in terms of patient mortality and drug resistance over  $\beta$ -lactams alone<sup>76</sup>. Instead, the combination fares slightly worse due to aminoglycoside nephrotoxicity<sup>76</sup>.

This highlights the need for ongoing research on the interplay between physiological drug interactions and resistance mutation trade-offs. It also points to areas for further improvement. One difficulty with multi-drug treatment is ensuring simultaneous delivery to target cells. Indeed, unequal absorption and penetration may lead to pockets of single drug exposure and faster evolution of resistance<sup>77</sup>. One potential solution to this problem is covalently linking antibiotics into hybrid compounds<sup>78,79</sup>. In addition to ensuring simultaneous delivery, hybrid drugs can combine the growth inhibition of one drug with the resistance evasion of another to both treat an infection and prevent resistance (**Chapter 3**).

## References

1. Abraham, E. P. *et al.* Further observations on penicillin. *Lancet* **238**, 177–189 (1941).
2. World Health Organization. Antimicrobial resistance: global report on surveillance. *Bulletin of the World Health Organization* (2014).
3. Centers for Disease Control and Prevention. *Antibiotic Resistance Threats in the United States, 2013*. 1–114 (2013).
4. Laxminarayan, R. Antibiotic effectiveness: balancing conservation against innovation. *Science* **345**, 1299–1301 (2014).
5. Drawz, S. M. & Bonomo, R. A. Three decades of beta-lactamase inhibitors. *Clin. Microbiol. Rev.* **23**, 160–201 (2010).
6. Wright, G. D. Resisting resistance: new chemical strategies for battling superbugs. *Chem Biol* **7**, R127–32 (2000).

7. Ball, P. Conclusions: the future of antimicrobial therapy-Augmentin® and beyond. *Int J Antimicrob Ag* **30**, 139–141 (2007).
8. King, A. M. *et al.* Aspergillomarasmine A overcomes metallo- $\beta$ -lactamase antibiotic resistance. *Nature* **510**, 503–506 (2014).
9. Allen, N. E., Alborn, W. E., Hobbs, J. N. & Kirst, H. A. 7-Hydroxytropolone: an inhibitor of aminoglycoside-2"-O-adenylyltransferase. *Antimicrob Agents Chemother* **22**, 824–831 (1982).
10. Roestamadji, J. & Grapsas, I. Mechanism-based inactivation of bacterial aminoglycoside 3'-phosphotransferases. *J Am Chem Soc* (1995). doi:10.1021/bi010574w
11. Clancy, J. *et al.* Assays to detect and characterize synthetic agents that inhibit the ErmC methyltransferase. *J Antibiot* **48**, 1273–1279 (1995).
12. Hajduk, P. J. *et al.* Novel Inhibitors of Erm Methyltransferases from NMR and Parallel Synthesis. *J Med Chem* **42**, 3852–3859 (1999).
13. Nelson, M. *et al.* Inhibition of the tetracycline efflux antiport protein by 13-thio-substituted 5-hydroxy-6-deoxytetracyclines. *J Med Chem* **36**, 370–377 (1993).
14. Renau, T. *et al.* Inhibitors of Efflux Pumps in *Pseudomonas aeruginosa* Potentiate the Activity of the Fluoroquinolone Antibacterial Levofloxacin. *J Med Chem* **42**, 4928–4931 (1999).
15. Neyfakh, A. A., Borsch, C. M. & Kaatz, G. W. Fluoroquinolone resistance protein NorA of *Staphylococcus aureus* is a multidrug efflux transporter. *Antimicrob Agents Chemother* **37**, 128–129 (1993).
16. Markham, P. N. & Neyfakh, A. A. Inhibition of the multidrug transporter NorA prevents emergence of norfloxacin resistance in *Staphylococcus aureus*. *Antimicrob Agents Chemother* **40**, 2673–2674 (1996).
17. Stermitz, F. R., Lorenz, P., Tawara, J. N., Zenewicz, L. A. & Lewis, K. Synergy in a medicinal plant: antimicrobial action of berberine potentiated by 5'-methoxyhydnocarpin, a multidrug pump inhibitor. *Proc Natl Acad Sci USA* **97**, 1433–1437 (2000).
18. Pagès, J.-M. & Amaral, L. Mechanisms of drug efflux and strategies to combat them: challenging the efflux pump of Gram-negative bacteria. *Biochim. Biophys. Acta* **1794**, 826–833 (2009).
19. Reading, C. & Cole, M. Clavulanic acid: a beta-lactamase-inhibiting beta-lactam from *Streptomyces clavuligerus*. *Antimicrob Agents Chemother* **11**, 852 (1977).
20. Chaïbi, E. B., Sirot, D., Paul, G. & Labia, R. Inhibitor-resistant TEM beta-

- lactamases: phenotypic, genetic and biochemical characteristics. *J Antimicrob Chemother* **43**, 447–458 (1999).
21. Sjölund, M., Wreiber, K., Andersson, D. I., Blaser, M. J. & Engstrand, L. Long-term persistence of resistant *Enterococcus* species after antibiotics to eradicate *Helicobacter pylori*. *Ann. Intern. Med.* **139**, 483–487 (2003).
  22. Sjölund, M., Tano, E., Blaser, M. J., Andersson, D. I. & Engstrand, L. Persistence of resistant *Staphylococcus epidermidis* after single course of clarithromycin. *Emerg Infect Dis* **11**, 1389–1393 (2005).
  23. De Gelder, L. *et al.* Combining mathematical models and statistical methods to understand and predict the dynamics of antibiotic-sensitive mutants in a population of resistant bacteria during experimental evolution. *Genetics* **168**, 1131–1144 (2004).
  24. Andersson, D. I. & Hughes, D. Antibiotic resistance and its cost: is it possible to reverse resistance? *Nat Rev Micro* **8**, 260–271 (2010).
  25. Hegreness, M., Shores, N., Damian, D., Hartl, D. & Kishony, R. Accelerated evolution of resistance in multidrug environments. *Proc Natl Acad Sci USA* **105**, 13977–13981 (2008).
  26. Michel, J., Yeh, P., Chait, R., Moellering, R. & Kishony, R. Drug interactions modulate the potential for evolution of resistance. *Proc Natl Acad Sci USA* **105**, 14918 (2008).
  27. Yeh, P. J., Hegreness, M. J., Aiden, A. P. & Kishony, R. Drug interactions and the evolution of antibiotic resistance. *Nat Rev Micro* **7**, 460–466 (2009).
  28. Yeh, P., Tschumi, A. I. & Kishony, R. Functional classification of drugs by properties of their pairwise interactions. *Nat Genet* **38**, 489–494 (2006).
  29. Bliss, C. I. The toxicity of toxins applied jointly. *Ann Appl Biol* **26**, 585–615 (1939).
  30. Loewe, S. Die quantitation probleme der pharmakologie. *Ergeb. Physiol.* **27**, 47–187 (1928).
  31. Cokol, M. *et al.* Large-Scale Identification and Analysis of Suppressive Drug Interactions. *Chem Biol* **21**, 541–551 (2014).
  32. Cokol, M. *et al.* Systematic exploration of synergistic drug pairs. *Mol Syst Biol* **7**, 1–9 (2011).
  33. Nichols, R. J. *et al.* Phenotypic landscape of a bacterial cell. *Cell* **144**, 143–156 (2011).
  34. Bollenbach, T., Quan, S., Chait, R. & Kishony, R. Nonoptimal Microbial Response

- to Antibiotics Underlies Suppressive Drug Interactions. *Cell* **139**, 707–718 (2009).
35. Allison, K. R., Brynildsen, M. P. & Collins, J. J. Metabolite-enabled eradication of bacterial persisters by aminoglycosides. *Nature* **473**, 216–220 (2011).
  36. Lee, H. H., Molla, M. N., Cantor, C. R. & Collins, J. J. Bacterial charity work leads to population-wide resistance. *Nature* **467**, 82–85 (2010).
  37. Vega, N. M., Allison, K. R., Samuels, A. N., Klempner, M. S. & Collins, J. J. *Salmonella typhimurium* intercepts *Escherichia coli* signaling to enhance antibiotic tolerance. *Proc Natl Acad Sci USA* **110**, 14420–14425 (2013).
  38. Malik, M. *et al.* Lethal synergy involving bicyclomycin: an approach for reviving old antibiotics. *J Antimicrob Chemoth* **69**, 3227–3235 (2014).
  39. Ejim, L. *et al.* Combinations of antibiotics and nonantibiotic drugs enhance antimicrobial efficacy. *Nat Chem Biol* **7**, 348–350 (2011).
  40. Taylor, P. L., Rossi, L., De Pascale, G. & Wright, G. D. A forward chemical screen identifies antibiotic adjuvants in *Escherichia coli*. *ACS Chem Biol* **7**, 1547–1555 (2012).
  41. Peña-Miller, R. & Lahnemann, D. The optimal deployment of synergistic antibiotics: a control-theoretic approach. *J R Soc Interface* **9**, (2012).
  42. Torella, J. P., Chait, R. & Kishony, R. Optimal drug synergy in antimicrobial treatments. *PLoS Comput Biol* **6**, e1000796 (2010).
  43. Chait, R., Craney, A. & Kishony, R. Antibiotic interactions that select against resistance. *Nature* **446**, 668–671 (2007).
  44. Chow, J. W. & Yu, V. L. Combination antibiotic therapy versus monotherapy for gram-negative bacteraemia: a commentary. *Int J Antimicrob Ag* **11**, 7–12 (1999).
  45. Safdar, N., Handelsman, J. & Maki, D. G. Does combination antimicrobial therapy reduce mortality in Gram-negative bacteraemia? A meta-analysis. *Lancet* **4**, 519–527 (2004).
  46. Tamma, P. D., Cosgrove, S. E. & Maragakis, L. L. Combination Therapy for Treatment of Infections with Gram-Negative Bacteria. *Clin. Microbiol. Rev.* **25**, 450–470 (2012).
  47. Wood, K. B., Wood, K. C., Nishida, S. & Cluzel, P. Uncovering Scaling Laws to Infer Multidrug Response of Resistant Microbes and Cancer Cells. *CellReports* **6**, 1073–1084 (2014).
  48. Munck, C., Gumpert, H. K., Wallin, A. I. N., Wang, H. H. & Sommer, M. O. A. Prediction of resistance development against drug combinations by collateral

- responses to component drugs. *Sci Transl Med* **6**, 262ra156 (2014).
49. Stogios, P. J. *et al.* Structure-guided optimization of protein kinase inhibitors reverses aminoglycoside antibiotic resistance. *Biochem. J.* **454**, 191–200 (2013).
  50. Szybalski, W. & Bryson, V. Genetic studies on microbial cross resistance to toxic agents. I. Cross resistance of *Escherichia coli* to fifteen antibiotics. *J Bacteriol* **64**, 489–499 (1952).
  51. Chait, R., Shrestha, S., Shah, A. K., Michel, J.-B. & Kishony, R. A differential drug screen for compounds that select against antibiotic resistance. *PLoS ONE* **5**, e15179 (2010).
  52. Szybalski, W. & Bryson, V. Genetic studies on microbial cross-resistance to toxic agents. III. Cross-resistance of *Mycobacterium ranae* to twenty-eight antimycobacterial agents. *Am Rev Tuberc* **69**, 267–279 (1954).
  53. Szybalski, W. Genetic studies on microbial cross resistance to toxic agents. IV. Cross resistance of *Bacillus megaterium* to forty-four antimicrobial drugs. *Appl Microbiol* **2**, 57–63 (1954).
  54. Lázár, V. *et al.* Bacterial evolution of antibiotic hypersensitivity. *Mol Syst Biol* **9**, 700 (2013).
  55. Imamovic, L. & Sommer, M. O. A. Use of collateral sensitivity networks to design drug cycling protocols that avoid resistance development. *Sci Transl Med* **5**, 204ra132 (2013).
  56. Hiramatsu, K. *et al.* Curing bacteria of antibiotic resistance: reverse antibiotics, a novel class of antibiotics in nature. *Int J Antimicrob Ag* **39**, 478–485 (2012).
  57. Chao, L. An unusual interaction between the target of nalidixic acid and novobiocin. *Nature* **271**, 385–386 (1978).
  58. Lukens, A. K. *et al.* Harnessing evolutionary fitness in *Plasmodium falciparum* for drug discovery and suppressing resistance. *Proc Natl Acad Sci USA* **111**, 799–804 (2014).
  59. Oz, T. *et al.* Strength of selection pressure is an important parameter contributing to the complexity of antibiotic resistance evolution. *Mol Biol Evol* **31**, 2387–2401 (2014).
  60. Suzuki, S., Horinouchi, T. & Furusawa, C. Prediction of antibiotic resistance by gene expression profiles. *Nat Commun* **5**, 1–12 (2014).
  61. Taber, H. W., Mueller, J. P., Miller, P. F. & Arrow, A. S. Bacterial uptake of aminoglycoside antibiotics. *Microbiol. Rev.* **51**, 439–457 (1987).

62. Alekshun, M. N. & Levy, S. B. Molecular Mechanisms of Antibacterial Multidrug Resistance. *Cell* **128**, 1037–1050 (2007).
63. Okusu, H., Ma, D. & Nikaido, H. AcrAB efflux pump plays a major role in the antibiotic resistance phenotype of *Escherichia coli* multiple-antibiotic-resistance (Mar) mutants. *J Bacteriol* **178**, 306–308 (1996).
64. Kim, S., Lieberman, T. D. & Kishony, R. Alternating antibiotic treatments constrain evolutionary paths to multidrug resistance. *Proc Natl Acad Sci USA* **111**, 14494–14499 (2014).
65. Bochner, B., Huang, H., Schieven, G. & Ames, B. Positive selection for loss of tetracycline resistance. *J Bacteriol* **143**, 926 (1980).
66. Podolsky, T., Fong, S. T. & Lee, B. T. Direct selection of tetracycline-sensitive *Escherichia coli* cells using nickel salts. *Plasmid* **36**, 112–115 (1996).
67. Merlin, T. L., Davis, G. E. & Anderson, W. L. Aminoglycoside uptake increased by tet gene expression. *Antimicrob Agents Chemother* **33**, 1549–1552 (1989).
68. Merlin, T. L., Corvo, D. L., Gill, J. H. & Griffith, J. K. Enhanced gentamicin killing of *Escherichia coli* by tet gene expression. *Antimicrob Agents Chemother* **33**, 230–232 (1989).
69. Griffith, J. K., Kogoma, T., Corvo, D. L., Anderson, W. L. & Kazim, A. L. An N-terminal domain of the tetracycline resistance protein increases susceptibility to aminoglycosides and complements potassium uptake defects in *Escherichia coli*. *J Bacteriol* **170**, 598–604 (1988).
70. Li, Q. *et al.* NB2001, a novel antibacterial agent with broad-spectrum activity and enhanced potency against beta-lactamase-producing strains. *Antimicrob Agents Chemother* **46**, 1262–1268 (2002).
71. Katayama, Y., Ito, T. & Hiramatsu, K. A new class of genetic element, staphylococcus cassette chromosome mec, encodes methicillin resistance in *Staphylococcus aureus*. *Antimicrob Agents Chemother* **44**, 1549–1555 (2000).
72. Chopra, I. & Roberts, M. Tetracycline antibiotics: mode of action, applications, molecular biology, and epidemiology of bacterial resistance. *Microbiol Mol Biol R* **65**, 232 (2001).
73. Martinez, J. L. & Baquero, F. Mutation Frequencies and Antibiotic Resistance. *Antimicrob Agents Chemother* **44**, 1771–1777 (2000).
74. Jawetz, E., Gunnison, J. B. & Speck, R. S. Antibiotic synergism and antagonism. *New Engl J Med* **245**, 966–968 (1951).
75. Plotz, P. H. & Davis, B. D. Synergism between streptomycin and penicillin: a

proposed mechanism. *Science* **135**, 1067–1068 (1962).

76. Marcus, R., Paul, M., Elphick, H. & Leibovici, L. Clinical implications of  $\beta$ -lactam-aminoglycoside synergism: systematic review of randomised trials. *Int J Antimicrob Ag* **37**, 491–503 (2011).
77. Moreno-Gamez, S. *et al.* Imperfect drug penetration leads to spatial monotherapy and rapid evolution of multi-drug resistance. *bioRxiv* (2014). doi:10.1101/013003
78. Pokrovskaya, V. & Baasov, T. Dual-acting hybrid antibiotics: a promising strategy to combat bacterial resistance. *Expert Opin. Drug Discov.* **5**, 883–902 (2010).
79. Silver, L. L. Multi-targeting by monotherapeutic antibacterials. *Nat Rev Drug Discov* **6**, 41–55 (2007).

## **Chapter 2: New compounds that select against the tetracycline resistance efflux pump<sup>1</sup>**

We developed a novel competition-based screening strategy to identify compounds that select against antibiotic resistance mechanisms. Using our assay, we screened over 20,000 compounds for the ability to select against TetA efflux pump-mediated tetracycline resistance in *E. coli* and identified two hits:  $\beta$ -thujaplicin and disulfiram. We demonstrate a two-phase treatment paradigm, where pre-treatment of a tetracycline resistant bacterial population with  $\beta$ -thujaplicin causes loss of the resistance gene, enabling an effective second-phase treatment with doxycycline.

---

<sup>1</sup> This collaborative work is being prepared for publication. The authors are Laura K. Stone, Tami D. Lieberman, Michael Baym, Remy Chait, Jon Clardy, Roy Kishony.



## Introduction

Antibiotic resistance is a growing public health concern<sup>1</sup>. The use of antibiotics promotes the emergence and spread of resistant strains reducing the drugs' efficacy. Turning this process around and driving a resistant pathogen population back to drug susceptibility is a major challenge. Since the cost of resistance is typically small<sup>2,3</sup>, a resistance allele will remain in the population after fixation, even in the absence of the antibiotic<sup>4-6</sup>. Selecting against resistance therefore requires a treatment that imposes a cost on the resistant bacteria thereby inverting their evolutionary advantage.

Collateral sensitivity can be used against resistant strains to select in favor of drug susceptibility<sup>7</sup>. Collateral sensitivity occurs when resistance to one drug confers increased sensitivity to another<sup>8</sup>. Therefore, while bacteria evolve resistance to drug A, they can be penalized by their increased sensitivity to drug B. Treating with drug B can then drive them back to become drug A susceptible<sup>7</sup>. Focusing on resistance through *de novo* mutations, specific instances of collateral sensitivity have been identified where mutations providing resistance to one drug confer sensitivity to another<sup>7-13</sup>. However, the major mode of clinical resistance for many drugs is not through *de novo* mutations, but rather through specialized resistance genes, such as efflux pumps, drug degrading enzymes, or modified targets<sup>14,15</sup>. Only a few drugs are known to select against specialized resistance genes and cassettes<sup>16-20</sup>, and systematic screens for such selection-inverting compounds have been limited<sup>21</sup>.

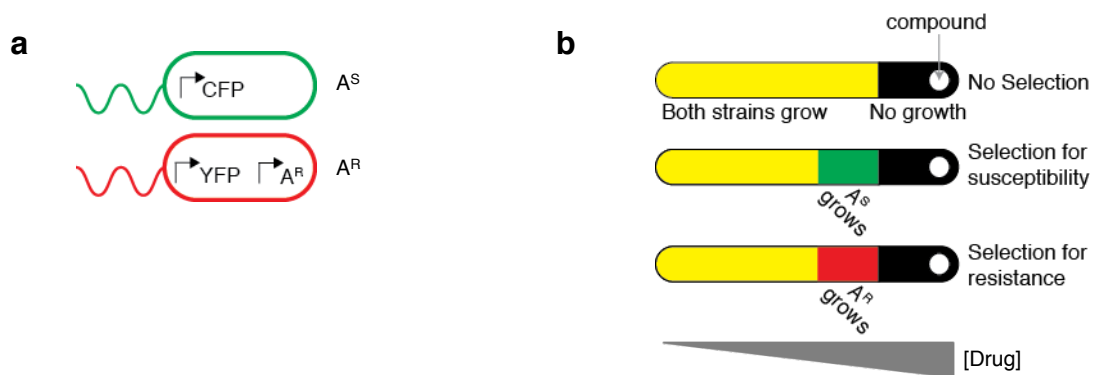
## Results

We designed a high-throughput screen to identify selection-inverting compounds: small molecules that confer a disadvantage to an antibiotic resistant strain competing with its

susceptible parent. In this assay, susceptible and resistant strains are differentially labeled with fluorescent proteins and competed on gradients of test compounds (**Fig. 2.1a**). Compounds that differentially select between these two strains will have an area along the gradient where only one of the strains can grow, appearing as a red or green band indicating selection for or against resistance, respectively (**Fig. 2.1b**). Custom 48-well channel plates and an automated imaging platform allow for high throughput automation of the assay (**Fig. S1.1, Methods**).

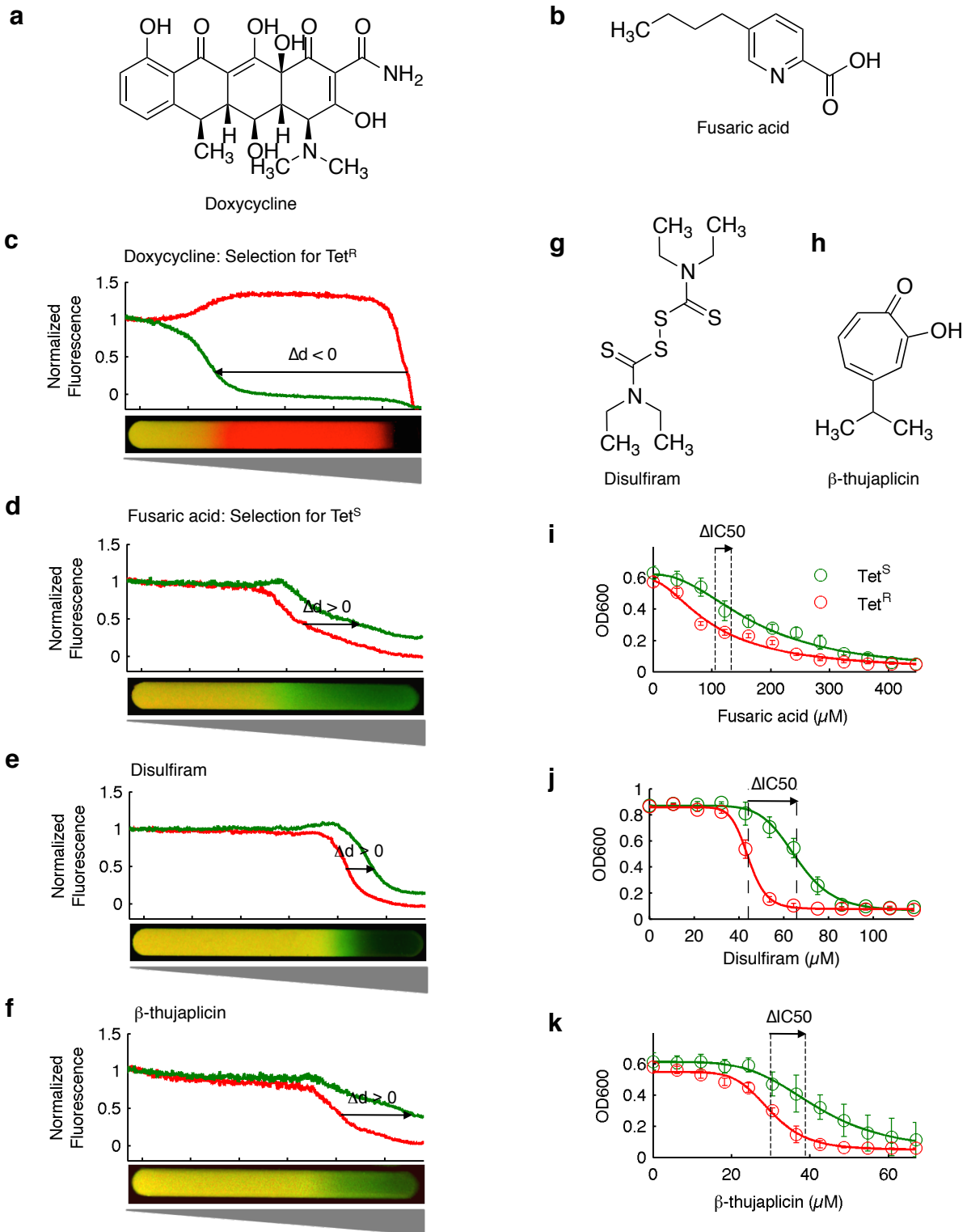
Using this assay, I screened for compounds that select against *E. coli* expressing the tetracycline resistance efflux pump, TetA. Tetracycline is a broad spectrum antibiotic whose use has dwindled, in part, due to widespread resistance<sup>4,22</sup>. The TetA efflux pump, often carried by transposons, is one of the most prevalent tetracycline resistance mechanisms<sup>2,22</sup>. As control compounds, I used doxycycline, a tetracycline analog that selects for tetracycline resistance (**Fig. 2.2a, c**), fusaric acid, a known molecule that selects against the TetA efflux pump but has toxicity issues<sup>16,23</sup> (**Fig. 2.2b, d**), and ciprofloxacin, an antibiotic eliciting no or slight selection for tetracycline resistance (**Fig. S1.2b**). The media was supplemented with anhydrous tetracycline (ATC) at concentrations that induce expression of TetA but have no detectable effects on growth (**Methods**).

I screened 20,529 compounds in this assay: 9,512 known bioactives, 6,441 natural product extracts, and 4,576 commercial library compounds. The primary screen identified 30 hits (0.29%) from the known bioactives collection, 8 hits (0.13%) in the natural extract libraries, and none in the commercial libraries. I verified positive hits by first retesting them in our assay, in duplicate with the dye swap (**Fig. S1.3**). Of our 38 initial hits, two hits from the bioactives collection retested positive in both replicates: disulfiram and  $\beta$ -thujaplicin (also known as hinokitiol) (**Fig. 2.2e-h**). Disulfiram is an FDA approved drug (Antabuse) for treating alcoholism



**Figure 2.1. A high throughput diffusion-based screen to identify compounds that select against antibiotic resistance.** (a) Matched fluorescent pairs of antibiotic susceptible ( $A^S$ , CFP, shown in green) and resistant ( $A^R$ , YFP, shown in red) strains are mixed 1:1 and added to gradients of test compound. A dye swap is also performed. (b) Fluorescent imaging reveals regions of selection on the compound gradient. Areas of no selection maintain a 1:1 ratio of  $A^S$  to  $A^R$  (yellow), while areas of no growth appear dark. Concentration regimes that select for susceptibility favor  $A^S$  growth (green), while regimes that select for resistance favor  $A^R$  growth (red). The white dot indicates where compound was spotted.

**Figure 2.2 Disulfiram and  $\beta$ -thujaplicin select against TetA-mediated tetracycline resistance.** Control compounds, (a) doxycycline and (b) fusaric acid select for tetracycline resistance and susceptibility, respectively. (c-f) Compounds that select against resistance were automatically identified by tracking the fluorescence of tetracycline resistant ( $Tet^R$ , TetA) and susceptible ( $Tet^S$ ) strains down the concentration gradients of test compounds (**Methods**). Automated image analysis identifies the highest points on the concentration gradient (corresponding to the distance from the top of the well) where each strain is at half-max growth. The difference between these points ( $\Delta d$ ) is used to score hits, with negative  $\Delta d$  indicating selection for resistance and positive  $\Delta d$  indicating selection against resistance. Hit compounds (g) disulfiram and (h)  $\beta$ -thujaplicin select for tetracycline susceptibility. (i-k) Dose responses for (i) fusaric acid, (j) disulfiram, and (k)  $\beta$ -thujaplicin in  $Tet^S$  and  $Tet^R$  strains, grown separately. The vertical black dashed lines indicate the mean IC50s for the  $Tet^R$  and  $Tet^S$  strains across six replicates. Error bars represent standard deviation across six replicates.



**Figure 2.2 (Continued). Disulfiram and  $\beta$ -thujaplicin select against TetA-mediated tetracycline resistance.**

and acts synergistically with tetracycline in susceptible strains<sup>24</sup>. Isolated from cedar trees,  $\beta$ -thujaplicin is natural product with widespread antifungal and antibacterial activity<sup>25</sup>. While these compounds were known to have antibacterial activity<sup>25,26</sup>, their ability to select against tetracycline resistance is a newly discovered property.

I evaluated potency and selectivity of the compounds by testing them on the resistant and susceptible strain separately and in competition. I measured the dose response of these two hits and fusaric acid for tetracycline susceptible ( $Tet^S$ ) and resistant ( $Tet^R$ ) strains grown separately in broth media and obtained their 50% inhibitory concentrations (IC50s, **Fig. 2.2i-k**). All three drugs had IC50s that are lower for the  $Tet^R$  strain than the  $Tet^S$  strain ( $Tet^R$ ,  $Tet^S$ ; disulfiram:  $44 \pm 1 \mu M$ ,  $66 \pm 3 \mu M$ ;  $\beta$ -thujaplicin:  $30 \pm 1 \mu M$ ,  $39 \pm 4 \mu M$ ; fusaric acid  $106 \pm 6 \mu M$ ,  $133 \pm 14 \mu M$ ; mean  $\pm$  standard deviation across six replicates). To quantify the competitive advantage conferred by the compounds, I performed a competition assay in liquid media, mixing fluorescently labeled  $Tet^S$  and  $Tet^R$  strains 1:1 and growing them in a linear dilution series of each compound. After an overnight incubation, I measured the number of  $Tet^S$  cells ( $N_{Tet^S}$ ) and  $Tet^R$  cells ( $N_{Tet^R}$ ) with flow cytometry (**Fig. 2.3a**). All three compounds select for  $Tet^S$  over  $Tet^R$  by at least an order of magnitude at some concentration (**Fig. 2.3b**, **Fig. S1.5a,b**). Its better potency ( $Tet^S$  IC50) and the availability of analogs lead us to focus on  $\beta$ -thujaplicin for further analysis.

To understand which chemical moieties of  $\beta$ -thujaplicin are critical for its potency and selection properties, I measured the IC50 of  $\beta$ -thujaplicin analogs for  $Tet^S$  and  $Tet^R$  strains and their effect on competition between  $Tet^S$  and  $Tet^R$  strains (**Fig. 2.3c**, **Fig. S1.4 & S1.5**, **Table S1.1**). In competition,  $\beta$ -thujaplicin selects for  $Tet^S$  over  $Tet^R$  by over two orders of magnitude (**Fig. 2.3b**), more than any other analog tested. Moreover,  $\beta$ -thujaplicin has the best combination

**Figure 2.3. Structure activity relationship for  $\beta$ -thujaplicin analogs.** (a) To quantify the degree of selection against tetracycline resistance, a 1:1 mixture of fluorescent Tet<sup>S</sup> (green) and Tet<sup>R</sup> (red) cells was added to a linear dilution series of each drug. Flow cytometry was used to count the number of Tet<sup>R</sup> ( $NTet^R$ ) and Tet<sup>S</sup> ( $NTet^S$ ) cells. The data shown are from a well with no drug (left) and a well with 43  $\mu$ M  $\beta$ -thujaplicin (right). (b) The ratio of Tet<sup>S</sup> to Tet<sup>R</sup> cells ( $NTet^S/NTet^R$ ) gives the selection for the Tet<sup>S</sup> strain at each drug concentration. This ratio is normalized to the ratio of  $NTet^S/NTet^R$  in wells with no drug and then averaged over a minimum of 5 replicates. The integral (gray) of the selection over all concentrations in which cells can grow is considered the total selection (selectivity) for Tet<sup>S</sup> by that compound. (c) The selection for Tet<sup>S</sup> over Tet<sup>R</sup> exerted by all compound gradients. Wells where there is no growth of either strain are in gray. (d) Examining all compounds for selectivity and potency (Tet<sup>S</sup> IC<sub>50</sub>) shows that  $\beta$ -thujaplicin exerts the greatest selection for Tet<sup>S</sup> among its analogs.

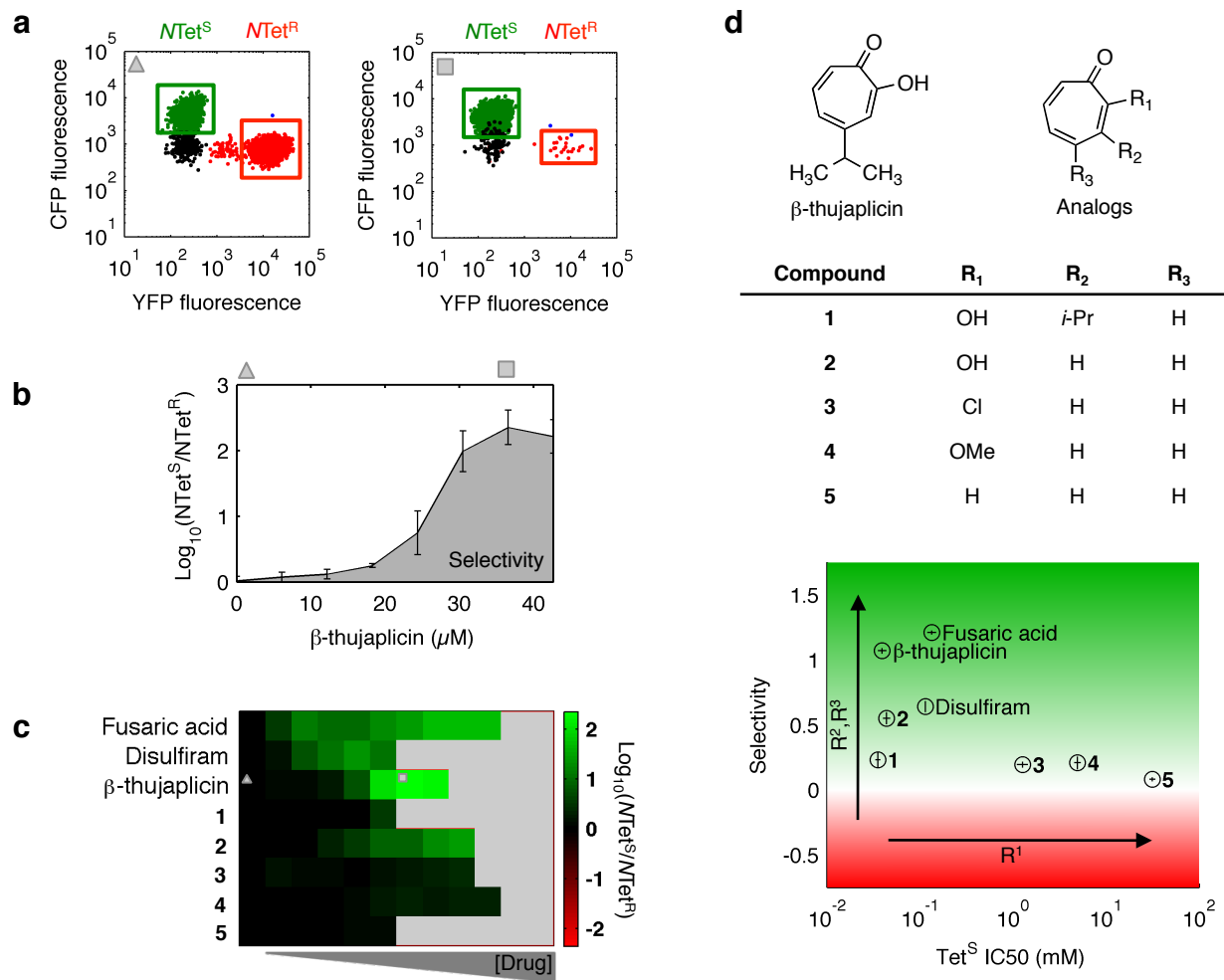


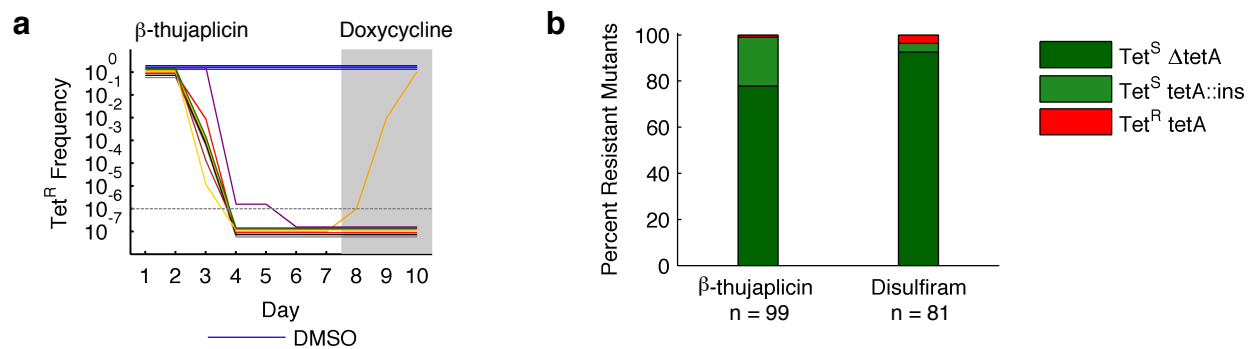
Figure 2.3 (Continued). Structure activity relationship for  $\beta$ -thujaplicin analogs.



of selection and potency (Tet<sup>S</sup> IC50) of the compounds tested (**Fig. 2.3d**). The closest analog,  $\alpha$ -thujaplicin, showed no difference in IC50 between the Tet<sup>S</sup> and Tet<sup>R</sup> strains and little selection either for or against the Tet<sup>R</sup> strain (**Fig. S1.4a & S1.5c, Table S1.1**). From this structure-activity relationship, I infer that the hydroxyl group is required for potency, while the presence and position of the isopropyl group determines the degree of selection.

While the compounds I identified advantage the Tet<sup>S</sup> over the Tet<sup>R</sup> strain, it remained unclear whether this advantage was enough to evolve a resistant population back to drug susceptibility. To answer this question, I propagated 8 replicate populations of the Tet<sup>R</sup> strain in increasing amounts of  $\beta$ -thujaplicin for 7 days and monitored the frequency of Tet<sup>R</sup> cells (**Fig. 2.4a**). In all 8 populations, the frequency of Tet<sup>R</sup> cells decreased until it fell below detectable levels (**Fig. 2.4a**). To see if these, now Tet<sup>S</sup>, populations would revert to Tet<sup>R</sup> upon treatment with doxycycline, I next passaged them in increasing amounts of doxycycline for 3 days. Only one of the eight populations regained resistance to doxycycline. Most cultures have permanently lost Tet<sup>R</sup> upon  $\beta$ -thujaplicin treatment, allowing effective doxycycline treatment in the second phase of this two-phase treatment protocol.

To understand the frequency of Tet<sup>R</sup> loss and its underlying genotypic mechanisms, I isolated  $\beta$ -thujaplicin resistant mutants of the Tet<sup>R</sup> strain and assayed their doxycycline phenotype (**Methods**). The vast majority of these isolates became doxycycline susceptible upon  $\beta$ -thujaplicin selection (98/99, **Fig. 2.4b**). PCR of the *tetA* gene showed that most had deleted *tetA* (77/99), while the rest had a 0.5-1 kb insertion in *tetA* (21/99, **Fig. 2.4b, Fig. S1.9**). Whole genome sequencing of 4 isolates with insertions in *tetA* confirmed the presence of insertion elements within *tetA* and sequencing of 6  $\Delta tetA$  isolates revealed that the entire Tn10 transposon carrying *tetA* has been deleted. Two of these  $\Delta tetA$  isolates also had single nucleotide



**Figure 2.4. β-thujaplicin and disulfiram select for loss of the tetracycline resistance phenotype and loss of *tetA*.** (a) When evolved in β-thujaplicin, eight parallel populations of the Tet<sup>R</sup> strain lose their tetracycline resistance phenotype until the frequency of Tet<sup>R</sup> cells falls below the detection limit ( $10^{-6}$ ). In comparison, populations evolved in DMSO (blue), do not lose their tetracycline resistance. After 7 days, the lineages were then evolved in doxycycline for three days. Only one of the eight lineages regains its tetracycline resistance. Points overlap and are offset slightly in the Tet<sup>R</sup> frequency axis for clarity. (b) Over 90% of β-thujaplicin and disulfiram resistant mutants selected from the Tet<sup>R</sup> background strain lose phenotypic resistance to tetracycline. These Tet<sup>S</sup> mutants had completely lost *tetA* or had insertions within the gene.

polymorphisms (SNP) elsewhere in the genome (**Table S1.2**). The one isolate that became  $\beta$ -thujaplicin resistant without losing *tetA* had a mutation in *marR*, the repressor of the multiple antibiotic resistance operon<sup>27</sup> (**Table S1.2**). Together, these data show that the vast majority of resistance to  $\beta$ -thujaplicin appears through null insertions or irreversible loss of the *tetA* gene, while only rare cases evolve resistance to  $\beta$ -thujaplicin through more general resistance pathways and without Tet<sup>R</sup> loss. Furthermore, these  $\Delta tetA$  mutants occur at much higher frequency ( $\sim 10^{-4}$ ) than SNP-based resistance mutations ( $\sim 10^{-6}$ ), in agreement with previous studies documenting loss of Tn10<sup>16</sup>. Similar results appear for disulfiram selection (78/81 lost Tet<sup>R</sup>: 75 due to loss of *tetA*, 1 due to an insertion in *tetA*, 2 due to other mutations, **Fig. S1.10**).

## Discussion

This work provides a proof of concept that selection-inverting compounds for well-optimized resistance genes can be found through a competition-based screening assay and can be used preceding their corresponding antibiotic in a two-phase treatment strategy against a resistant bacterial population. This methodology can be adapted to other organisms and resistance mechanisms. Two-phase treatment protocols beginning with selection-inverting drugs followed by conventional antibiotics may provide novel antimicrobial treatments that are effective against resistant pathogens by first reverting them to drug susceptibility. However, this strategy is not without limitations. The population that became  $\beta$ -thujaplicin resistant without completely losing its tetracycline resistance suggests that, while it might be rare, it is possible for bacteria to escape collateral sensitivity. Firstly, it is possible that some members of the population remained  $\beta$ -thujaplicin sensitive and tetracycline resistant even after  $\beta$ -thujaplicin selection. Secondly, there are other paths to  $\beta$ -thujaplicin resistance, as demonstrated by the *marR* mutant that became  $\beta$ -

thujaplicin resistant without losing its tetracycline resistance. Thirdly, the  $\beta$ -thujaplicin resistant mutants with insertions in TetA, instead of complete deletions, may more easily revert to Tet<sup>R</sup>.

Furthermore, the need to remove antibiotic resistance from the bacterial population must be balanced with the need to cure the patient. In acute infections such as septicemia, a selection-inverting compound must not only drive the loss of resistance mechanisms, it must also lower the bacterial load—and quickly. In this scenario, clinically useful selection-inverting compounds must be powerful antibiotics in their own right and the speed of clearance may obviate the need for the second-phase of treatment. Therefore, in life-threatening short-term infections, a two-phase treatment strategy does not offer much more benefit to the individual patient than a traditional antibiotic, even though broad implementation may reduce the prevalence of resistance genes in the general population. Instead, this two-phase treatment strategy is likely to be more useful in long-term chronic infections such as *Pseudomonas aeruginosa* in cystic fibrosis patients or chronic tuberculosis infections. These infections typically require long treatment durations with multiple drugs at once to limit the emergence of resistance. Two-phase treatment strategies designed against common resistance mechanisms in these pathogens may cure the infection, stave off resistance, and avoid the toxicity risk that often comes with concurrent multi-drug treatment.

As antibiotic resistance rates rise, new strategies are needed to combat infections. Current treatments overwhelmingly favor the evolution of resistance and most strategies employed to curb the spread of resistance do little to reduce that selective pressure. Ideally, therapeutic design would consider evolutionary and ecological dynamics and create treatment regimens that can reverse the evolution of resistance. Two-phase treatments beginning with selection-inverting

compounds that counteract the evolutionary advantage of resistance could add valuable tools to our antimicrobial arsenal.

## Methods

### Strains and Media

All experiments were conducted in low salt LB broth (RPI, catalog #L24065), supplemented with bactoagar (BD Falcon) when noted. Drug solutions were made from powder stocks (anhydrotetracycline hydrochloride (ATC), catalogue no. 37919 (Sigma); doxycycline hyclate, catalogue no. D9891 (Sigma); ciprofloxacin, catalogue no. 17850 (Fluka); fusaric acid, catalogue no. AC19896 (Fisher);  $\beta$ -thujaplicin, catalogue no. 469521 (Sigma); disulfiram, catalogue no. 86720 (Sigma);  $\alpha$ -thujaplicin (analog **1**), catalogue no. 088-08701, (Wako); tropolone (analog **2**), catalogue no. T89702 (Sigma); 2-Chloro-2,4,6-cycloheptatrien-1-one (analog **3**, chlorotropone), catalogue no. 669571, (Sigma); 2-Methoxy-2,4,6-cycloheptatrien-1-one (analog **4**, methoxytropone), catalogue no. 137-15711 (Wako); tropone (analog **5**), catalogue no. 252832 (Sigma)) and filter-sterilized. All drug stocks were dissolved in DMSO at 15 mg/mL, except anhydrotetracycline hydrochloride, which was dissolved in EtOH at 1 mg/mL.

Strain construction and designations are given below. Plasmids expressing YFP or CFP under the  $P_R$  promoter<sup>28</sup> were constructed from the pZ vector system<sup>29</sup>. Assay strains were grown from single colonies to saturation in low salt LB. Cell concentrations were measured by OD600 and plate count, and aliquots were stored in 15% glycerol at -80°C. Fresh aliquots were used for each experiment.

**Table 2.1: Strains**

Strain	Type	Tetracycline resistance	Source
CAG18478	MG1655, <i>ycaD-ycaM::Tn10</i>	Tet <sup>R</sup>	Ref. 30
WT	MC4100	Tet <sup>S</sup>	Ref. 31
t17c	MC4100, <i>ycaD-ycaM::Tn10</i> , <i>galK::CFP</i> , Amp <sup>R</sup>	Tet <sup>R</sup>	Ref. 32
t17	MC4100, <i>ycaD-ycaM::Tn10</i>	Tet <sup>R</sup>	P1 <sub>vir</sub> (t17c) → MC4100
pY	MC4100 / pZS2R-YFP	Tet <sup>S</sup>	Plasmid pZS2R-YFP into WT
pC	MC4100 / pZS2R-CFP	Tet <sup>S</sup>	Plasmid pZS2R-CFP into WT
t17pY	MC4100, <i>ycaD-ycaM::Tn10</i> / pZS2R-YFP	Tet <sup>R</sup>	Plasmid pZS2R-YFP into t17
t17pC	MC4100, <i>ycaD-ycaM::Tn10</i> / pZS2R-CFP	Tet <sup>R</sup>	Plasmid pZS2R-CFP into t17

**Custom Assay Plate**

I tailored Remy Chait's design for 48 well plates composed of 2 rows of 24 lanes<sup>21</sup> to be compatible with high throughput screening robots by lowering the plate's skirt and adding spacing bars so that air can escape as the agar cools while the plates are stacked (**Fig. S1.1**).

**Screen for Selection Inverters**

Custom 48 well screening plates were filled with 352  $\mu$ L/well low salt LB 1.5% bactoagar containing 80 ng/mL ATC using a Wellmate Stacker (ThermoScientific). Approximately 1  $\mu$ L/well test compounds were pinned onto the top of each lane using AFIX384FP6 (V&P Scientific) with FP6S pins (V&P Scientific) in rows A and I. Approximately 1  $\mu$ L/well control compounds were pinned onto the top of each lane by hand using AFIX384FP (V&P Scientific) with FP6S pins (V&P Scientific) in appropriate wells. Each screening plate had at least one of each control: 15 mg/mL doxycycline, 15 mg/mL fusaric acid, 15 mg/mL ciprofloxacin, and

DMSO vehicle control. Plates were stored at 4°C for 24 hours to allow the compounds to diffuse, creating concentration gradients down the length of the wells. Plates were then inoculated using a Wellmate Stacker with 112 µL/well frozen cell aliquots diluted 1:100 in low salt LB 0.75% bactoagar containing 80 ng/mL ATC. Each test compound is tested twice, with the fluorescent markers switched between the tetracycline susceptible and resistant strains to identify autofluorescent compounds. One replicate is inoculated with a 1:1 ratio of pY:t17pC and the other is inoculated with a 1:1 ratio of pC:t17pY. Plates were incubated at 30°C and 70% humidity for 16-18 h, and automatically imaged using a custom-built robotic fluorescent imaging device constructed by Michael Baym and Remy Chait and programmed by Michael Baym. Images in three channels, brightfield, CFP(436/20ex, 480/40em), and YFP(500/20ex, 530/20em) were acquired with a Canon T3i.

### **Screen Analysis**

The images were processed using a custom MATLAB script (deposited at <https://github.com/lkstone/StoneThesis>). The blue channel from the CFP image and the green channel from the YFP image are reduced to grayscale images. Nonuniformity in the field of illumination are corrected by normalizing each image to a fluorescent standard. The images are further processed by subtracting the background (the median intensity of an area of no bacterial growth) and normalizing to an area of neutral selection (the median intensity of the DMSO controls). Next, an RGB overlay image is created with the susceptible strain image in the green channel and the resistant strain image in the red channel, regardless of the fluorescent proteins involved. Using this overlay, the pixel intensity data is isolated for each well and the median is taken across the width of the well for the red and green channels. Wells with no inhibition of

either strain are filtered out using a minimum intensity threshold. The remaining wells are scored by subtracting the distance to the half-max growth of the resistant strain from the distance to the half-max growth of the susceptible strain down the length of the well ( $\Delta d$ ). Overlay images were evaluated by eye in addition to the automated ranking of hits. Using the  $\Delta d$  metric, doxycycline (selection for resistance control) and fusaric acid (selection against resistance control) were identified in comparison to ciprofloxacin (inhibition with no selection control) and DMSO (no inhibition or selection control). The  $Z'$  factor was 0.62 for the fusaric acid control and 0.87 for the doxycycline control.

### **Petri Competition Assay**

Petri dishes (100mm x 15 mm, BD Falcon) were filled with 20 mL low salt LB 1.5% bactoagar containing 80 ng/mL ATC. Drug stocks were pipetted onto the plate (3  $\mu$ L of 15 mg/mL fusaric acid, 1  $\mu$ L of 15 mg/mL  $\beta$ -thujaplicin, and 6  $\mu$ L of 15 mg/mL disulfiram dissolved in DMSO) and allowed to diffuse at 4°C for 24 h. The plates were then inoculated with 100  $\mu$ L of a 1:100 dilution of frozen cell aliquots in phosphate buffered saline (PBS). One replicate is inoculated with a 1:1 ratio of pY:t17pC and the other is inoculated with a 1:1 ratio of pC:t17pY. Plates were incubated at 30°C and 70% humidity for 16-18 h, then imaged in brightfield, CFP(436/20ex, 480/40em), and YFP(500/20ex, 530/20em) with a Canon T3i.

### **IC50 Measurements**

Clear, flat-bottomed 96-well plates (Corning 3370) were filled with 150  $\mu$ L/well low salt LB containing linear dilution series of drug,  $\sim 10^4$  cfu/mL WT (Tet<sup>S</sup>), and  $\sim 10^4$  cfu/mL t17 (Tet<sup>R</sup>) cells. Experiments are run in parallel: at least 6 replicates with and 6 replicates without 80 ng/mL



ATC to show that fitness differences are dependent on the expression of the TetA pump. The plates are sealed with Aeraseal (EXCEL) to limit evaporation and incubated for 24 h at 30°C with shaking at 900 rpm on Titramax 1000 (Heidolph). Growth was measured by optical density at 600 nm (OD600) on a Victor3 plate reader (Perkin Elmer). The dose responses are fit to a 4 parameter logistic function  $c + (d - c)/(1 + (x/a)^b)$  where a is the IC50, b is the slope parameter, c is the minimum response level, and d is the maximum response level.

### **FACS Competition Assay**

Clear, flat-bottomed 96-well plates (Corning 3370) were filled with 150  $\mu$ L/well low salt LB containing linear dilution series of drug and  $\sim 10^4$  cfu/mL fluorescently-labeled Tet<sup>S</sup> and  $\sim 10^4$  cfu/mL fluorescently-labeled Tet<sup>R</sup> cells. Experiments are run in parallel with a dye swap (pY & t17pC in one set of plates and pC & t17pY in another set) to show that fitness differences do not depend on the fluorescent proteins and with and without 80 ng/mL ATC to show that fitness differences are dependent on the expression of the TetA pump. The plates are sealed with Aeraseal (EXCEL) to limit evaporation and incubated for 24 h at 30°C with shaking at 900 rpm on Titramax 1000 (Heidolph). The saturated cultures were diluted 1:100 by pinning  $\sim 1.5$   $\mu$ L/well culture into 150  $\mu$ L PBS with VP407 (V&P Scientific). Cells were counted by flow cytometry (Becton Dickinson LSRII; CFP excited at 405nm, emission detected through 505LP and 525/550nm filters; YFP excited at 488nm, emission also detected through 505LP and 525/550nm filters). The ratio of Tet<sup>S</sup> to Tet<sup>R</sup> cells ( $N_{TetS}/N_{TetR}$ ) was normalized to the  $N_{TetS}/N_{TetR}$  of eight no drug wells on each plate. Results in Figure 2.3 are the average of 5 replicates performed with pC and t17pY cells and 80 ng/mL ATC.

## Passaging Experiment

Clear, flat-bottomed 96-well plates (Corning 3370) were filled to a final volume of 150  $\mu\text{L}$ /well low salt LB with 80 ng/mL ATC. Each column contained a linear dilution series of  $\beta$ -thujaplicin or doxycycline. Each plate included one column inoculated with WT ancestral control, one column inoculated with t17 ancestral control, and one column with no bacteria to control for contamination. Nine columns contained replicate populations of t17 passaged each day into fresh  $\beta$ -thujaplicin for 7 days, then in doxycycline for 3 days ( $\beta$ -thujaplicin evolved strains). In addition, 3 replicate populations of t17 were passaged in a fixed DMSO concentration equivalent to the highest DMSO concentration used in the  $\beta$ -thujaplicin dilution series (DMSO evolved strains). Plates were inoculated with  $\sim 10^4$  cfu/mL. The plates are sealed with Aeraseal (EXCEL) to limit evaporation and incubated for 22 h at 30°C with shaking at 900 rpm on Titramax 1000 (Heidolph). Growth was measured by optical density at 600 nm (OD600) on a Victor3 plate reader (Perkin Elmer). For each evolved strain, the well containing the highest drug concentration with  $\text{OD}_{600} \geq 0.4$  was diluted and propagated daily into fresh drug plates with  $\sim 10^4$  cfu/mL. The remainder of the well was stored in 15% glycerol at -80°C. The wells with WT and t17 ancestral controls and no drug were also stored in 15% glycerol at -80°C to serve as controls for later follow up. One of the nine  $\beta$ -thujaplicin lineages was contaminated in storage and is excluded from Figure 2.4.

The Tet<sup>R</sup> frequency was measured by creating a 10-fold dilution series of stored evolved strains and ancestral controls in PBS. Using VP407,  $\sim 1.5$   $\mu\text{L}$ /well of these dilution series and the storage wells were pinned onto one non-treated omnitray (Thermo Scientific) containing 30 mL low salt LB 1.5% bactoagar and one non-treated omnitray containing 30 mL low salt LB 1.5%

bactoagar and 20  $\mu\text{g}/\text{mL}$  doxycycline. The plates were incubated at 30°C for 22 h then imaged. Growth was then measured by eye with positive growth meaning that at least one colony grew from the spot. The cfu/mL of the dilution series was calibrated by plating 50  $\mu\text{L}$  of select wells onto petri dishes containing 20 mL low salt LB 1.5% bactoagar. The data from pinning is precise to one order of magnitude. The accuracy of this method was confirmed by plating 50  $\mu\text{L}/\text{well}$  of a subset of samples onto petri dishes containing 20 mL low salt LB 1.5% bactoagar and onto petri dishes containing 20 mL low salt LB 1.5% bactoagar and 20  $\mu\text{g}/\text{mL}$  doxycycline.

### **Resistant Mutant Selection**

The t17 strain was streaked on a low salt LB 1.5% bactoagar petri dish and grown overnight at 30°C. A single colony was picked and grown overnight in low salt LB to saturation ( $\sim 2 \times 10^9$ ). This culture was spun down at 3000 rpm & 4°C and the supernatants decanted. The culture was re-suspended in PBS, spun down again, the supernatants decanted, and re-suspended in PBS to a density of  $\sim 10^7$  cfu/mL. Petri dishes containing 20 mL low salt LB 1.5% bactoagar, 80 ng/mL ATC, and either 40  $\mu\text{g}/\text{mL}$  disulfiram or 15  $\mu\text{g}/\text{mL}$   $\beta$ -thujaplicin were inoculated with  $\sim 10^6$  t17 cfu/plate. The plates were incubated at 30°C, 70% humidity, protected from light. Disulfiram plates were incubated for 3 days and  $\beta$ -thujaplicin plates were incubated for 6 days.

One hundred colonies from the  $\beta$ -thujaplicin and disulfiram selection plates were streaked onto LB agar petri dishes and incubated overnight at 30°C. One colony from each streak was transferred to deep 96 well plates containing 1 mL/well low salt LB. A subset of the plate was inoculated with WT or t17 ancestral controls or left empty to control for cross contamination. The plates were sealed with Aeraseals and incubated at 30°C with 600 rpm shaking on a

Titramax. Using VP407, ~1.5  $\mu\text{L}$ /well was transferred from these overnight plates onto omnitrays containing low salt LB 1.5% bactoagar, 80 ng/mL ATC, and drug (5, 10, 15, 20, 25, 30  $\mu\text{g}/\text{mL}$   $\beta$ -thujaplicin; 10, 20, 30, 40, 50, 60  $\mu\text{g}/\text{mL}$  disulfiram; 0, 0.1, 1, 5, 10, 20, 40, 60, 80, 100  $\mu\text{g}/\text{mL}$  doxycycline). Omnitrays were incubated at 30°C for 20 h. Plates were imaged and growth was recorded (single colonies or films were recorded as no growth). The minimum inhibitory concentration (MIC) was determined as the lowest concentration at which the strains did not grow.

### Detection of *tetA* by PCR

The *tetA* gene was amplified with the primers below (**Table 2.2**) in 25  $\mu\text{L}$  reactions using 0.2  $\mu\text{L}$  OneTaq (New England Biolabs) according to the supplier's protocol. Reactions were cycled 30 times, with an annealing temperature of 57°C. PCR product size was determined by gel electrophoresis on a 1% agarose gel (**Fig. S1.9-11**). The bands were compared to a 1 kb DNA ladder (New England Biolabs) and their size was determined within 0.5 kb. The expected band size is 1086 bp if *tetA* is present and uninterrupted.

**Table 2.2. Primers**

Primer	Sequence
<i>tetA</i> forward	GCTAACCACTTTGGCGTATTG
<i>tetA</i> reverse	AGCACTTGTCTCCTGTTTACTC

### Genomic sequencing of $\beta$ -thujaplicin resistant colonies

Genomic DNA was extracted from 1 mL cultures of eleven colonies and the ancestral t17 control using illustra bacteria GenomicPrep Mini Spin Kit (GE Healthcare) following the supplier's protocol, except eluting with water instead of elution buffer. Purified DNA was quantified using the Quant-iT™ High-Sensitivity DNA Assay Kit (Life Technologies). Sequencing libraries were prepared using the Nextera XT DNA Sample Preparation Kit (Illumina), using a previously described protocol<sup>33</sup>. Samples were sequenced using 100bp paired-end reads on the HiSeq platform at Axeq Technologies, Seoul, South Korea. Tami Lieberman performed genomic sequencing analysis. Adaptors were removed using cutadapt<sup>34</sup>, reads were trimmed using Sickle, and trimmed reads were aligned to both the *E. coli* MC4100 reference genome and Tn10 (Genbank accession numbers NC\_012759.1 and AF162223.1, respectively) using Bowtie2<sup>35</sup>. Over 99.7% of reads aligned to the reference genome, and average coverage across a sample ranged between 33x and 134x (median 65x). SNPs were identified using SAMtools<sup>36</sup> and consensus quality (FQ score) cutoff of less than -55 for inclusion. At each variant position that met this cutoff in at least one strain, a best call was made based on the aligned reads for each strain, and positions where all reads supported a variant were discarded. Small insertions and deletions (indels) were called using Dindel<sup>37</sup>. Candidate indels found in one strain were explicitly tested for in all strains; indels with at least 70% of reads in the region supporting the indel and that were at positions with an average of at least 10x coverage across isolates were accepted. Tn10 deletions were identified by the absence of reads aligning to the coding section of AF162223.1. Insertion elements were identified using RetroSeq<sup>38</sup> (FL score of 6 or 8).

## **Contributions**

L.K.S., J.C., and R.K. designed research; L.K.S. performed research and analyzed data; T.D.L. analyzed genomic sequencing data; M.B. and R.C. built the custom imaging setup and M.B. wrote the robotic scripts; R.C. contributed the initial plate and assay design; L.K.S. and R.K. wrote the manuscript.

## Acknowledgements

We thank D. Rudner, R. Mazitschek, and R. Moellering for helpful insights. We thank J. Horn and J. Marchionna for custom screening plates and technical advice. We thank D. Flood and S. Rudnicki for technical support in the primary screen. We thank Jodene Moore and Jue Wang for sharing their flow cytometry expertise. All primary screening was performed at Harvard Medical School ICCB-L Screening Facility. This work was supported in part by National Institute of Allergy and Infectious Diseases grant U54 AI057159, US National Institutes of Health grant R01 GM081617 (to R.K.), European Research Council FP7 ERC Grant 281891, Hoffman-LaRoche, and a National Science Foundation Graduate Fellowship (to L.K.S.).

## References

1. World Health Organization. Antimicrobial resistance: global report on surveillance. *Bulletin of the World Health Organization* (2014).
2. Lenski, R. E., Simpson, S. C. & Nguyen, T. T. Genetic analysis of a plasmid-encoded, host genotype-specific enhancement of bacterial fitness. *J Bacteriol* **176**, 3140–3147 (1994).
3. Andersson, D. I. & Hughes, D. Antibiotic resistance and its cost: is it possible to reverse resistance? *Nat Rev Micro* **8**, 260–271 (2010).
4. De Gelder, L. *et al.* Combining mathematical models and statistical methods to understand and predict the dynamics of antibiotic-sensitive mutants in a population of resistant bacteria during experimental evolution. *Genetics* **168**, 1131–1144 (2004).

5. Sjölund, M., Wreiber, K., Andersson, D. I., Blaser, M. J. & Engstrand, L. Long-term persistence of resistant *Enterococcus* species after antibiotics to eradicate *Helicobacter pylori*. *Ann. Intern. Med.* **139**, 483–487 (2003).
6. Sjölund, M., Tano, E., Blaser, M. J., Andersson, D. I. & Engstrand, L. Persistence of resistant *Staphylococcus epidermidis* after single course of clarithromycin. *Emerg Infect Dis* **11**, 1389–1393 (2005).
7. Imamovic, L. & Sommer, M. O. A. Use of collateral sensitivity networks to design drug cycling protocols that avoid resistance development. *Sci Transl Med* **5**, 204ra132 (2013).
8. Szybalski, W. & Bryson, V. Genetic studies on microbial cross resistance to toxic agents. I. Cross resistance of *Escherichia coli* to fifteen antibiotics. *J Bacteriol* **64**, 489–499 (1952).
9. Lázár, V. *et al.* Bacterial evolution of antibiotic hypersensitivity. *Mol Syst Biol* **9**, 700 (2013).
10. Hiramatsu, K. *et al.* Curing bacteria of antibiotic resistance: reverse antibiotics, a novel class of antibiotics in nature. *Int J Antimicrob Ag* **39**, 478–485 (2012).
11. Szybalski, W. Genetic studies on microbial cross resistance to toxic agents. IV. Cross resistance of *Bacillus megaterium* to forty-four antimicrobial drugs. *Appl Microbiol* **2**, 57–63 (1954).
12. Chao, L. An unusual interaction between the target of nalidixic acid and novobiocin. *Nature* **271**, 385–386 (1978).
13. Lukens, A. K. *et al.* Harnessing evolutionary fitness in *Plasmodium falciparum* for drug discovery and suppressing resistance. *Proc Natl Acad Sci USA* **111**, 799–804 (2014).
14. Blair, J. M. A., Webber, M. A., Baylay, A. J., Ogbolu, D. O. & Piddock, L. J. V. Molecular mechanisms of antibiotic resistance. *Nat Rev Micro* **13**, 42–51 (2015).
15. Wright, G. D. Molecular mechanisms of antibiotic resistance. *Chemical Communications* **47**, 4055 (2011).
16. Bochner, B., Huang, H., Schieven, G. & Ames, B. Positive selection for loss of tetracycline resistance. *J Bacteriol* **143**, 926 (1980).
17. Podolsky, T., Fong, S. T. & Lee, B. T. Direct selection of tetracycline-sensitive *Escherichia coli* cells using nickel salts. *Plasmid* **36**, 112–115 (1996).
18. Merlin, T. L., Corvo, D. L., Gill, J. H. & Griffith, J. K. Enhanced gentamicin killing of *Escherichia coli* by tet gene expression. *Antimicrob Agents Chemother* **33**, 230–232 (1989).
19. Griffith, J. K., Kogoma, T., Corvo, D. L., Anderson, W. L. & Kazim, A. L. An N-terminal

- domain of the tetracycline resistance protein increases susceptibility to aminoglycosides and complements potassium uptake defects in *Escherichia coli*. *J Bacteriol* **170**, 598–604 (1988).
20. Merlin, T. L., Davis, G. E. & Anderson, W. L. Aminoglycoside uptake increased by tet gene expression. *Antimicrob Agents Chemother* **33**, 1549–1552 (1989).
  21. Chait, R., Shrestha, S., Shah, A. K., Michel, J.-B. & Kishony, R. A differential drug screen for compounds that select against antibiotic resistance. *PLoS ONE* **5**, e15179 (2010).
  22. Chopra, I. & Roberts, M. Tetracycline antibiotics: mode of action, applications, molecular biology, and epidemiology of bacterial resistance. *Microbiol Mol Biol R* **65**, 232 (2001).
  23. Wang, H. & Ng, T. B. Pharmacological activities of fusaric acid (5-butylpicolinic acid). *Life Sci.* **65**, 849–856 (1999).
  24. Ejim, L. *et al.* Combinations of antibiotics and nonantibiotic drugs enhance antimicrobial efficacy. *Nat Chem Biol* **7**, 348–350 (2011).
  25. Anderson, A. B. & Sherrard, E. C. Dehydroperillic Acid, an Acid from Western Red Cedar (*Thuja Plicata* Don) 2. *J Am Chem Soc* **55**, 3813–3819 (1933).
  26. Phillips, M., Malloy, G., Nedunchezian, D., Lukrec, A. & Howard, R. G. Disulfiram inhibits the in vitro growth of methicillin-resistant *Staphylococcus aureus*. *Antimicrob Agents Chemother* **35**, 785–787 (1991).
  27. Alekshun, M. N. & Levy, S. B. Molecular mechanisms of antibacterial multidrug resistance. *Cell* **128**, 1037–1050 (2007).
  28. Meyer, B. J., Maurer, R. & Ptashne, M. Gene regulation at the right operator (OR) of bacteriophage lambda. II. OR1, OR2, and OR3: their roles in mediating the effects of repressor and cro. *J Mol Biol* **139**, 163–194 (1980).
  29. Lutz, R. & Bujard, H. Independent and tight regulation of transcriptional units in *Escherichia coli* via the LacR/O, the TetR/O and AraC/I1-I2 regulatory elements. *Nucleic acids research* **25**, 1203 (1997).
  30. Singer, M. *et al.* A collection of strains containing genetically linked alternating antibiotic resistance elements for genetic mapping of *Escherichia coli*. *Microbiol Mol Biol R* **53**, 1 (1989).
  31. Casadaban, M. J. Transposition and fusion of the lac genes to selected promoters in *Escherichia coli* using bacteriophage lambda and Mu. *J Mol Biol* **104**, 541–555 (1976).
  32. Chait, R., Craney, A. & Kishony, R. Antibiotic interactions that select against resistance. *Nature* **446**, 668–671 (2007).



33. Baym, M., Kryazhimskiy, S., Lieberman, T. D. & Chung, H. Inexpensive Multiplexed Library Preparation for Megabase-Sized Genomes. *bioRxiv* (2015). doi:10.1101/013771
34. Martin, M. Cutadapt removes adapter sequences from high-throughput sequencing reads. *EMBnet.Journal* **17**, 10–11 (2011).
35. Langmead, B. & Salzberg, S. L. Fast gapped-read alignment with Bowtie 2. *Nat Chem Biol* **9**, 357–359 (2012).
36. Li, H. *et al.* The Sequence Alignment/Map format and SAMtools. *Bioinformatics* **25**, 2078–2079 (2009).
37. Albers, C. A. *et al.* Dindel: Accurate indel calls from short-read data. *Genome Research* **21**, 961–973 (2011).
38. Keane, T. M., Wong, K. & Adams, D. J. RetroSeq: transposable element discovery from next-generation sequencing data. *Bioinformatics* **29**, 389–390 (2013).

## **Chapter 3: A hybrid antibiotic restricts evolutionary paths to resistance by evading activation of the multiple antibiotic resistance operon<sup>1</sup>**

Hybrid drugs are a promising strategy to address the growing problem of drug resistance, but the mechanism by which they modulate the evolution of resistance is poorly understood. Integrating high-throughput resistance measurements and genomic sequencing, we compared *Escherichia coli* evolved in a hybrid antibiotic that links ciprofloxacin and neomycin to *E. coli* evolved in combinations of the component drugs. We find that populations evolved in the hybrid gain less resistance than those evolved in the equivalent mixture of the hybrid's components because the hybrid evades resistance mediated by the multiple antibiotic resistance (*mar*) operon. Furthermore, we establish that the ciprofloxacin moiety of the hybrid inhibits bacterial growth while the neomycin moiety diminishes the effectiveness of *mar* activation. Together, comparative investigation of the phenotypic and genotypic paths to resistance can help pinpoint unique properties of new compounds that limit the emergence of resistance.

---

<sup>1</sup> This collaborative work has been submitted for publication. The authors are Kathy K. Wang, Laura K. Stone, Tami D. Lieberman, Michal Shavit, Timor Baasov, Roy Kishony.

## Introduction

Drug resistance is a growing problem in cancer and infectious disease<sup>1,2</sup>. Prolonged use of chemotherapeutic agents inevitably selects for resistance in the target organisms, reducing drug efficacy. Most anticancer and antimicrobial drugs target a single essential process, allowing resistance to rapidly emerge by spontaneous mutations or horizontal transfer of resistance genes<sup>1,3</sup>.

Drug combinations have long been employed to slow down the evolution of resistance. Drugs with different mechanisms of action often require different resistance mutations, such that the probability of any cell simultaneously gaining resistance to both drugs is extremely low<sup>4,5</sup>. Furthermore, when combinations are used, synergistic or antagonistic drug interactions can alter the evolution of resistance<sup>5,6</sup>. In addition, the evolution of resistance to drug combinations can be slowed if a mutation that confers resistance to one drug increases sensitivity to another drug<sup>7-11</sup>.

Another intriguing possibility is that chemically linking two drugs into a single hybrid molecule can incorporate the properties of both compounds and attack the target cell via two modes of action<sup>12-14</sup>. This dual-action strategy could be used to ensure simultaneous delivery of two drugs to the target cells, improve pharmacokinetic and pharmacodynamic properties<sup>15</sup>, avoid toxicity<sup>16</sup>, lead to better uptake<sup>17</sup>, and increase retention<sup>18,19</sup>. Furthermore, these hybrid compounds often surpass their component drugs, either alone or in combination, by maintaining their activity against cells that are resistant to one or both of the component drugs<sup>19-24</sup>, and can even decrease the frequency of resistant mutants<sup>19,24</sup>.

However, it is unclear how hybrid compounds affect resistance acquisition<sup>25</sup>. Indeed, some hybrid antibiotics select for high levels of resistance<sup>22,26</sup>. In cases where resistance is impeded, the hybrid's ability to stave off resistance may result from a range of mechanisms,

including increased target affinity, drug interactions or collateral sensitivity between its components, a new mode of action, or the ability to escape efflux or degradation.

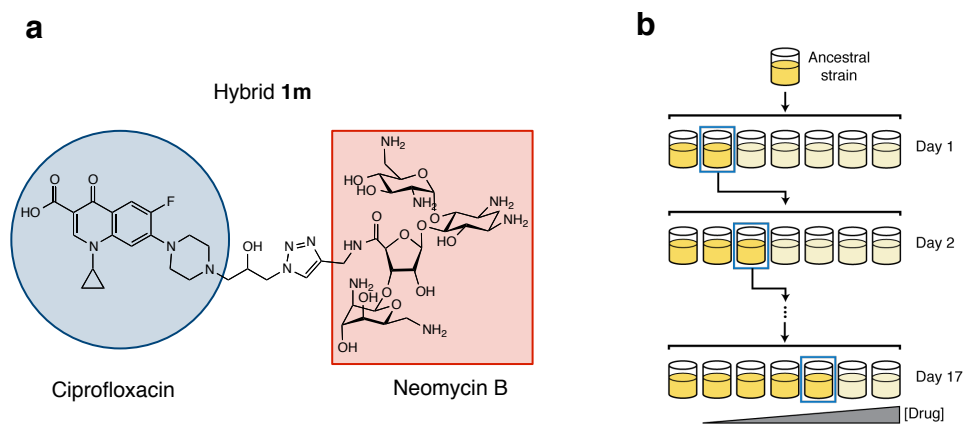
Here, we focus on a hybrid that links two commonly used antibiotics, ciprofloxacin (Cpr) and neomycin B (NeoB). A Cpr-NeoB hybrid may take advantage of a dual mode of action<sup>24</sup>. Cpr is a fluoroquinolone that inhibits DNA replication by binding to DNA gyrase and topoisomerase IV<sup>27,28</sup>. NeoB is an aminoglycoside that inhibits protein translation by binding to the 30S ribosomal subunit<sup>29</sup>. Hybrid compounds of these two antibiotics were shown to have increased *in vitro* affinity to Cpr targets, with slightly reduced *in vitro* activity on the NeoB target<sup>24</sup>. These Cpr-NeoB hybrids were able to overcome resistance by both horizontally transferred mechanisms, such as modification by plasmid-born neomycin resistance genes, and vertical evolution<sup>24</sup>.

To understand the way and extent to which these Cpr-NeoB hybrid compounds limit the evolution of resistance, we followed the phenotypic and genotypic evolution of resistance to a hybrid and to combinations of its component antibiotics. We measured the cross-resistance of experimentally evolved strains and used genomic sequencing to identify adaptive mutations in each condition. Comparing these data across different drug conditions, we identified genotypic constraints that limit resistance to the hybrid antibiotic.

## Results




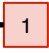

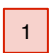


*Escherichia coli* evolve less resistance to the hybrid antibiotic than to an equimolar mixture of its components.

We measured how *E. coli* K-12 MG1655 evolve resistance to the **1m** hybrid (**Fig. 3.1a**)<sup>24</sup> compared to four combinations of its parent antibiotics, Cpr and NeoB (**Table 3.1**). *E. coli* were



**Figure 3.1. Assessing resistance to antibiotic hybrid 1m.** (a) Hybrid compound **1m** chemically links two antibiotics, ciprofloxacin and neomycin B. (b) Schematic of the serial passage selection procedure for a single population. Darker yellow culture color indicates higher bacterial density. In total, 50 parallel populations were evolved in 5 drug selection conditions, and 4 parallel populations were evolved in no drug, over 17 days. The populations were evolved in 2-fold dilution series of compound(s). For each population, the well growing at the highest concentration of drug was propagated daily into fresh drug. On each day of passage, the drug concentration range was adjusted such that the highest concentration was at least 8x the greatest minimum inhibitory concentration (MIC) across all populations in that drug.

**Table 3.1. Initial and final minimum inhibitory concentrations (MICs) in each of five antibiotic treatments.**

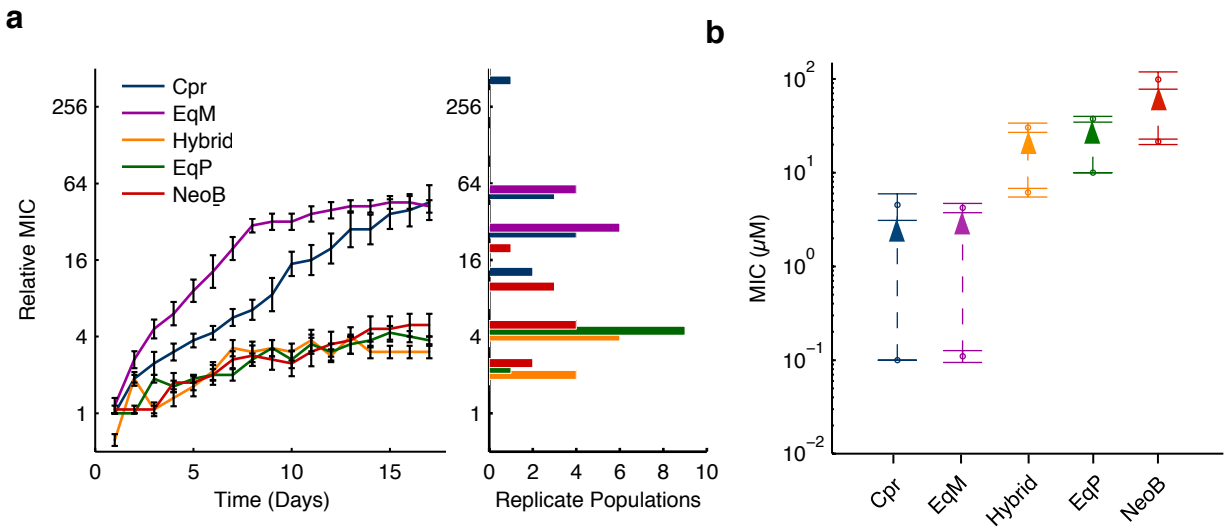
	Antibiotic(s)	Day 1 MIC ( $\mu\text{M}$ )	Day 17 MIC ( $\mu\text{M}$ )	Fold MIC Increase (Day 17/Day 1)
	Ciprofloxacin (Cpr)	$0.1 \pm 0.0$	$4.5 \pm 1.4$	$45.3 \pm 14.2$
	Neomycin B (NeoB)	$21.4 \pm 1.5$	$98.5 \pm 20.5$	$4.6 \pm 1.0$
 	Hybrid	$6.2 \pm 0.7$	$30.3 \pm 3.4$	$4.9 \pm 0.7$
 	Cpr: NeoB = 1:1 Molar (EqM)	$0.11 \pm 0.02 \mu\text{M}$	$4.2 \pm 0.48$	$36.8 \pm 5.1$
 	Cpr:NeoB = $\text{MIC}_{\text{Cpr}}:\text{MIC}_{\text{NeoB}}$ (EqP)	$0.05:10 \pm 0.0:0.0$	$0.19:37.3 \pm 0.01:2.6$	$3.7 \pm 0.3$

The table lists, for each antibiotic selection condition, the average MIC values of the ancestral strain (Day 1 MIC) and evolved strains (Day 17 MIC), and the fold increase in MIC  $\pm$  standard error of the mean. Day 1 and 17 MICs are averages of the ten populations evolved in parallel. The five drug selection conditions are ciprofloxacin only (Cpr, blue circle), neomycin B only (NeoB, red square), the hybrid compound, Cpr and NeoB mixed in a 1:1 M ratio, and Cpr and NeoB mixed in a ratio proportional to their initial MICs ( $\text{MIC}_{\text{Cpr}}:\text{MIC}_{\text{NeoB}}$ ). The  $\text{MIC}_{\text{Cpr}}:\text{MIC}_{\text{NeoB}}$  mixture is intended to compensate for the dissimilar MICs of Cpr and NeoB and maintain selective pressure on bacteria to develop resistance to both compounds.

evolved in Cpr and NeoB individually and in two different mixtures. The equimolar (EqM) mixture contains Cpr and NeoB in the same ratio as the hybrid: one molecule of Cpr per molecule of NeoB (**Table 3.1**). The equipotent (EqP) mixture compensates for the different potencies of Cpr and NeoB by mixing them in a ratio proportional to their minimal inhibitory concentrations (MICs), thus applying selective pressure on both drugs' targets simultaneously (**Table 3.1**). The equipotent ratio is based on the MICs of the ancestral strain and is kept constant for the duration of the experiment (**Fig. S2.1**). To account for the stochasticity of the evolutionary process, 10 replicate, parallel populations of *E. coli* were evolved in each of the five drug selection conditions. All populations were evolved through 17 days of serial selection in twofold dilution series of drug, passaging from the highest drug concentration allowing growth (**Fig. 3.1b, Fig. S2.2, Methods**).

Assuming that chemically linking Cpr and NeoB does not change their individual activities and the spectrum of resistance mutations, resistance to the hybrid and to the EqM mixture should evolve similarly because both conditions contain one molecule of Cpr per molecule of NeoB. Furthermore, under this assumption, evolution in the hybrid and the EqM should be similar to evolution in Cpr alone. The initial MIC of Cpr is ~200 times less than that of NeoB (**Table 3.1, Fig. S2.1**), making it the vastly more potent of the two components and the main evolutionary pressure.

Despite this expectation, strains evolved in the hybrid gained much less resistance than strains evolved in the EqM mixture and strains evolved in Cpr. On average, populations evolved in Cpr or the EqM mixture developed a 40-fold increase in resistance (**Fig. 3.2a**). However, strains evolved in the hybrid averaged only a 4.6-fold increase in resistance (**Table 3.1, Fig. 3.2a**). In fact, selection in the hybrid resulted in a rate and level of MIC increase resembling



**Figure 3.2. Evolution of resistance to hybrid compound follows a different trajectory than an equimolar mixture of components. (a)** Mean resistance trajectories. Populations were evolved in each of five drug conditions and serially passaged daily for 17 days. Each line indicates average minimum inhibitory concentration (MIC: highest drug concentration where  $\text{OD}_{600} < 0.2$ ) of 10 replicate populations relative to the ancestral control strain on the same plate. Error bars indicate standard error. The histogram at right shows the distribution of day 17 MICs. **(b)** Increase (arrow) in absolute MIC between day 1 (start point) and day 17 (end point) of the evolution experiment. Error bars indicate standard error.

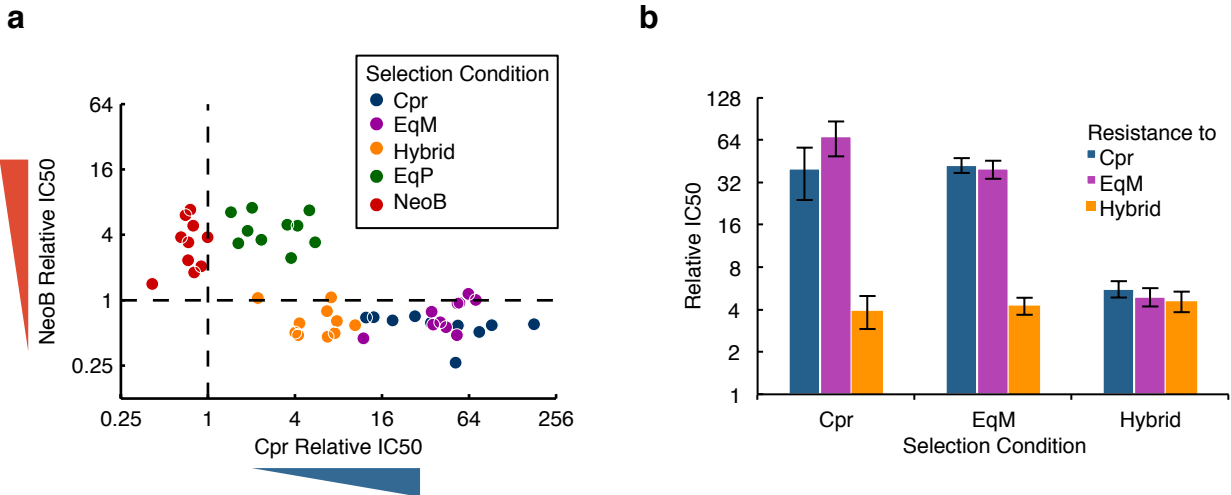


selection in NeoB and the EqP mixture (**Fig. 3.2**). This could be explained by the hybrid unexpectedly acting through its NeoB moiety, or acting through its Cpr moiety but avoiding a specific resistance mechanism.

***Phenotypic cross-resistances of evolved strains suggest that the hybrid primarily inhibits Cpr targets***

To understand the basis of this diminished resistance, we tested the cross-resistance phenotypes of all evolved strains to all selection conditions (**Fig. S2.3**) and found evidence that the hybrid restricts growth primarily through its Cpr moiety. Firstly, all strains evolved in the hybrid gained Cpr resistance (2.2-10 fold), suggesting that the hybrid's Cpr moiety may drive the evolution of hybrid resistance (**Fig. 3.3a**). Secondly, the strains evolved in the hybrid are not NeoB resistant, but actually show increased sensitivity to NeoB (**Fig. 3.3a**). This could imply that the NeoB moiety does not place sufficient pressure on the cell to select for resistance, or it could mean that NeoB resistance mutations are incompatible with Cpr resistance mutations. Contrary to the latter hypothesis, the populations evolved in the EqP mixture gain both Cpr and NeoB resistance (**Fig. 3.3a**), proving that it is possible to evolve resistance to both drugs. Therefore, the Cpr moiety appears to be responsible for the hybrid's inhibitory effect, while the antibacterial contribution of its NeoB moiety is negligible.

While the hybrid acts primarily through its Cpr moiety, the hybrid-evolved strains do not gain as much Cpr resistance as the Cpr-evolved strains (**Fig. 3.3b**). Cpr-evolved strains developed a 7.4-fold higher increase in Cpr resistance than hybrid-evolved strains, suggesting that strains evolved in the hybrid do not access all Cpr resistance mutations (**Fig. 3.3b**). Furthermore, high Cpr resistance does not translate into high hybrid resistance; strains evolved in Cpr gain only as much hybrid resistance as strains evolved in the hybrid (**Fig. 3.3b, Fig. S2.3**),



**Figure 3.3. Selection for resistance to hybrid 1m and molar mixture is driven by the ciprofloxacin component.** (a)  $\log_2$  ciprofloxacin and neomycin B  $IC_{50}$ s of day 17 isolates relative to the ancestral strain. Each point represents a single isolate from one evolved population. Isolates were evolved in Cpr (blue); NeoB (red); equipmolar (EqM) mixture (purple); equipotent (EqP) mixture (green); hybrid compound (orange). (b) Mean Cpr and hybrid resistance ( $IC_{50}$  relative to the ancestral strain) of isolates selected in Cpr and the hybrid. Bars represent averages of 10 single colonies, one picked from each final evolved population. Error bars indicate standard error. (c) Mean EqM and hybrid resistance (relative  $IC_{50}$ ) of isolates selected in EqM and the hybrid. Bars represent averages of 10 single colonies, one picked from each final evolved population. Error bars indicate standard error.

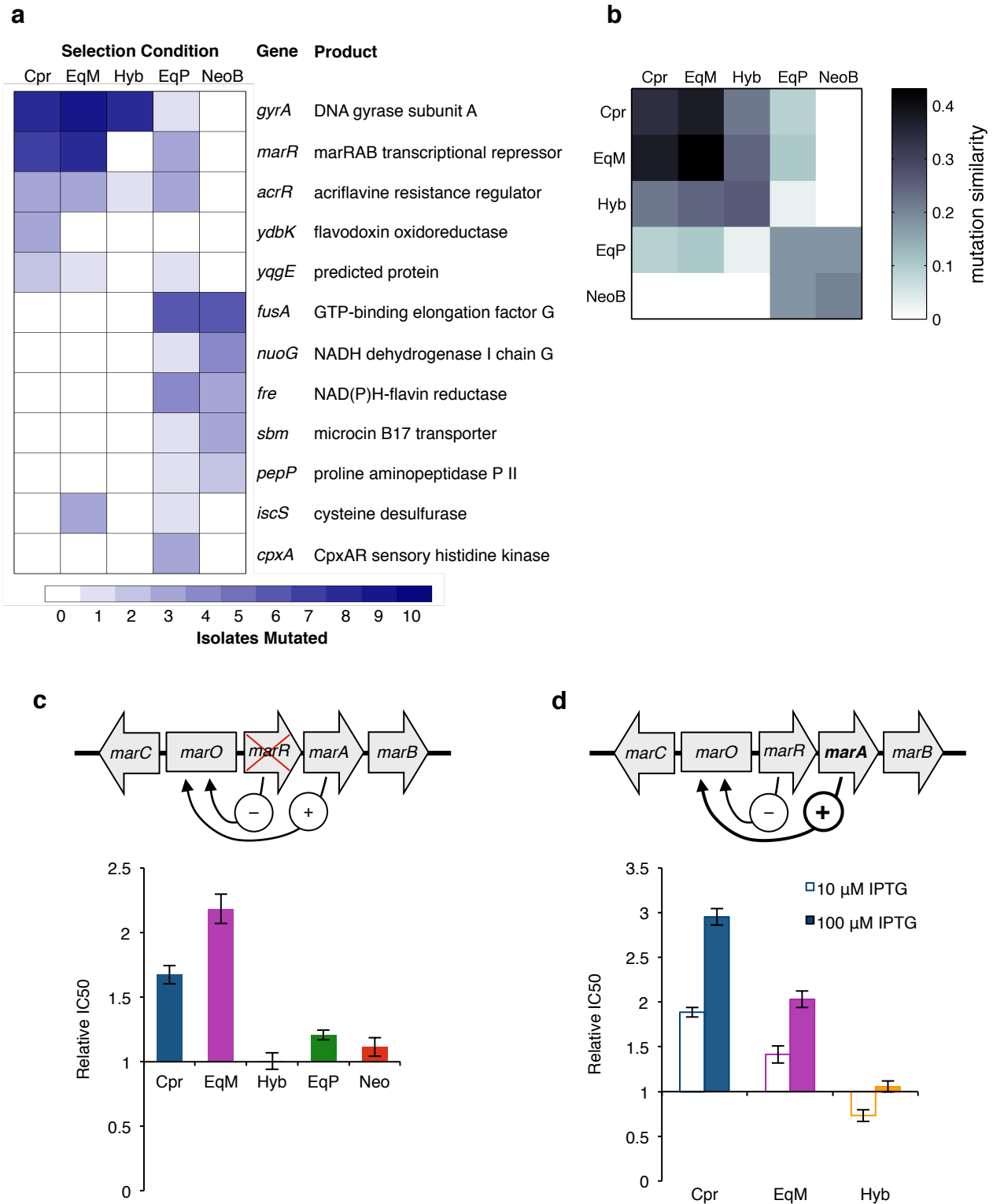
suggesting that only a subset of the Cpr resistance mutations provides resistance to the hybrid. The EqM-evolved strains match the phenotype of the Cpr-evolved strains: an 8.1-fold higher increase in resistance to the EqM mixture arose in EqM-evolved strains compared to hybrid-evolved strains (**Fig. 3.3b**, **Fig. S2.3**). This shows that the mere presence of NeoB does not limit Cpr resistance. Only when NeoB is linked to Cpr, as in the hybrid, is an EqM ratio of Cpr and NeoB able to limit resistance.

### ***Genotypic data reveals constraints on the evolution of resistance to the hybrid***

To identify the resistance mutations and understand the constraints on evolution to the hybrid, we sequenced the whole genomes of isolates from all 50 evolved populations, as well as the ancestral strain and 4 isolates from populations passaged without drug selection. We identified single-nucleotide polymorphisms (SNPs) and small insertions and deletions (indels) that differed from the wild-type *E. coli* MG1655 genome and were not present in the no-drug controls (**Methods**). A total of 219 mutations were identified in 104 unique genes (**Table S2.1**). Mutations displayed strong parallelism, with 51% of mutations present in genes that were mutated in at least 3 different populations (**Fig. 3.4a**).

The mutational profiles mimicked the phenotypic results, with isolates evolved in the hybrid having mutation profiles similar to those evolved in Cpr and different from those evolved in NeoB. The gene *gyrA*, which encodes the Cpr target DNA gyrase, was mutated in 9 out of 10 parallel populations evolved in Cpr, all 10 populations evolved in the EqM mixture, and in 9 out of 10 populations evolved in the hybrid (**Fig. 3.4a**). In contrast, *fusA*, which encodes the ribosomal translocase elongation factor G, was mutated in 7 out of 10 parallel NeoB-evolved populations, but was not mutated in any of the hybrid-evolved populations (**Fig. 3.4a**). In line

**Figure 3.4. The hybrid antibiotic limits evolution of resistance by restricting the effect of *marR* mutations.** (a) Resistance mutations found by genomic sequencing of single colonies, grouped by each antibiotic selection condition. Genes mutated in at least three independent isolates are included. Colors indicate the total number of mutated isolates in each selection condition. Selection conditions are: Cpr, equimolar mixture (EqM), hybrid **1m** (Hyb), equipotent mixture (EqP), and NeoB. (b) Similarity of mutated genes, assessed by mean fraction of total mutated genes shared between any two of fifty random mutants from either the same or different selection condition. (c) Relative IC<sub>50</sub> of *E. coli* BW25113  $\Delta marR$  compared to wild-type BW25113. Schematic represents regulation of *marRAB* operon, with *marR* deletion indicated. (d) Relative IC<sub>50</sub>s of *E. coli* BW25113 transformed with ASKA *marA* overexpression vector compared to *E. coli* BW25113 transformed with control vector. Expression was induced with 10  $\mu$ M or 100  $\mu$ M IPTG. Error bars indicate standard error.



**Figure 3.4 (Continued).** The hybrid antibiotic limits evolution of resistance by restricting the effect of *marR* mutations.

with these results, group analysis across all mutated genes showed that hybrid-selected populations are similar to Cpr-selected populations and distinct from NeoB-selected populations (**Fig. 3.4b**). In total, this data suggests that both the hybrid compound and the EqM mixture mainly inhibit cell growth through the Cpr component.

### ***Absence of marR mutations limits resistance to the hybrid antibiotic***

Surprisingly, mutations in one gene, *marR*, arise from selection in the EqM mixture and Cpr, but not in the hybrid antibiotic. The *marR* transcriptional repressor is the negative regulator of the *marRAB* operon, which controls the multiple antibiotic resistance (Mar) phenotype (**Fig. 3.34c**). Mutations in *marR* arose in 8 out of 10 isolates evolved in Cpr and in 9 out of 10 isolates evolved in the EqM mixture (**Fig. 3.4a**). However, no *marR* mutations arose in any hybrid-evolved strains (**Fig. 3.4a**). Given this mutational pattern, we hypothesized that *marR* is responsible for the disparity in phenotypic cross-resistance between the hybrid and Cpr.

To investigate whether *marR* mutations confer resistance to the hybrid, we compared the activities of the hybrid, Cpr, the EqM mixture, and NeoB against a *marR* knockout and wild-type *E. coli*. As expected from the genomic data, the *marR* knockout was 1.7-fold more resistant to Cpr and 2.2-fold more resistant to the EqM mixture (**Fig. 3.4c**). However, this mutant was not resistant to the hybrid (**Fig. 3.4c**). Therefore, inactivating mutations in *marR* confer resistance specifically to Cpr and the EqM mixture but not to the hybrid. Differences in resistance conferred by *marR* deletion account for 16% of discrepancy in resistance between hybrid-evolved strains and Cpr-evolved strains (**Fig. 3.3b, 3.4c**), and 23% of the discrepancy between hybrid and EqM-evolved strains (**Fig. 3.3c, 3.4c**). Overexpression of *marA* also confers resistance to Cpr and the EqM mixture in a dose-dependent manner, but has no effect of

resistance to the hybrid (**Fig. 3.4d**). Thus, the inability of the *mar* phenotype to confer resistance to the hybrid explains why the hybrid selected for less resistance in the evolution experiment, compared to Cpr and the EqM mixture. We hypothesize that the hybrid drug evades *marRAB*-regulated drug efflux, a major mode of multidrug resistance, thereby greatly restricting the paths to resistance.

## Discussion

Using a combination of experimental evolution, cross-resistance profiling, and genomic sequencing, we show that linking antibiotics can produce unexpected properties. The **1m** hybrid inhibits bacterial growth through its Cpr moiety and limits resistance through its NeoB moiety. Our results suggest that the hybrid drug binds effectively to the well-known Cpr target, *gyrA*, as bacteria evolved resistance to the hybrid primarily through mutations in this gene. The absence of *marR* mutations in hybrid- and NeoB-evolved strains suggests that the NeoB component is limiting efflux-mediated resistance to the hybrid.

MarR is a repressor of the *marRAB* operon that regulates the AcrAB-TolC efflux system, outer membrane porins such as OmpF, and other genes that modulate susceptibility to multiple antibiotics<sup>30-32</sup>. Mutations in *marR* are known to increase resistance to a broad spectrum of antibiotics, including fluoroquinolones (such as Cpr),  $\beta$ -lactams, tetracycline, and chloramphenicol<sup>33,34</sup>. However, aminoglycosides such as NeoB are highly hydrophilic and cannot be exported through the AcrAB-TolC efflux system upregulated by *marR* mutations<sup>35,36</sup>. Therefore, the NeoB component could limit *marR*-mediated efflux of the hybrid, thereby removing *marR* as a path to hybrid resistance.

To the best of our knowledge, the **1m** Cpr-NeoB hybrid antibiotic studied here is the first quinolone that can evade resistance mediated by the multiple antibiotic resistance (*mar*) operon. Furthermore, this Cpr-NeoB hybrid series has higher *in vitro* affinity to the quinolone targets, DNA gyrase and topoisomerase IV, than Cpr itself<sup>24</sup>. However, the **1m** Cpr-NeoB hybrid has inferior whole-cell activity compared to Cpr (**Table 3.1**), suggesting poor permeability. The size and hydrophilicity of the NeoB moiety may be responsible for both the hybrid's poor penetration and its ability to evade the *mar* pathway. Since the hybrid's antibacterial activity does not rely on NeoB binding to the ribosome, it is likely that the NeoB moiety may be substituted with chemically similar groups or substructures of NeoB to find a compromise between increasing import and evading the *mar* pathway.

These results can inform the future design of hybrid compounds that aim to prevent the emergence of multidrug resistance. Hybrids can have properties beyond those of its individual components, and important functions other than binding canonical drug targets. Therefore, even when the two component drugs of a hybrid have dissimilar molar MICs, combining the drugs can have a beneficial effect. In this case, a potent antibiotic whose efficacy is eventually limited by efflux-mediated resistance is linked to a less potent antibiotic that prevents efflux, resulting in a compound that combines the benefits of the first component's mechanism and the second component's restriction on resistance. Future hybrid compounds could be developed according to this principle to limit the emergence of multidrug resistance in cancer and infectious disease.

The approach developed here represents a general way to evaluate new hybrid compounds for function and resistance evolution potential. By comparing the mutational pathways between a hybrid compound and its components, we can tease apart each moiety's contribution to efficacy and resistance. We anticipate this comparative approach may be useful



not only for hybrid drugs, but also for evaluating analogs of the same chemical scaffold.

Assessing the mutational paths that a compound prevents—not just those taken—is a powerful tool for understanding, predicting, and manipulating the evolution of resistance.

## Methods

### Strains

*Escherichia coli* K-12 MG1655, a gram-negative laboratory strain with minimal genetic manipulation and no plasmids, was used as the ancestral strain during experimental evolution<sup>37</sup>. A single colony of *E. coli* MG1655 was picked and grown overnight to saturation at 37°C with shaking at 225 rpm. Aliquots of the ancestral strain were stored at -80°C in 16.7% glycerol and were used to initiate the evolution experiment and to serve as ancestral controls (1/500 dilution). The  $\Delta marR$  strain was generated by using pCP20-delivered FLP recombinase<sup>38</sup> to remove *kanR* from the  $\Delta marR::kanR$  strain (JW5248) of the *E. coli* BW25113 Keio collection<sup>39</sup>. The *marA* overexpression strain was generated by transformation of the ASKA ORF library *marA* vector into *E. coli* BW25113<sup>40</sup>.

### Drug conditions

Stocks of antibiotics Cpr only, NeoB only, the equimolar (EqM) mixture, and the equipotent (EqP) MIC<sub>Cpr</sub>:MIC<sub>NeoB</sub> mixture were prepared in LB media from powder stocks, by two-fold dilution in 25mL of LB, starting at ~512 times their MICs. Stocks were stored at 4°C. Conditions with hybrid were prepared fresh each day, from 2 mg/mL stocks in dH<sub>2</sub>O stored at -20°C, due to limited quantities of the drug.

## **Experimental evolution**

Evolution experiments were conducted in 96-well Corning microtiter plates with a final volume of 150  $\mu$ L per well. Each of the 12 columns contained a 2-fold dilution series of one drug condition. The drug concentration range for the hybrid was adjusted daily such that the highest concentration was at least 8 times the MIC of the most resistant lineage. Minimum inhibitory concentration (MIC) was set as the lowest drug concentration where  $OD_{600} < 0.2$ . Each plate included one column for the ancestral control, and one column with no bacteria as a control for contamination. Each of the remaining 10 columns contained replicate populations of bacteria. Each day, the 600 nm absorbance ( $OD_{600}$ ) of the cultures was measured using the Victor3 Multilabel Plate Counter (PerkinElmer). For each population (each column excluding ancestral controls and blanks), the well with an  $OD_{600}$  above 0.4 at the highest concentration of antibiotic was propagated. An aliquot of each selected well was diluted 1/500 into a new antibiotic gradient plate. Each plate was covered with an AeraSeal (EXCEL) and incubated for 21 hours at 37°C, with shaking at 900 rpm on a Titramax 1000 (Appleton Woods). The remaining population in each selected well was stored at -80°C, in 5% DMSO. Populations were evolved for 17 days. As a control, four ancestral populations of *E. coli* MG1655 were also propagated in 150  $\mu$ L of LB without antibiotic selection.

## **Retrospective phenotyping of evolved strains**

At the end of 17 days of selection, samples from all 54 cultures, one for each final evolved population, were streaked onto LB agar plates and grown overnight at 37°C without antibiotic selection. Single colonies were picked and grown to saturation in 2 mL of LB at 37°C, and then separated into aliquots for either (1) storage at -80°C in 5% DMSO, (2) assessment for resistance to all five drug conditions using the same conditions and plate layout as that used in the

evolution experiment, or (3) genomic DNA extraction. In the retrospective assessment of resistance to all drug conditions, the final OD<sub>600</sub> measurements at each drug concentration were fit to a four-parameter logistic model to find the concentration of 50% inhibition (IC<sub>50</sub>).

### **Genomic sequencing**

A total of 55 single colonies were sequenced: 10 isolates evolved in each of 5 conditions (Cpr only, Neo only, EqM mix, EqP mix, and hybrid), 4 no-selection controls, and 1 ancestral control. Genomic DNA was extracted from 500 µL cultures of each colony using the PureLink Pro 96 Genomic DNA Purification Kit (Invitrogen) according to the supplier's protocol. Purified DNA was quantified using the Quant-iT™ High-Sensitivity DNA Assay Kit (Life Technologies). Sequencing libraries were prepared using the Nextera XT DNA Sample Preparation Kit (Illumina) with 0.2 ng of input DNA. 42 samples were sequenced at Axseq Technologies, Seoul, South Korea, on an Illumina HiSeq 2000, on one lane of a 100 bp paired-end run. The remaining samples were sequenced at the Harvard Medical School Biopolymers Facility, on an Illumina HiSeq 2500, on one lane of a 100 bp paired-end run. Reads were trimmed using Sickle and aligned to the *E. coli* MG1655 reference genome (Genbank accession number U00096.2) with Bowtie2<sup>41</sup>. Over 99.7% of reads aligned to the reference genome, and average coverage across a sample ranged between 5x and 65x (median 32x). SNPs were identified using SAMtools<sup>42</sup> and consensus quality (FQ score) cutoff of less than -55 for inclusion. Each variant position that met this cutoff in at least one strain was investigated in remaining strains, and a best call was made based on the aligned reads. Several co-localized false-SNP calls near a large 15kb deletion were manually discarded. Small insertions and deletions (indels) were called using Dindel<sup>43</sup>. Candidate indels found in one strain were explicitly tested for in all strains; indels with a quality score greater than 20, with at least 30% of reads in the region supporting the indel, and that were

not found in any of the control strains were accepted. Gene names and products not annotated in the Genbank were annotated using UniProt and GeneExpDB.

### **Growth of mutant strains**

Growth of the  $\Delta marR$  strain was compared with growth of wild-type *E. coli* BW25113. Growth of the ASKA *marA* overexpression strain was compared with growth of *E. coli* BW25113 transformed with ASKA/ $\Delta pYFP$  control vector. ASKA vectors were induced with 10  $\mu M$  or 100  $\mu M$  IPTG. Cultures were diluted 1/500 into 150  $\mu L$  final volume of LB with two-fold drug dilutions and incubated at 37°C for 21 hours with shaking at 900 rpm. For each strain, OD<sub>600</sub> measurements at each drug concentration were pooled from three replicates and fit to a four-parameter logistic model to determine the concentration of 50% inhibition (IC50).

### **Contributions**

T.B. and R.K. conceived the study; K.K.W., L.K.S., T.B., and R.K. designed research; M.S. synthesized **1m**; K.K.W. performed experiments; K.K.W. and T.D.L. analyzed genomic data; K.K.W., L.K.S., and R.K. analyzed data; K.K.W., L.K.S., T.D.L. and R.K. wrote the paper.

### **Acknowledgements**

We thank S. Kim and A. Palmer for constructive discussions, H. Chung, M. Baym, and T. Phulchung for technical assistance, and G.C. Lai for comments on the manuscript. This work was supported in part by US National Institutes of Health grant R01 GM081617 (to R.K.), European Research Council FP7 ERC Grant 281891, Hoffman-LaRoche, The Israel Science

Foundation (ISF) grant 1845/14 (to T. B.), and a National Science Foundation Graduate Fellowship (to L.K.S.).

## References

1. Ramos, P. & Bentires-Alj, M. Mechanism-based cancer therapy: resistance to therapy, therapy for resistance. *Oncogene* (2014). doi:10.1038/onc.2014.314
2. World Health Organization. Antimicrobial resistance: global report on surveillance. *Bulletin of the World Health Organization* (2014).
3. Walsh, C. *Antibiotics: Actions, Origins, Resistance*. (ASM Press, 2003).
4. Zhanel, G. G., Mayer, M., Laing, N. & Adam, H. J. Mutant prevention concentrations of levofloxacin alone and in combination with azithromycin, ceftazidime, colistin (Polymyxin E), meropenem, piperacillin-tazobactam, and tobramycin against *Pseudomonas aeruginosa*. *Antimicrob Agents Chemother* **50**, 2228–2230 (2006).
5. Michel, J., Yeh, P., Chait, R., Moellering, R. & Kishony, R. Drug interactions modulate the potential for evolution of resistance. *Proc Natl Acad Sci USA* **105**, 14918 (2008).
6. Hegreness, M., Shores, N., Damian, D., Hartl, D. & Kishony, R. Accelerated evolution of resistance in multidrug environments. *Proc Natl Acad Sci USA* **105**, 13977–13981 (2008).
7. Szybalski, W. & Bryson, V. Genetic studies on microbial cross resistance to toxic agents. I. Cross resistance of *Escherichia coli* to fifteen antibiotics. *J Bacteriol* **64**, 489–499 (1952).
8. Lázár, V. *et al.* Bacterial evolution of antibiotic hypersensitivity. *Mol Syst Biol* **9**, 700 (2013).
9. Imamovic, L. & Sommer, M. O. A. Use of collateral sensitivity networks to design drug cycling protocols that avoid resistance development. *Sci Transl Med* **5**, 204ra132 (2013).
10. Kim, S., Lieberman, T. D. & Kishony, R. Alternating antibiotic treatments constrain evolutionary paths to multidrug resistance. *Proc Natl Acad Sci USA* **111**, 14494–14499 (2014).
11. Pluchino, K. M., Hall, M. D., Goldsborough, A. S., Callaghan, R. & Gottesman, M. M. Collateral sensitivity as a strategy against cancer multidrug resistance. *Drug Resist. Updat.* **15**, 98–105 (2012).
12. Barbachyn, M. R. in *Annual reports in medicinal chemistry* **43**, 281–290 (Academic Press,

- 2008).
13. Pokrovskaya, V. & Baasov, T. Dual-acting hybrid antibiotics: a promising strategy to combat bacterial resistance. *Expert Opin. Drug Discov.* **5**, 883–902 (2010).
  14. Fortin, S. & Bérubé, G. Advances in the development of hybrid anticancer drugs. *Expert Opin. Drug Discov.* **8**, 1029–1047 (2013).
  15. Albrecht, H. A. *et al.* Cephalosporin 3'-quinolone esters with a dual mode of action. *J Med Chem* **33**, 77–86 (1990).
  16. Grapsas, I., Lerner, S. A. & Mobashery, S. Conjoint molecules of cephalosporins and aminoglycosides. *Arch. Pharm. (Weinheim)* **334**, 295–301 (2001).
  17. Alovero, F., Nieto, M., Mazzieri, M. R., Then, R. & Manzo, R. H. Mode of action of sulfanilyl fluoroquinolones. *Antimicrob Agents Chemother* **42**, 1495–1498 (1998).
  18. Bremner, J. B. Some approaches to new antibacterial agents. *Pure and applied chemistry* **79**, 2143–2153 (2007).
  19. Robertson, G. T. *et al.* In vitro evaluation of CBR-2092, a novel rifamycin-quinolone hybrid antibiotic: microbiology profiling studies with staphylococci and streptococci. *Antimicrob Agents Chemother* **52**, 2324–2334 (2008).
  20. Hubschwerlen, C., Specklin, J.-L., Sigwalt, C., Schroeder, S. & Locher, H. H. Design, synthesis and biological evaluation of oxazolidinone-quinolone hybrids. *Bioorg Med Chem* **11**, 2313–2319 (2003).
  21. Jones, R. N., Barry, A. L. & Thornsberry, C. Antimicrobial activity of Ro 23-9424, a novel ester-linked codrug of fleroxacin and desacetylcefotaxime. *Antimicrob Agents Chemother* **33**, 944–950 (1989).
  22. Gu, J. W. & Neu, H. C. In vitro activity of Ro 23-9424, a dual-action cephalosporin, compared with activities of other antibiotics. *Antimicrob Agents Chemother* **34**, 189–195 (1990).
  23. Bremner, J. B., Ambrus, J. I. & Samosorn, S. Dual action-based approaches to antibacterial agents. *Curr. Med. Chem.* **14**, 1459–1477 (2007).
  24. Pokrovskaya, V., Belakhov, V., Hainrichson, M., Yaron, S. & Baasov, T. Design, synthesis, and evaluation of novel fluoroquinolone-aminoglycoside hybrid antibiotics. *J Med Chem* **52**, 2243–2254 (2009).
  25. Pokrovskaya, V. & Baasov, T. Dual-acting hybrid antibiotics: a promising strategy to combat bacterial resistance. *Expert Opin. Drug Discov.* **5**, 883–902 (2010).
  26. Robertson, G. T. *et al.* In vitro evaluation of CBR-2092, a novel rifamycin-quinolone hybrid antibiotic: studies of the mode of action in *Staphylococcus aureus*. *Antimicrob*

- Agents Chemother* **52**, 2313–2323 (2008).
27. Wolfson, J. S. & Hooper, D. C. The fluoroquinolones: structures, mechanisms of action and resistance, and spectra of activity in vitro. *Antimicrob Agents Chemother* **28**, 581–586 (1985).
  28. Khodursky, A. B., Zechiedrich, E. L. & Cozzarelli, N. R. Topoisomerase IV is a target of quinolones in *Escherichia coli*. *Proc Natl Acad Sci USA* **92**, 11801–11805 (1995).
  29. Fourmy, D., Recht, M. I. & Puglisi, J. D. Binding of neomycin-class aminoglycoside antibiotics to the A-site of 16 S rRNA. *J Mol Biol* **277**, 347–362 (1998).
  30. Cohen, S. P., McMurry, L. M. & Levy, S. B. marA locus causes decreased expression of OmpF porin in multiple-antibiotic-resistant (Mar) mutants of *Escherichia coli*. *J Bacteriol* **170**, 5416–5422 (1988).
  31. Okusu, H., Ma, D. & Nikaido, H. AcrAB efflux pump plays a major role in the antibiotic resistance phenotype of *Escherichia coli* multiple-antibiotic-resistance (Mar) mutants. *J Bacteriol* **178**, 306–308 (1996).
  32. Alekshun, M. N. & Levy, S. B. The mar regulon: multiple resistance to antibiotics and other toxic chemicals. *Trends Microbiol* **7**, 410–413 (1999).
  33. Maneewannakul, K. & Levy, S. B. Identification for mar mutants among quinolone-resistant clinical isolates of *Escherichia coli*. *Antimicrob Agents Chemother* **40**, 1695–1698 (1996).
  34. Alekshun, M. N. & Levy, S. B. Regulation of chromosomally mediated multiple antibiotic resistance: the mar regulon. *Antimicrob Agents Chemother* **41**, 2067–2075 (1997).
  35. Aires, J. R. & Nikaido, H. Aminoglycosides are captured from both periplasm and cytoplasm by the AcrD multidrug efflux transporter of *Escherichia coli*. *J Bacteriol* **187**, 1923–1929 (2005).
  36. Elkins, C. A. & Nikaido, H. Substrate specificity of the RND-type multidrug efflux pumps AcrB and AcrD of *Escherichia coli* is determined predominately by two large periplasmic loops. *J Bacteriol* **184**, 6490–6498 (2002).
  37. Blattner, F. R., Plunkett, G., Bloch, C. A., Perna, N. T. & Burland, V. The complete genome sequence of *Escherichia coli* K-12. *Science* **277**, 1453–1462 (1997).
  38. Datsenko, K. A. & Wanner, B. L. One-step inactivation of chromosomal genes in *Escherichia coli* K-12 using PCR products. *Proc Natl Acad Sci USA* **97**, 6640–6645 (2000).
  39. Baba, T. *et al.* Construction of *Escherichia coli* K-12 in-frame, single-gene knockout mutants: the Keio collection. *Mol Syst Biol* **2**, (2006).

40. Kitagawa, M. *et al.* Complete set of ORF clones of *Escherichia coli* ASKA library (A Complete Set of E. coli K-12 ORF Archive): Unique Resources for Biological Research. *DNA Research* **12**, 291–299 (2006).
41. Langmead, B. & Salzberg, S. L. Fast gapped-read alignment with Bowtie 2. *Nat Chem Biol* **9**, 357–359 (2012).
42. Li, H. *et al.* The Sequence Alignment/Map format and SAMtools. *Bioinformatics* **25**, 2078–2079 (2009).
43. Albers, C. A. *et al.* Dindel: Accurate indel calls from short-read data. *Genome Research* **21**, 961–973 (2011).



## Chapter 4: Concluding Remarks

Antibiotic resistance is a worldwide public health concern. The work described here builds upon two strategies in the growing arsenal of tools to stave off resistance.

Several recent works have put collateral sensitivity in the spotlight as a potential strategy to reduce the evolution of resistance. This interest combined with the screening platform described here (**Chapter 2**) will lead to the identification of more collateral sensitivity relationships for well-optimized resistance genes and cassettes. This work provides valuable proof of concept that compounds that select against well-optimized resistance genes and cassettes can be found through high-throughput screening. An industrial-sized screen would likely reveal many more compounds that select against resistance mechanisms. Moreover, this methodology can be easily adapted to other organisms and resistance mechanisms. Combining selection-inverting drugs with conventional antibiotics may provide novel antimicrobial treatments that are effective against resistant pathogens, prevent susceptible infections from developing resistance, and potentially even revert resistant bacterial populations back to susceptibility.

Such selection-inverting drugs would be most useful paired with a traditional antibiotic in a two-phase treatment strategy against long-term resistant infections. A long-term infection has a higher probability of developing resistance and would allow time for both treatment phases. This strategy requires monitoring the infection with rapid diagnostics to identify the resistance profile of the pathogen and the resistance mechanism(s) present.

Particularly promising are compounds that select against resistance genes and cassettes present on mobile elements. These mobile elements enable resistance genes to spread quickly to new strains and species. However, because of the genetic instability that allows them to move

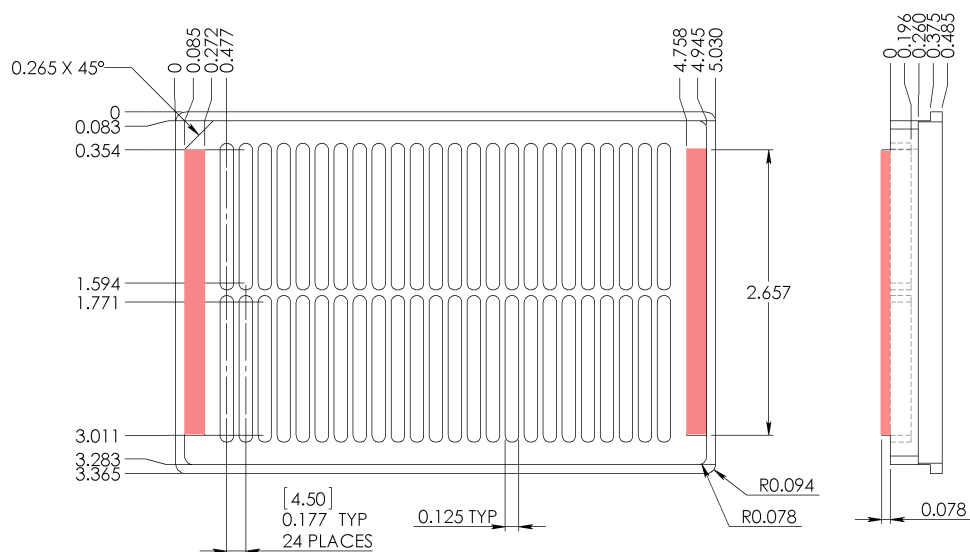
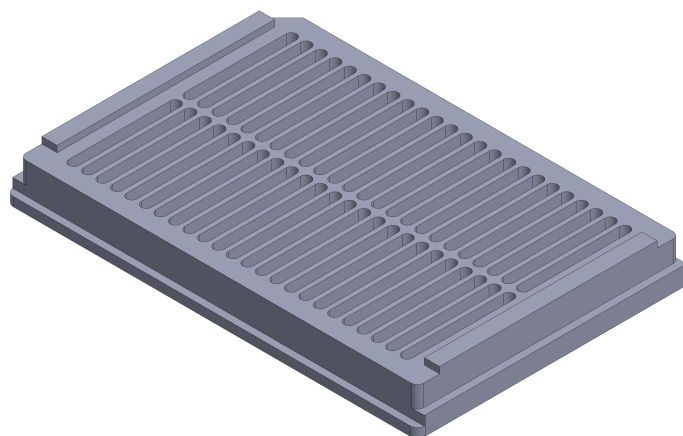
around, the spontaneous loss of a mobile element occurs much more frequently than a SNP resistance mutation. Furthermore, as the most dangerous resistance cassettes contain multiple antibiotic resistance genes, a compound that selects successfully for loss of the mobile element may confer additional susceptibilities. This also implies, however, that a selection-inverting compound may prove less effective if administered at the same time as another drug to which the transposon provides resistance. Additionally, if the resistance mechanism is not on a mobile element, than nullifying mutations in the resistance gene are likely to occur at similar frequencies to SNP resistance mutations elsewhere in the genome, compromising the selection-inverting compound's ability to remove the resistance gene from the population.

More broadly, drugs designed to alter the competition between strains rather than wipe out all bacteria present may be used in a host of settings. For example, selection-inverting compounds could be used to lower agricultural reservoirs of antibiotic resistance. The success of this strategy would likely require the absence of the corresponding antibiotic. In addition to modulating the competition between resistant and sensitive strains, compounds could be used to alter competition to favor symbiotic strains and species over pathogenic ones. For example, a therapy that alters the balance between *Clostridium difficile* and other gut bacteria could be used to encourage recolonization of beneficial species in patients with dysbiosis.

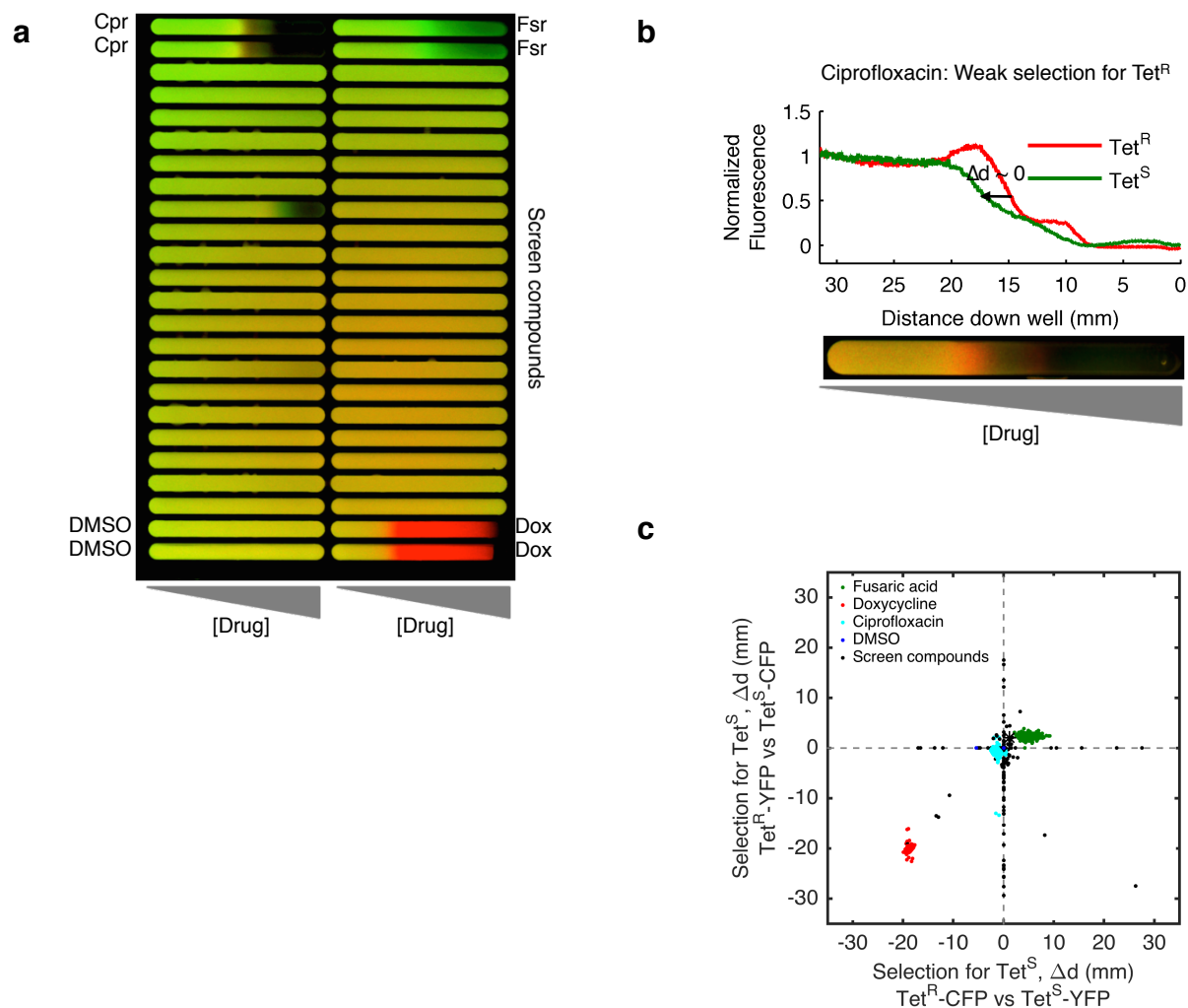
Antibiotic combinations have also received renewed attention for their ability to reduce the evolution of resistance. However, drug pairs with promising *in vitro* properties may fail to deliver results in the clinic due to different pharmacokinetic and pharmacodynamic profiles. Linking the two compounds together into one hybrid molecule can ensure they are absorbed and delivered at equimolar levels across the body, avoiding spatial monotherapy. In addition to creating compounds with two mechanisms of action, hybrids can combine the antibacterial

activity of one component with the resistance evasion of the other to reduce the evolution of resistance compared to an unlinked mixture (**Chapter 3**). In this way, hybrid antibiotics can avoid the canonical resistance mutations of their components and restrict the paths to resistance. Chapter 3 represents the most extensive examination of hybrid compound resistance evolution to date. Applying our comparative phenotypic and genetic approach to hybrids composed of different antibiotic classes will help determine if other drug combinations can similarly limit resistance when linked.

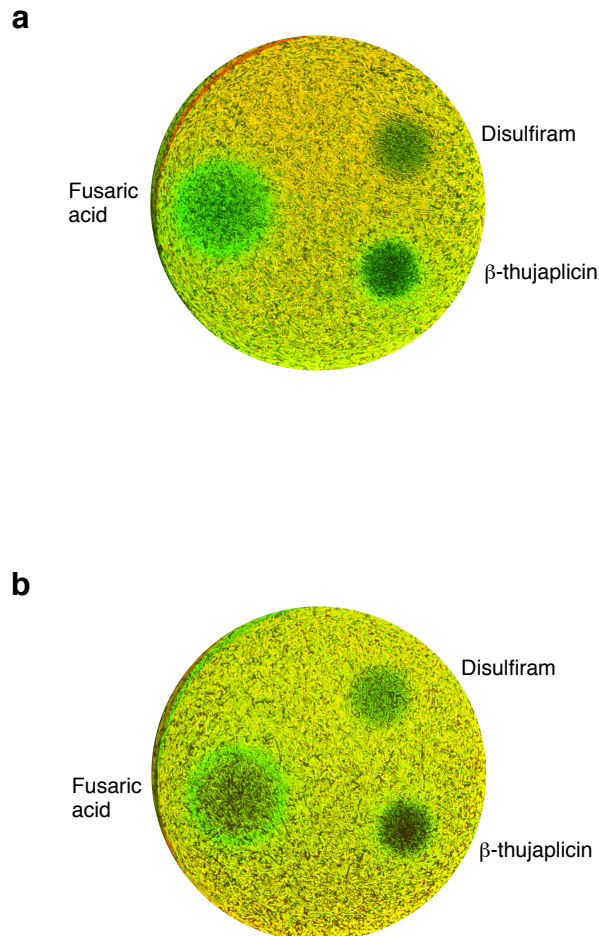
**Appendix 1: Supplementary Materials for Chapter 2: New  
compounds that select against the tetracycline resistance  
efflux pump (S1)**



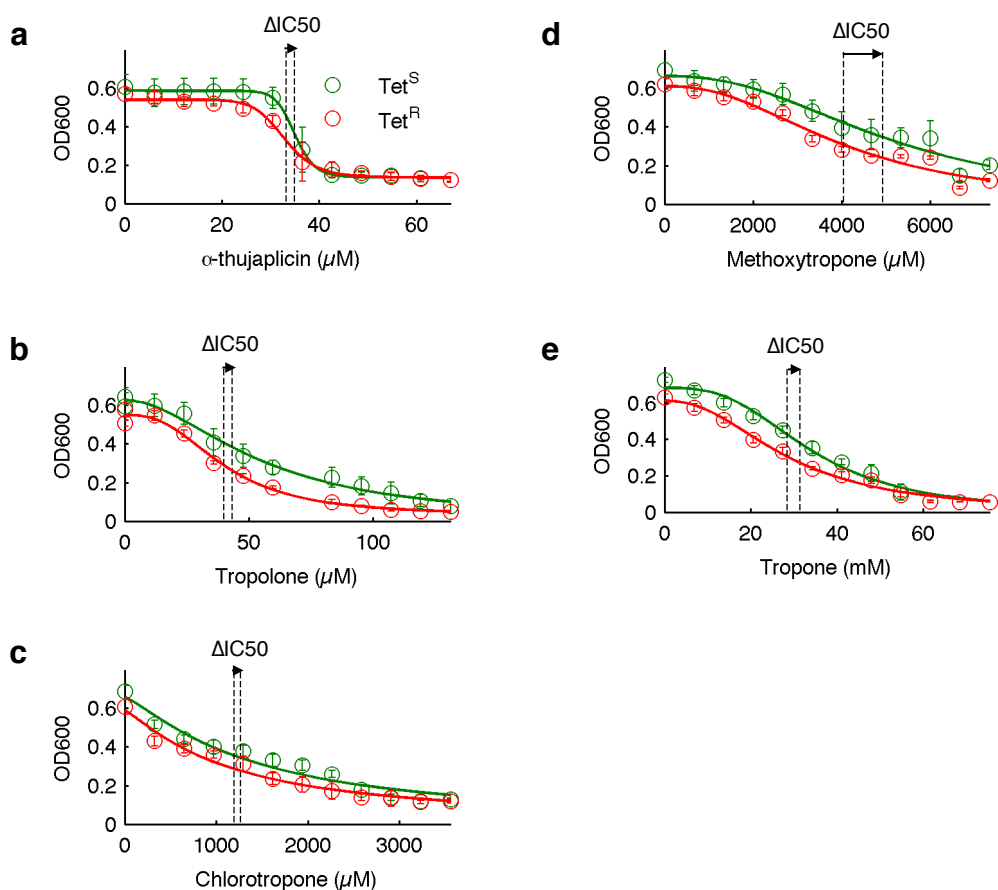
**Figure S1.1. Custom 48-well screening plate.** We adapted a design for 48-well plates<sup>1</sup> to be compatible with high-throughput screening robots and 384-well compound storage plates. The plates have ANSI/SLAS standard dimensions, with 24 columns corresponding to those of a 384-well plate and 2 rows beginning at the A and I positions of a 384-well plate. The plates are machined from polycarbonate sheet and additional polycarbonate spacers (in pink) are affixed with chloromethane. Measurements are in inches.



**Figure S1.2. Automated image analysis identifies hit compounds.** (a) An assay plate from the screen. Compounds are pinned at the top of each well, then diffuse through the agar creating concentration gradients. A top agar seeded with fluorescently-tagged tetracycline susceptible (Tet<sup>S</sup>) and resistant (Tet<sup>R</sup>) bacteria is applied on top of the concentration gradients. Wells A1-A2, A23-A24, B1-B2, and B23-24 contain fusaric acid, doxycycline, ciprofloxacin, and DMSO vehicle control respectively. The hit compound in B9 is disulfiram. (b) Ciprofloxacin is included as a control for compounds that exhibit no or weak selection for Tet<sup>R</sup>. Automated image analysis identifies the highest points on the concentration gradient (corresponding to the distance from the top of the well) where each strain is at half-max growth. The difference between these points ( $\Delta d$ ) is used to score hits. (c) Comparing the  $\Delta d$  of test compounds in one strain pair to their  $\Delta d$  in the dye swap can be used to remove autofluorescent compounds from further analysis. Compounds that have positive  $\Delta d$  for both strain pairs select against tetracycline resistance, compounds that have negative  $\Delta d$  for both strain pairs select for tetracycline resistance, while compounds that have a positive  $\Delta d$  in one strain pair and a negative  $\Delta d$  in the other are autofluorescent.

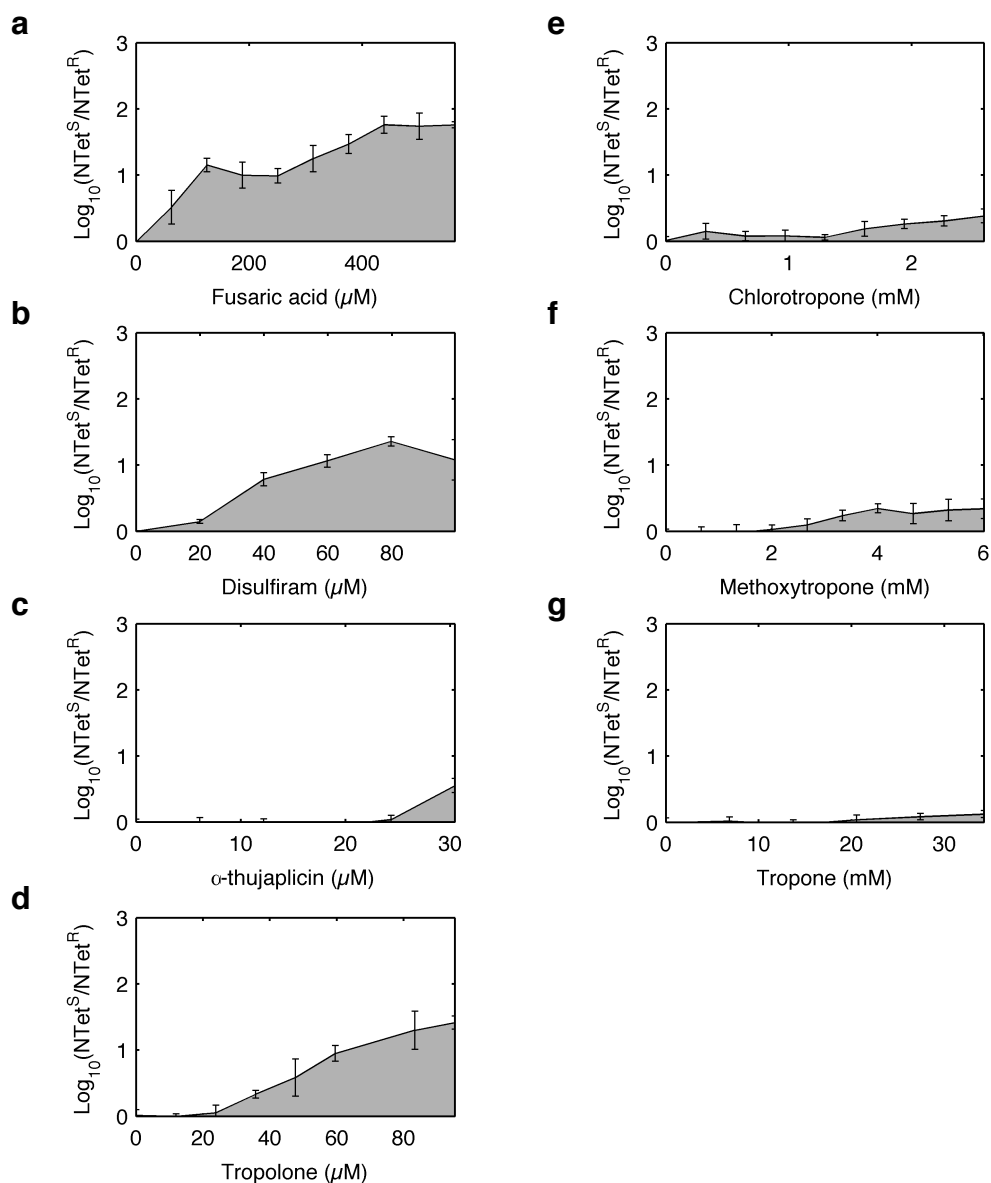


**Figure S1.3.  $\beta$ -thujaplicin and disulfiram reproducibly select against Tet<sup>R</sup>.** The competition assay was repeated with compound fresh from the manufacturers to verify disulfiram and  $\beta$ -thujaplicin's differential activity against Tet<sup>R</sup>. Petri dishes were spotted with 1  $\mu$ L  $\beta$ -thujaplicin, 6  $\mu$ L disulfiram, and 3  $\mu$ L fusaric acid, all dissolved in DMSO at 15 mg/mL. The drugs were allowed to diffuse for 24 h. Then, the plates were inoculated with a 1:1 mixture of Tet<sup>S</sup> (shown in green) and Tet<sup>R</sup> (shown in red) *E. coli* and incubated for 16-18 h. Fluorescent imaging reveals the level of competition between the two strains. The assay is performed in duplicate with a dye swap. (a) Competition between pC (Tet<sup>S</sup>, CFP-tagged, shown in green) and t17pY (Tet<sup>R</sup>, YFP-tagged, shown in red). (b) Competition between pY (Tet<sup>S</sup>, YFP-tagged, shown in green) and t17pC (Tet<sup>R</sup>, CFP-tagged, shown in red).

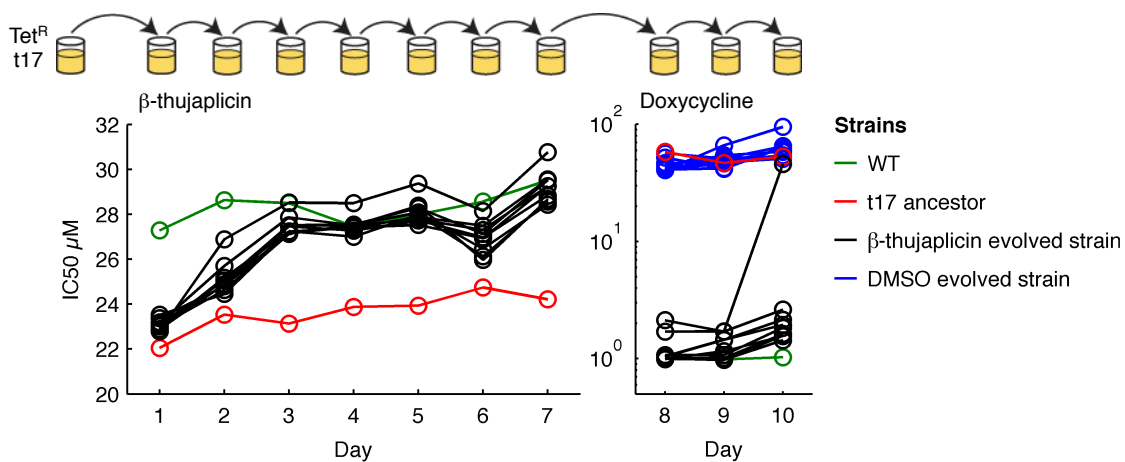


**Figure S1.4. Dose responses for  $\beta$ -thujaplicin analogs.**  $Tet^S$  (WT) and  $Tet^R$  (t17) cells are inoculated on a linear dilution series of compound with media supplemented with ATC to induce *tetA* expression and incubated for 24 h. Growth is measured by OD600. The linear black dashed lines indicate the mean  $IC_{50}$ s for the  $Tet^R$  and  $Tet^S$  strains across six replicates. Error bars indicate standard deviation across six replicates. Shown are dose responses for (a)  $\alpha$ -thujaplicin, (b) tropolone, (c) chlorotropone, (d), methoxytropone, (e), and tropone.

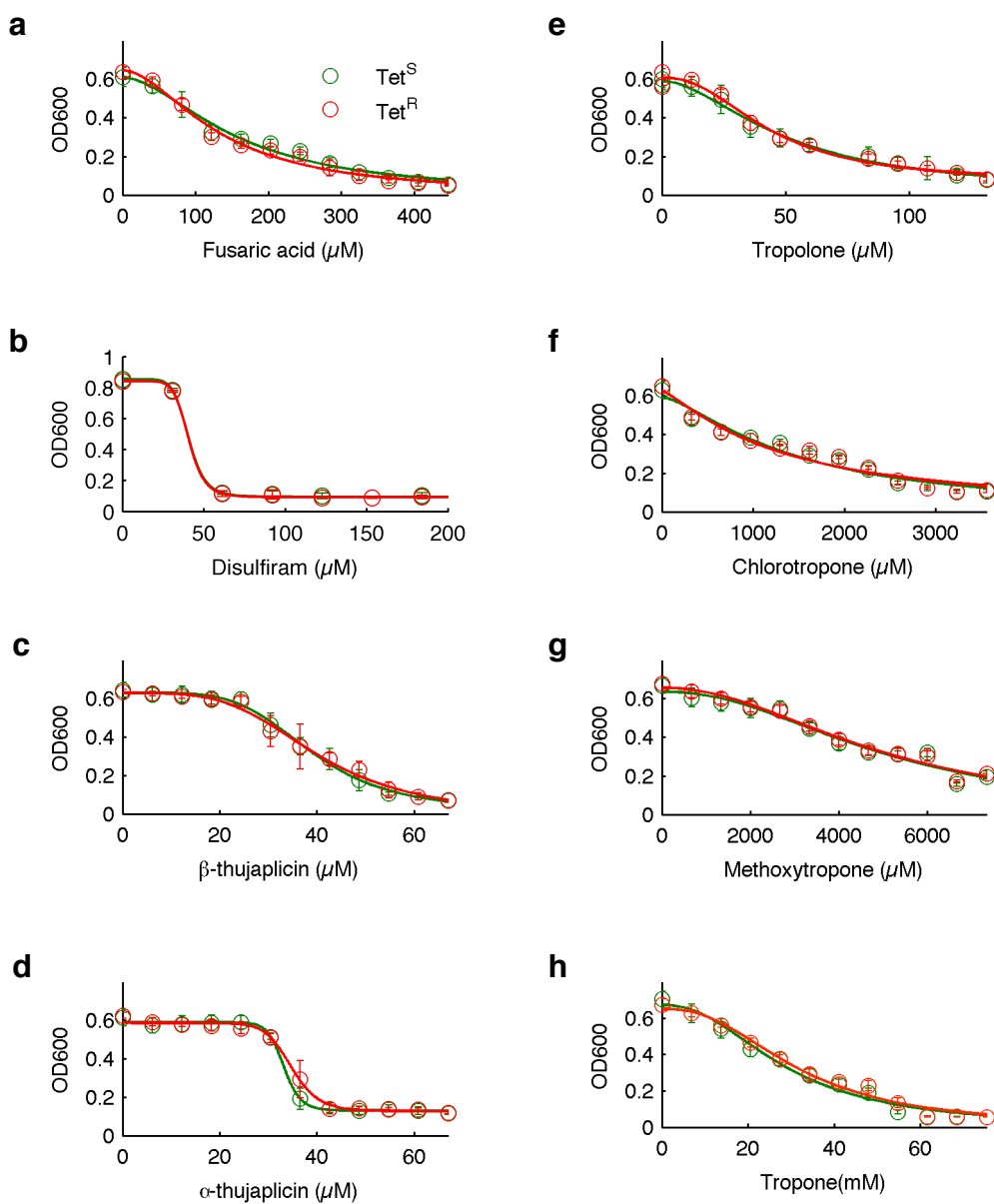




**Figure S1.5. Selection for Tet<sup>S</sup> over Tet<sup>R</sup> measured by flow cytometry.** To quantify the degree of selection against tetracycline resistance, a 1:1 mixture of CFP-tagged Tet<sup>S</sup> (pC) and YFP-tagged Tet<sup>R</sup> (t17pY) cells was added to a linear dilution series of each drug and incubated for 24 h. The media was supplemented with ATC to induce expression of *tetA*. Flow cytometry was used to count the number of Tet<sup>R</sup> (*NTet<sup>R</sup>*) and Tet<sup>S</sup> (*NTet<sup>S</sup>*) cells. The ratio of Tet<sup>S</sup> to Tet<sup>R</sup> cells (*NTet<sup>S</sup>/NTet<sup>R</sup>*) gives the selection for the Tet<sup>S</sup> strain at each drug concentration. This ratio is normalized to the ratio of *NTet<sup>S</sup>/NTet<sup>R</sup>* in wells with no drug and then averaged over a minimum of 5 replicates. The integral (gray) of the selection over all concentrations in which cells can grow is considered the total selection (selectivity) for Tet<sup>S</sup> by that compound. At concentrations above those shown, neither Tet<sup>S</sup> nor Tet<sup>R</sup> cells grow. Error bars indicate standard deviation across a minimum of five replicates. Shown are results for (a) fusaric acid, (b) disulfiram, (c) α-thujaplicin, (d) tropolone, (e) chlorotropone, (f) methoxytropone, and (g) tropone.

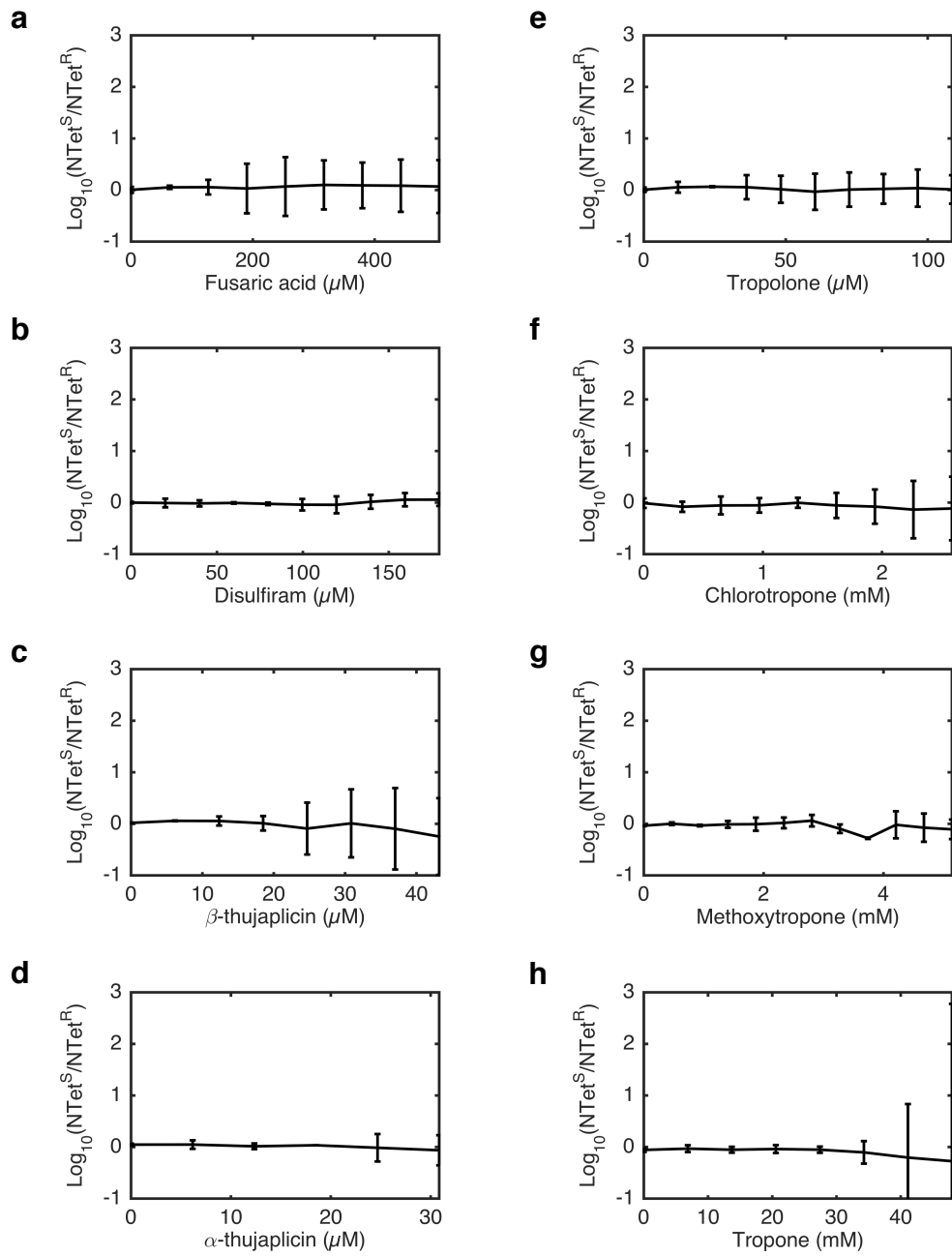


**Figure S1.6. Tet<sup>R</sup> strain loses its tetracycline resistance when evolved in β-thujaplicin.** Eight populations (black) of the Tet<sup>R</sup> t17 strain were serially transferred in dilution series of β-thujaplicin for 7 days, then in dilution series of doxycycline for 3 days. For each population, the well growing at the highest concentration of drug was transferred daily. Each strain became more β-thujaplicin resistant, eventually matching the WT strain (green), which is equivalent to the t17 ancestor without Tn10. When transferred to doxycycline, all of the β-thujaplicin evolved strains were doxycycline susceptible (Tet<sup>S</sup>). All but one of the β-thujaplicin evolved strains remained Tet<sup>S</sup>, even after selection in doxycycline, indicating that seven out of eight populations have permanently lost their Tet<sup>R</sup> phenotype. In contrast, three populations of the Tet<sup>R</sup> t17 strain that were serially transferred in a fixed concentration of DMSO (blue), equivalent to the highest DMSO concentration in the β-thujaplicin dilution series, remained Tet<sup>R</sup>.



**Figure S1.7. Dose responses of all compounds in *Tet<sup>S</sup>* and *Tet<sup>R</sup>* without ATC induction of *tetA*.** *Tet<sup>S</sup>* (WT) and *Tet<sup>R</sup>* (t17) cells are inoculated on a linear dilution series of compound and incubated for 24 h, without ATC induction of *tetA*. Growth is measured by OD600. Error bars indicate standard deviation across six replicates. Shown are dose responses for (a) fusaric acid, (b) disulfiram, (c)  $\beta$ -thujaplicin, (d)  $\alpha$ -thujaplicin, (e) tropolone, (f) chlorotropone, (g) methoxytropone, and (h) tropone. Without ATC induction of *tetA*, the *Tet<sup>R</sup>* and *Tet<sup>S</sup>* dose response are equivalent for all compounds.

**Figure S1.8. Selection for Tet<sup>S</sup> over Tet<sup>R</sup> measured by flow cytometry without ATC induction of *tetA*.** To quantify the degree of selection against tetracycline resistance, a 1:1 mixture of fluorescently tagged Tet<sup>S</sup> and Tet<sup>R</sup> cells was added to a linear dilution series of each drug and incubated for 24 h, without ATC induction of *tetA*. Flow cytometry was used to count the number of Tet<sup>R</sup> ( $NTet^R$ ) and Tet<sup>S</sup> ( $NTet^S$ ) cells. The ratio of Tet<sup>S</sup> to Tet<sup>R</sup> cells ( $NTet^S/NTet^R$ ) gives the selection for the Tet<sup>S</sup> strain at each drug concentration. This ratio is normalized to the ratio of  $NTet^S/NTet^R$  in wells with no drug and then averaged between two dye-swapped replicates. One replicate contains CFP-tagged Tet<sup>S</sup> (pC) and YFP-tagged Tet<sup>R</sup> (t17pY) cells. The other replicate contains YFP-tagged Tet<sup>S</sup> (pY) and CFP-tagged Tet<sup>R</sup> (t17pC) cells. Error bars indicate standard deviation between two replicates. Shown are results for (a) fusaric acid, (b) disulfiram, (c)  $\beta$ -thujaplicin, (d)  $\alpha$ -thujaplicin, (e) tropolone, (f) chlorotropone, (g) methoxytropone, and (h) tropone.



**Figure S1.8 (Continued). Figure S1.8. Selection for  $Tet^S$  over  $Tet^R$  measured by flow cytometry without ATC induction of *tetA*.**

**Figure S1.9. PCR amplification of *tetA* from  $\beta$ -thujaplicin resistant t17 mutants.**

The presence and size of the *tetA* gene was detected by PCR amplification and gel electrophoresis. The expected band size is 1086 bp if *tetA* is present and uninterrupted. Numbered wells are colonies selected on 15  $\mu\text{g}/\text{mL}$   $\beta$ -thujaplicin. Wells marked WT and t17 contain the PCR product amplified from Tet<sup>S</sup> and Tet<sup>R</sup> ancestral controls, respectively. Wells marked E contain reactions with no template. Wells marked M contain 1 kb DNA ladder (New England Biolabs). All WT controls had  $\beta$ -thujaplicin minimum inhibitory concentrations (MICs) of 20  $\mu\text{g}/\text{mL}$ , doxycycline MICs of 5  $\mu\text{g}/\text{mL}$ , and no PCR product. All t17 controls had a  $\beta$ -thujaplicin MICs of 15  $\mu\text{g}/\text{mL}$ , doxycycline MICs of 80  $\mu\text{g}/\text{mL}$ , and a  $\sim$ 1 kb PCR product. All  $\beta$ -thujaplicin resistant mutants had  $\beta$ -thujaplicin MICs of 20  $\mu\text{g}/\text{mL}$ , doxycycline MICs of 5  $\mu\text{g}/\text{mL}$ , and no PCR product or a 1.5-2 kb PCR product (indicating a large insertion in *tetA*), unless otherwise indicated. (a) Colonies 1-14. Colony 2 has a  $\beta$ -thujaplicin MIC of 15  $\mu\text{g}/\text{mL}$  and is therefore considered  $\beta$ -thujaplicin susceptible and not included in Fig. 3b analysis. Colony 2 also has a doxycycline MIC of 80  $\mu\text{g}/\text{mL}$  and a 1 kb PCR product, indicating *tetA* is present and intact. Colony 3 has a  $\beta$ -thujaplicin MIC of 20  $\mu\text{g}/\text{mL}$ , a doxycycline MIC of >100  $\mu\text{g}/\text{mL}$ , and a 1 kb PCR product, indicating *tetA* is present and intact. Genomic sequencing of colony 3 revealed a frameshift mutation in *marR* and an IS10 insertion in *ynbA* (**Table S1.2**). (b) Colonies 15-27. (c) Colonies 28-40. (d) Colonies 41-50. (e) Colonies 51-64. Measurement of the starred t17 control (\*1) was repeated (**Fig. S1.11**). (f) Colonies 71-77. (g) Colonies 78-90. (h) Colonies 91-100.

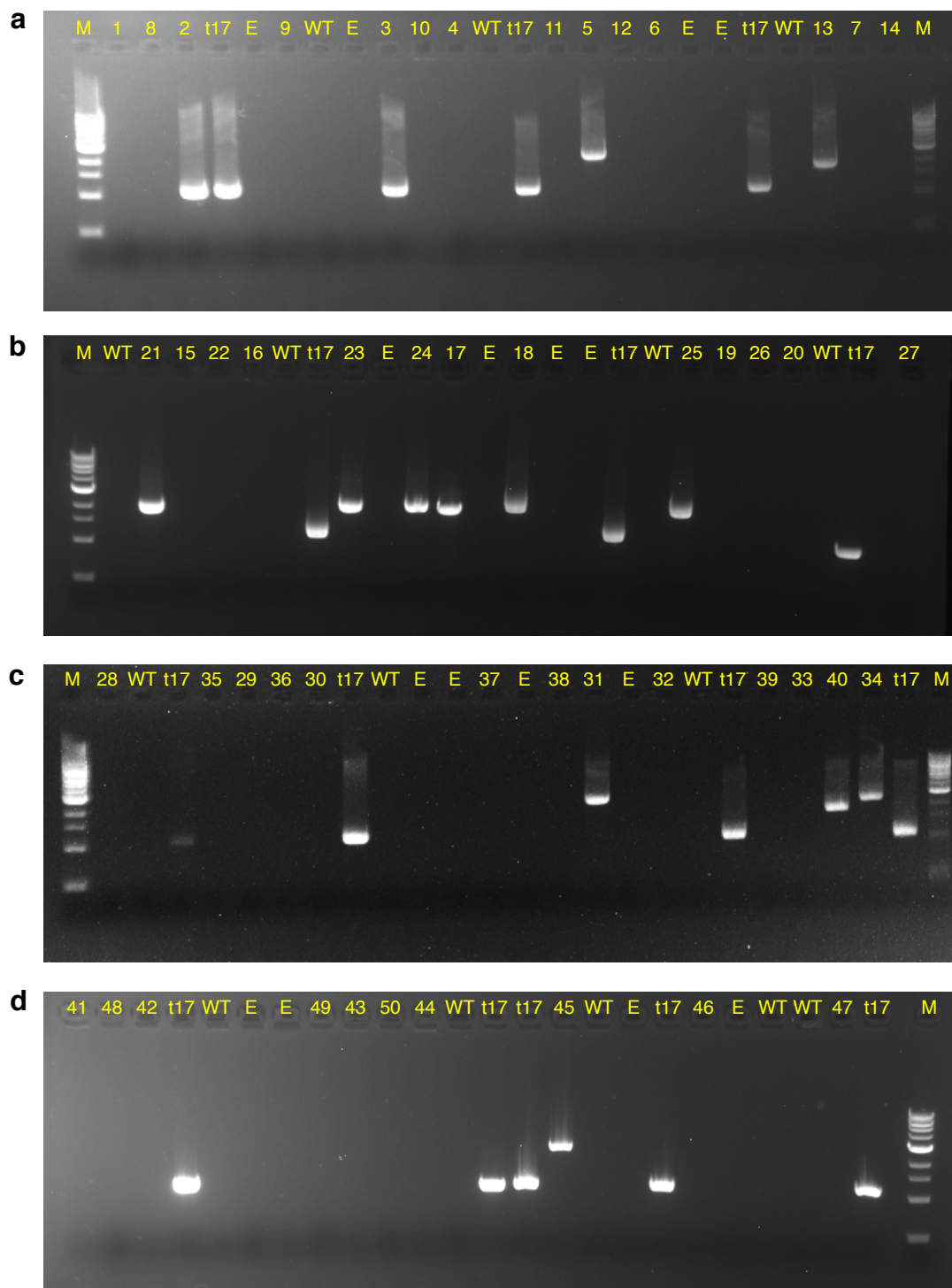
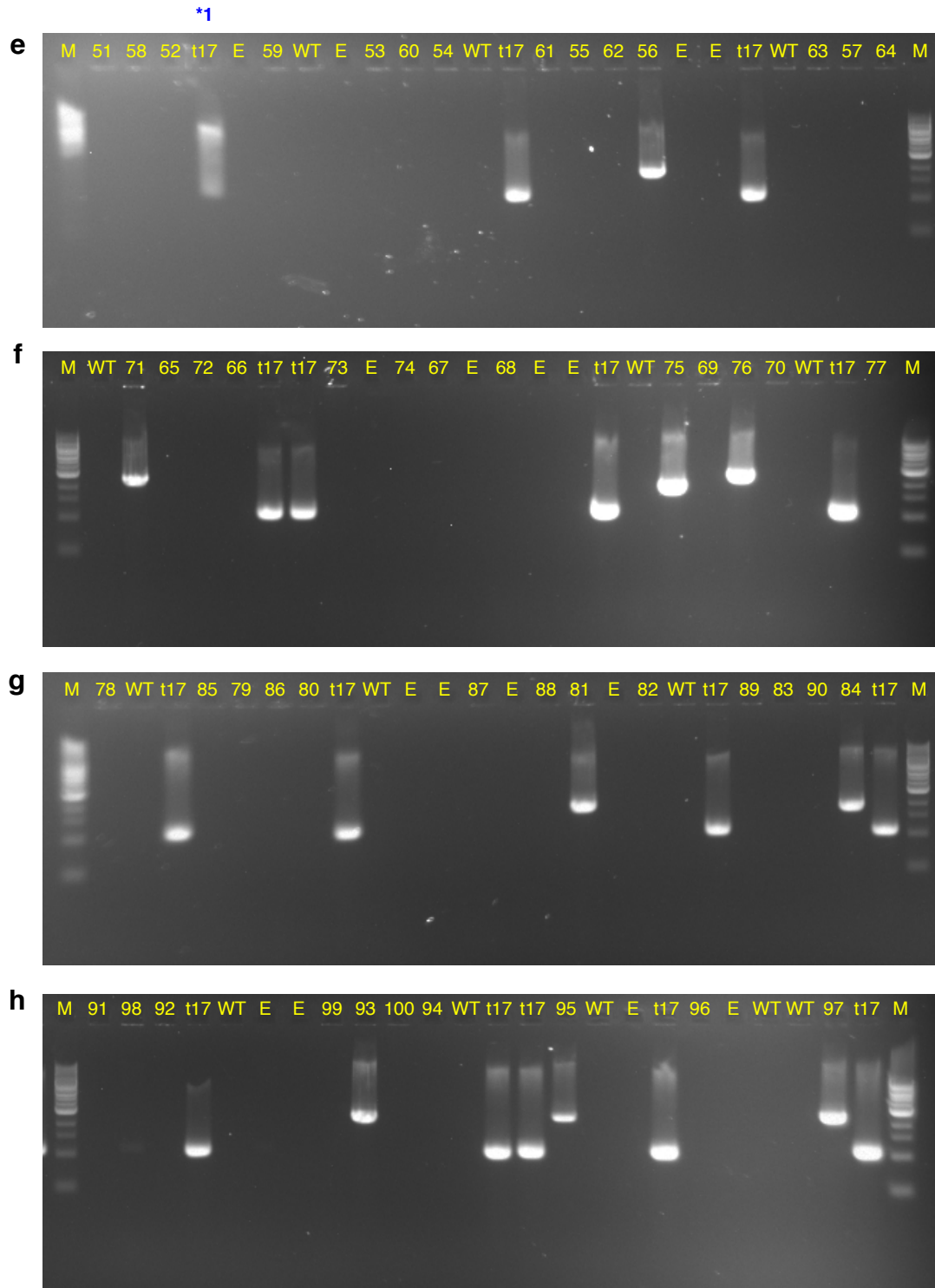


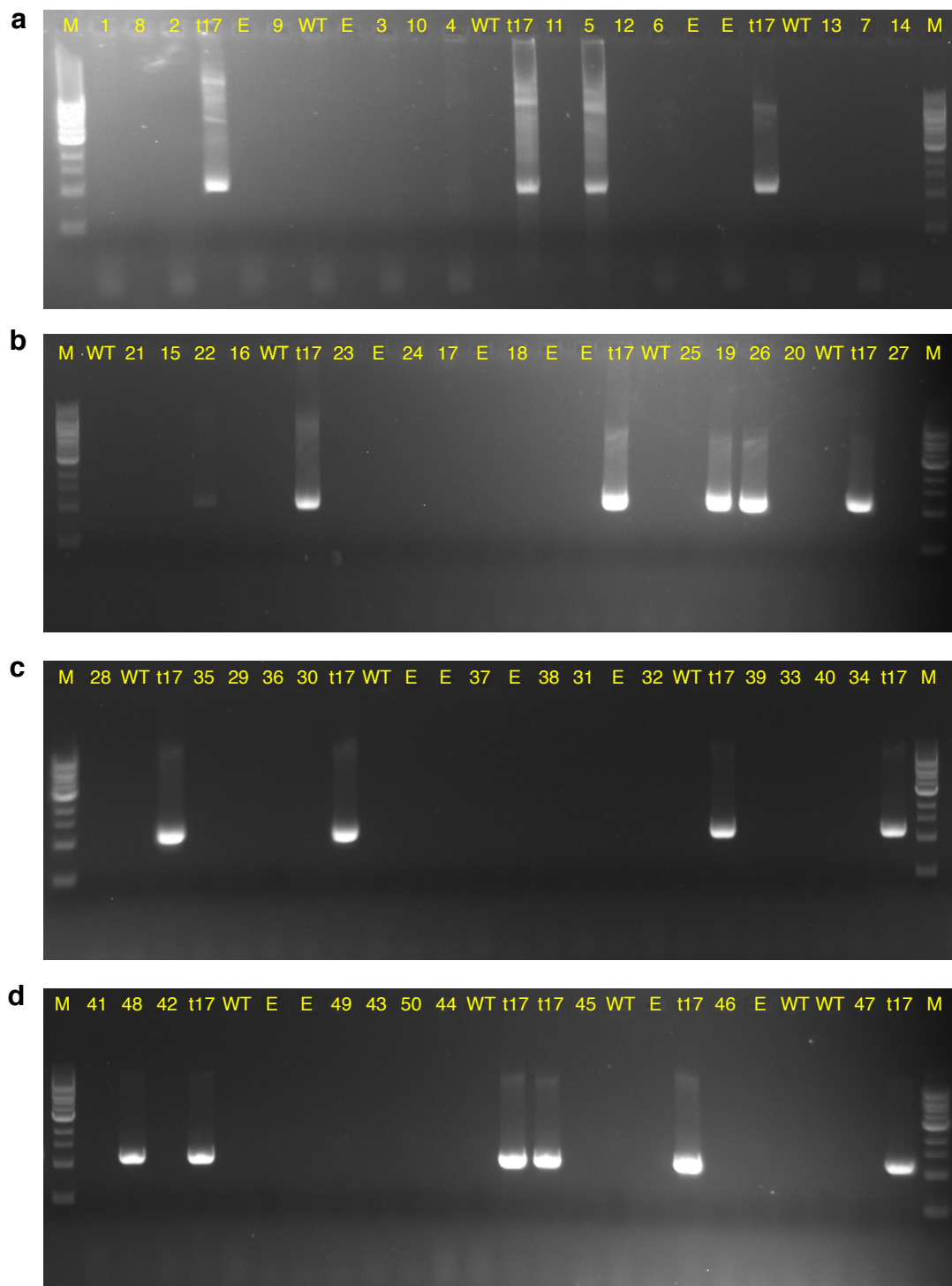
Figure S1.9 (Continued). PCR amplification of *tetA* from b-thujaplicin resistant t17 mutants.



**Figure S1.9 (Continued).** PCR amplification of *tetA* from b-thujaplicin resistant t17 mutants.

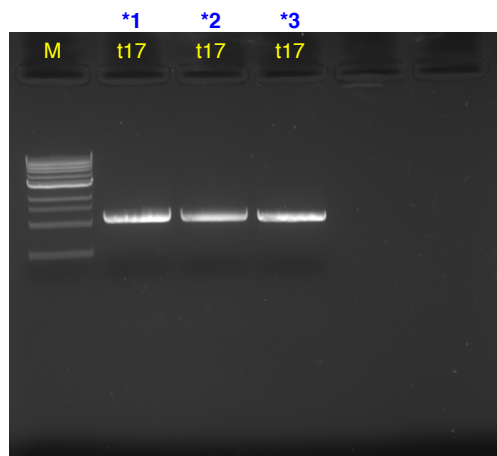


**Figure S1.10. PCR amplification of *tetA* from disulfiram resistant t17 mutants.** The presence and size of the *tetA* gene was detected by PCR amplification and gel electrophoresis. The expected band size is 1086 bp if *tetA* is present and uninterrupted. Numbered wells are colonies selected on 40  $\mu\text{g}/\text{mL}$  disulfiram. Wells marked WT and t17 contain the PCR product amplified from Tet<sup>S</sup> and Tet<sup>R</sup> ancestral controls, respectively. Wells marked E contain reactions with no template. Wells marked M contain 1 kb DNA ladder (New England Biolabs). All WT controls had doxycycline MICs of 5  $\mu\text{g}/\text{mL}$  and no PCR product. All t17 controls had doxycycline MICs of 80  $\mu\text{g}/\text{mL}$  and a  $\sim 1$  kb PCR product. The WT controls had a disulfiram MIC of  $16 \pm 7.8$   $\mu\text{g}/\text{mL}$  (mean and standard deviation across 28 replicates). The t17 controls had a disulfiram MIC of  $12 \pm 4.1$   $\mu\text{g}/\text{mL}$  disulfiram (mean and standard deviation across 29 replicates). Therefore, a disulfiram MIC of 30  $\mu\text{g}/\text{mL}$  or higher was used as the threshold for declaring a colony disulfiram resistant. All disulfiram resistant mutants had disulfiram MICs of 30  $\mu\text{g}/\text{mL}$  or greater, doxycycline MICs of 5  $\mu\text{g}/\text{mL}$ , and no PCR product or a 1.5-2 kb PCR product (indicating a large insertion in *tetA*), unless otherwise indicated. Colonies 5, 8, 15, 17, 23, 26, 34, 48, 54, & 64 have Dsf MICs of 10  $\mu\text{g}/\text{mL}$  and are therefore not considered disulfiram resistant. Colonies 14, 20, 80 have Dsf MICs of 20  $\mu\text{g}/\text{mL}$  and are therefore not considered disulfiram resistant. (a) Colonies 1-14. (b) Colonies 15-27. Colony 19 has a  $\sim 1$  kb PCR product, but still has a doxycycline MIC of 5  $\mu\text{g}/\text{mL}$ , suggesting *tetA* might be present, but mutated. (c) Colonies 28-40. (d) Colonies 41-50. (e) Colonies 51-64. Colony 51 has a  $\sim 1$  kb PCR product and a doxycycline MIC of 80  $\mu\text{g}/\text{mL}$ , suggesting *tetA* is present and intact. (f) Colonies 65-77. (g) Colonies 78-90. Colony 83 has a  $\sim 1$  kb PCR product and a doxycycline MIC of 80  $\mu\text{g}/\text{mL}$  suggesting *tetA* is present and intact. Colony 87 has a  $\sim 1$  kb PCR product, but still has a doxycycline MIC of 5  $\mu\text{g}/\text{mL}$ , suggesting *tetA* might be present, but mutated. (h) Colonies 91-96. Measurement of the starred t17 controls (\*2 and \*3) was repeated (Fig. S1.11).



**Figure S1.10 (Continued). PCR amplification of *tetA* from disulfiram resistant t17 mutants.**





**Figure S1.11. Repeat measurement of PCR product for starred t17 controls by gel electrophoresis.** Measuring the PCR product size from starred t17 controls from **Fig. S1.9e** and **Fig. S1.10h** was repeated by gel electrophoresis.

**Table S1.1. IC50 values for  $\beta$ -thujaplicin analogs in Tet<sup>S</sup> and Tet<sup>R</sup> strains.**

	<b>Compound</b>	<b>Tet<sup>S</sup> IC50 (<math>\mu</math>M)</b>	<b>Tet<sup>R</sup> IC50 (<math>\mu</math>M)</b>
<b>1</b>	$\alpha$ -thujaplicin	35 $\pm$ 2	33 $\pm$ 4
<b>2</b>	Tropolone	43 $\pm$ 4	40 $\pm$ 1
<b>3</b>	Chlorotropone	1300 $\pm$ 170	1200 $\pm$ 340
<b>4</b>	Methoxytropone	4900 $\pm$ 390	4000 $\pm$ 220
<b>5</b>	Tropone	31000 $\pm$ 2300	28000 $\pm$ 1900

Tet<sup>S</sup> (WT) and Tet<sup>R</sup> (t17) cells are inoculated on a linear dilution series of compound with media supplemented with ATC to induce *tetA* expression and incubated for 24 h. Growth is measured by OD600. IC50s are a mean of the IC50 values from 6 replicates  $\pm$  the standard deviation. The IC50 for each replicate is determined by fitting to a four parameter logistic function.

**Table S1.2. Genomic sequencing of  $\beta$ -thujaplicin resistant t17 mutants.**

Label	Colony	Bth MIC ( $\mu$ g/mL)	Dox MIC ( $\mu$ g/mL)	tetA PCR product	Mutation*
BthRP1A8	5	20	5	2kb	IS10 insertion in tetA (Tn10:6200)
BthRP1B11	13	20	5	2kb	IS1 insertion in tetA (Tn10:6150)
BthRP1C6	17	20	5	2kb	IS1 insertion in tetA (Tn10:6150)
BthRP2G12	97	20	5	2kb	IS10 insertion tetA (Tn10:5900)
BthRP1A12	7	20	5	0kb	Deletion of all coding portions of Tn10**; SNP in cydD, Q101K
BthRP1A6	4	20	5	0kb	Deletion of all coding portions of Tn10**
BthRP1A9	6	20	5	0kb	Deletion of all coding portions of Tn10**
BthRP1A5	3	20	80	1kb	1bp deletion (-G) in marR (NC_012759:1509511); IS10 insertion in ynbA (NC_012759:136820)
1H02	101	20	5	ND	Deletion of all coding portions of Tn10
1H05	102	20	5	ND	Deletion of all coding portions of Tn10; SNP 64bp upstream of tyrP (NC_012759:1880124)
1H07	103	20	5	ND	Deletion of all coding portions of Tn10**

Colonies 100-103 were isolated from a different inoculating culture than colonies 1-100. Their tetA PCR product was not determined.

\*Positions reported relative to NC\_012759 (MC4100, WT) or AF162223 (Tn10). Insertion site of IS elements rounded to nearest 50bp, as RetroSeq does not give precise results. Genomic sequencing reveals that Tn10 in ancestral strain t17 was inserted near 849200 of NC\_012759.

\*\*These deletions of Tn10 were accompanied by extra copies of IS10 in chromosome near NC\_012759:850000 (A12), 850750 (A6), 851100 (A9), and 909700 (1H07).

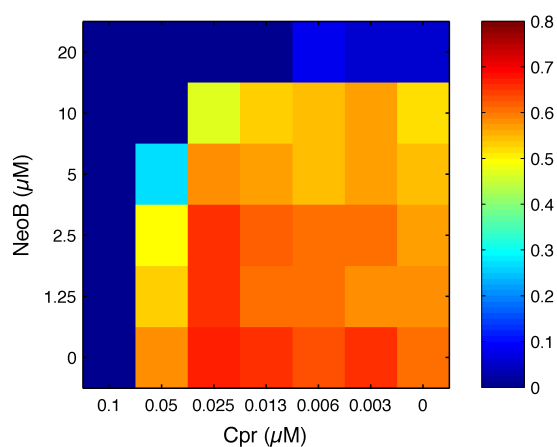
**Table S1.3. IC50 values for all compounds in Tet<sup>S</sup> and Tet<sup>R</sup> strains without ATC to induce TetA.**

	<b>Compound</b>	<b>Tet<sup>S</sup> IC50 (μM)</b>	<b>Tet<sup>R</sup> IC50 (μM)</b>
	Fusaric acid	155 ± 8	174 ± 14
	Disulfiram	40 ± 1	40 ± 2
	β-thujaplicin	39 ± 2.6	41 ± 2.5
<b>1</b>	α-thujaplicin	33 ± 0.98	35 ± 2.4
<b>2</b>	Tropolone	49 ± 7.7	54 ± 8.2
<b>3</b>	Chlorotropone	1400 ± 80	1400 ± 210
<b>4</b>	Methoxytropone	4900 ± 350	5000 ± 860
<b>5</b>	Tropone	28000 ± 2200	34000 ± 1400

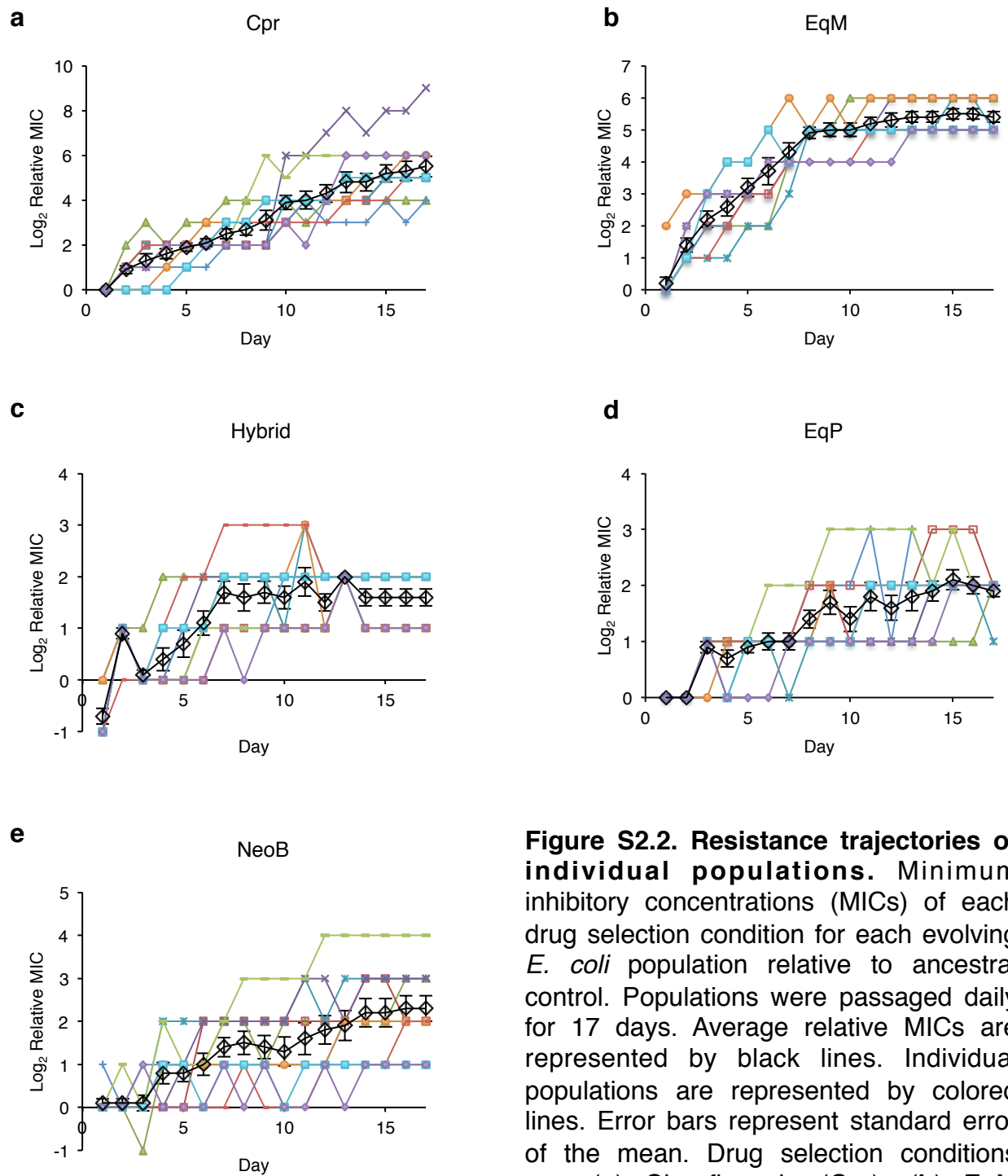
Tet<sup>S</sup> (WT) and Tet<sup>R</sup> (t17) cells are inoculated on a linear dilution series of compound and incubated for 24 h, without ATC induction of *tetA*. Growth is measured by OD600. IC50s are a mean of the IC50 values from 6 replicates ± the standard deviation. The IC50 for each replicate is determined by fitting to a four parameter logistic function. The Tet<sup>R</sup> and Tet<sup>S</sup> IC50s are equivalent for all compounds.

**Appendix 2: Supplementary Materials for Chapter 3: A  
hybrid antibiotic restricts evolutionary paths to resistance  
by evading activation of the multiple antibiotic resistance  
operon (S2)**



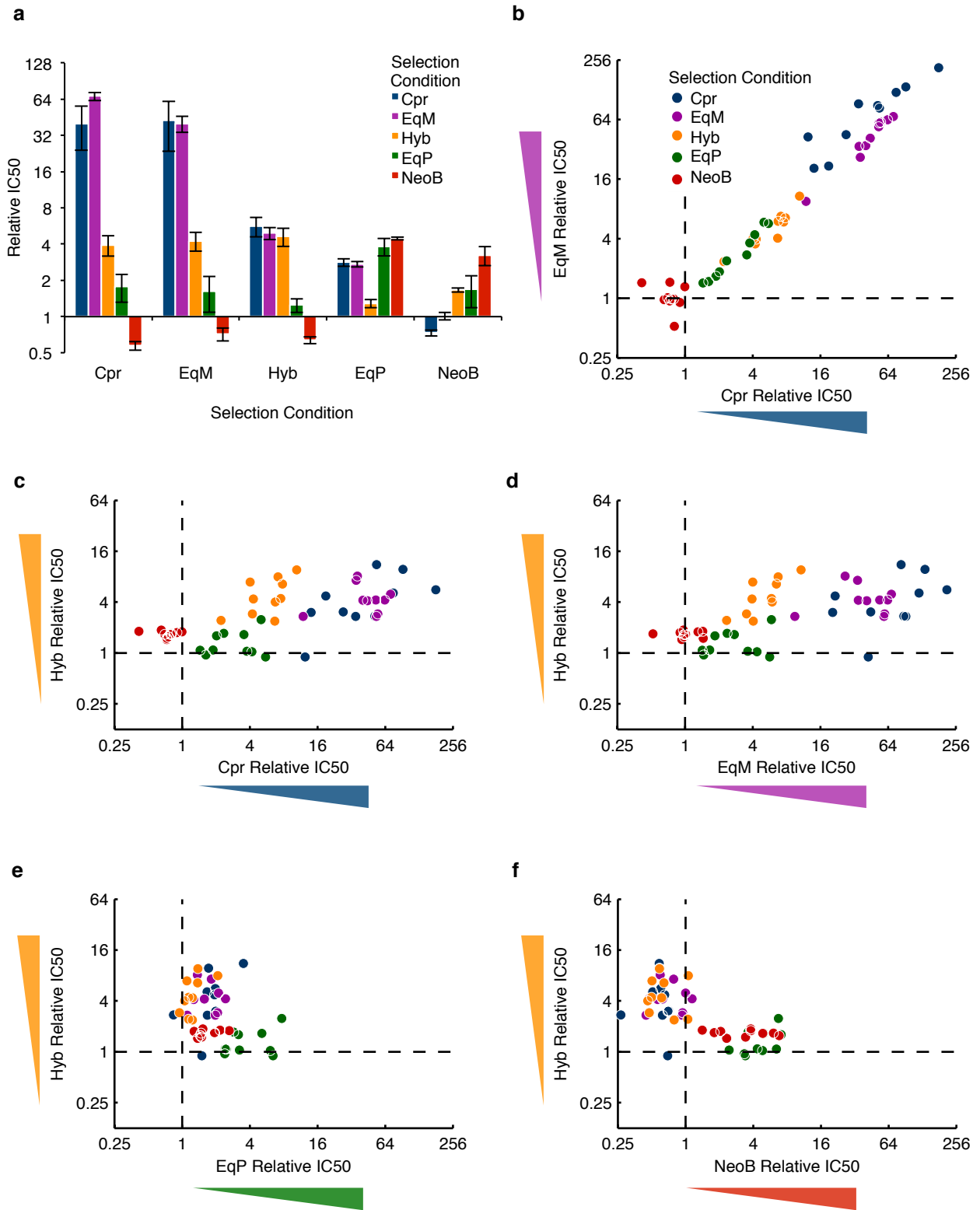


**Figure S2.1. 2-D checkerboard MICs of ciprofloxacin (Cpr) and neomycin B (NeoB).** Two-dimensional 2-fold drug gradients were prepared on two 96-well plates with a final volume of 150  $\mu\text{L}$  per well. Plates were inoculated with a 1:500 dilution of the ancestral freezer stock, incubated overnight at 37°C with shaking at 900 rpm. Results shown are the average  $\text{OD}_{600}$  measurements of each corresponding well between two replicate plates



**Figure S2.2. Resistance trajectories of individual populations.** Minimum inhibitory concentrations (MICs) of each drug selection condition for each evolving *E. coli* population relative to ancestral control. Populations were passaged daily for 17 days. Average relative MICs are represented by black lines. Individual populations are represented by colored lines. Error bars represent standard error of the mean. Drug selection conditions are: (a) Ciprofloxacin (Cpr); (b) EqM mixture of Cpr and NeoB; (c) Hybrid; (d) EqP mixture; (e) Neomycin B (NeoB).

**Figure S2.3. Retrospective cross-resistance profiles of final evolved strains. (a)** Bars indicate the mean resistances (IC50) of each evolved population relative to ancestral IC50. Each bar represents the average relative resistances of 10 single colonies, one picked from each final evolved population. Error bars indicate standard error. **(b-f)** Each point indicates the relative IC50 of one colony isolated from final evolved population, by susceptibility to drugs indicated on the axes. Blue: isolates evolved in Cpr. Red: isolates evolved in NeoB. Purple: isolates evolved in 1:1 M mixture. Green: isolates evolved in  $MIC_{Cpr}:MIC_{NeoB}$  mixture. Orange: isolates evolved in hybrid compound. **(b)** Resistance to ciprofloxacin vs. EqM mixture. **(c)** Resistance to ciprofloxacin vs. hybrid. **(d)** Resistance to EqM vs. hybrid. **(e)** Resistance to EqP vs. hybrid. **(f)** Resistance to NeoB vs. hybrid.



**Figure S2.3 (Continued). Retrospective cross-resistance profiles of final evolved strains.**

**Table S2.1. All mutations found in final (Day 17) evolved strains from genomic sequencing<sup>1</sup>.**

Strain	Type*	Position in U00096.2	NT position	NT Ref	NT Mutation	AA pos	AA Mut	Locustag	Gene	Annotation**
Cpr-1	N	485070	86	T	G	29	V29G	b0464	acrR	acrAB operon repressor
	N	1617277	77	T	A	26	V26E	b1530	marR	multiple antibiotic resistance protein; repressor of mar operon
	B	1669360		G	C			b1597	asr	384-b1596, -13-b1597
Cpr-2	D	2335601	1842	C	-GCGCCACGAGTG	614		b2231	gyrA	DNA gyrase, subunit A, type II topoisomerase
	N	1438226	583	C	A	195	E195*	b1378	ydbK	putative oxidoreductase, Fe-S subunit
	D	1617459	259	G	-C	87		b1530	marR	multiple antibiotic resistance protein; repressor of mar operon
	N	3876758	1385	A	T	462	L462H	b3699	gyrB	DNA gyrase subunit B, type II topoisomerase, ATPase activity
Cpr-3	D	3980699	71	T	-C	24		b3798	leuT	tRNA-Leu
	N	4182977	3710	A	T	1237	H1237L	b3987	rpoB	RNA polymerase, beta subunit
	D	1617501	301	C	-ACCAAGAATTAACAAAA	101		b1530	marR	multiple antibiotic resistance protein; repressor of mar operon
	D	1617548	348	T	-GAGTATTGCTTAA	116		b1530	marR	multiple antibiotic resistance protein; repressor of mar operon
	N	2337196	247	A	C	83	S83A	b2231	gyrA	DNA gyrase, subunit A, type II topoisomerase
Cpr-4	D	2432951	708	C	-G	236		b2318	truA	pseudouridylate synthase I
	D	485064	80	A	-G	27		b0464	acrR	acrAB operon repressor
	D	1617286	86	C	-T	29		b1530	marR	multiple antibiotic resistance protein; repressor of mar operon
	R	1989967	45	T	C	15		b1910	cysT	tRNA-Cys
	N	2337201	242	C	T	81	G81D	b2231	gyrA	DNA gyrase, subunit A, type II topoisomerase
	N	3172110	1309	T	G	437	I437L	b3030	parE	DNA topoisomerase IV subunit B
	D	3174309	547	C	-GTTACGCAGA	183		b3032	cpdA	cyclic 3',5'-adenosine monophosphate phosphodiesterase

**Table S2.1 (Continued). All mutations found in final (Day 17) evolved strains from genomic sequencing<sup>1</sup>.**

Cpr-5	N	485319	335	T	G		112	I112S	b0464	acrR	acrAB operon repressor
	N	2336299	1144	C	T		382	A382T	b2231	gyrA	DNA gyrase, subunit A, type II topoisomerase
	N	4632739	595	T	G		199	T199P	b4396	rob	right origin-binding protein
	N	646200	533	C	T		178	G178D	b0613	citG	orf, hypothetical protein
Cpr-6	N	1435600	3209	G	T		1070	P1070Q	b1378	ydbK	putative oxidoreductase, Fe-S subunit
	D	1617300	100	G	-C		34		b1530	marR	multiple antibiotic resistance protein; repressor of mar operon
	N	2335495	1948	T	C		650	T650A	b2231	gyrA	DNA gyrase, subunit A, type II topoisomerase
	N	2337183	260	T	C		87	D87G	b2231	gyrA	DNA gyrase, subunit A, type II topoisomerase
	N	4115627	487	T	G		163	I163L	b3927	glpF	facilitated diffusion of glycerol
	D	4627442	1104	C	-A		368		b4391	yjyK	putative ATP-binding component of a transport system
Cpr-7	N	646200	533	C	T		178	G178D	b0613	citG	orf, hypothetical protein
	N	1435600	3209	G	T		1070	P1070Q	b1378	ydbK	putative oxidoreductase, Fe-S subunit
	D	1617300	100	G	-C		34		b1530	marR	multiple antibiotic resistance protein; repressor of mar operon
	N	2335495	1948	T	C		650	T650A	b2231	gyrA	DNA gyrase, subunit A, type II topoisomerase
	N	2337183	260	T	C		87	D87G	b2231	gyrA	DNA gyrase, subunit A, type II topoisomerase
	N	4115627	487	T	G		163	I163L	b3927	glpF	facilitated diffusion of glycerol
Cpr-8	R	696046	8	A	G		3		b0668	glnW	synonyms: glnU, glnU-beta, SuB, supB, sufG
	N	1617390	190	T	C		64	W64R	b1530	marR	multiple antibiotic resistance protein; repressor of mar operon
	D	2337193	250	C	-CGA		84		b2231	gyrA	DNA gyrase, subunit A, type II topoisomerase
	I	3091177	291	G	+CT		97		b2948	yqgE	orf, hypothetical protein
	N	3307638	1622	A	C		541	I541S	b3164	pnp	polynucleotide phosphorylase; cytidylate kinase activity

**Table S2.1 (Continued). All mutations found in final (Day 17) evolved strains from genomic sequencing<sup>1</sup>.**

	D	3517056	232	C	-AA	78	b3390	aroK	shikimate kinase I
	R	696046	8	A	G	3	b0668	glnW	synonyms: glnU, glnU-beta, SuB, supB, sufG
Cpr-9	N	1617390	190	T	C	64	W64R	marR	multiple antibiotic resistance protein; repressor of mar operon
	D	2337193	250	C	-CGA	84	b2231	gyrA	DNA gyrase, subunit A, type II topoisomerase
	I	3091177	291	G	+CT	97	b2948	yqgE	orf, hypothetical protein
	D	3517056	232	C	-AA	78	b3390	aroK	shikimate kinase I
	D	4466404	757	G	-CAATGGTGATT	253	b4242	mgfA	Mg2+ transport ATPase, P-type 1
Cpr-10	N	2335621	1822	G	A	608	P608S	gyrA	DNA gyrase, subunit A, type II topoisomerase
	N	2337087	356	G	T	119	A119E	gyrA	DNA gyrase, subunit A, type II topoisomerase
	I	2910027	1647	C	+CGCCACCAATCG	549	b2784	relA	(p)ppGpp synthetase I (GTP pyrophosphokinase); regulation of RNA synthesis; stringent factor
	I	2919119	1004	A	+AC	335	b2789	gudP	putative D-glucarate permease (MFS family)
	D	4275926	435	C	-GCACGCTTGCTGGA	145	b4063	soxR	redox-sensing activator of soxS
NeoB-1	N	123050	34	A	T	12	I12F	aceE	pyruvate dehydrogenase (decarboxylase component)
	I	395879	17	T	+C	6	b0377	sbmA	sensitivity to microcin B17, possibly envelopprotein
	B	583715		T	A		b0564	appY	62-b0564, 188-b0565
	N	3469892	1645	A	C	549	Y549D	fusA	GTP-binding protein chain elongation factorEF-G
NeoB-2	D	3052789	74	G	-C	25	b2908	pepP	proline aminopeptidase P II
	N	3472345	230	T	A	77	H77L	rpsL	30S ribosomal subunit protein S12
NeoB-3	D	396780	918	G	-A	306	b0377	sbmA	sensitivity to microcin B17, possibly envelopprotein
	D	3182873	72	G	-A	24	b3042	yqiC	orf, hypothetical protein
	N	3469993	1544	T	G	515	Y515S	fusA	GTP-binding protein chain elongation factorEF-G

**Table S2.1 (Continued). All mutations found in final (Day 17) evolved strains from genomic sequencing<sup>1</sup>.**

	N	4025016	467	C	A		156	S156*	b3844	fre	ferrisiderophore reductase; flavin reductase(NADPH:flavin oxidoreductase)
NeoB-4	N	2161771	872	T	G		291	L291R	b2078	baeS	sensor protein (for BaeR)
	N	2396241	1953	C	A		651	W651C	b2283	nuoG	NADH dehydrogenase I chain G
	N	2427482	779	A	T		260	F260Y	b2312	purF	amidophosphoribosyltransferase = PRPPamidotransferase
	N	3469708	1829	G	A		610	P610L	b3340	fusA	GTP-binding protein chain elongation factorEF-G
NeoB-5	N	4024688	139	C	T		47	R47C	b3844	fre	ferrisiderophore reductase; flavin reductase(NADPH:flavin oxidoreductase)
	N	3469576	1961	A	T		654	I654N	b3340	fusA	GTP-binding protein chain elongation factorEF-G
	N	1263253	317	G	C		106	G106A	b1210	hemA	glutamyl-tRNA reductase
	N	2396294	1900	G	A		634	Q634*	b2283	nuoG	NADH dehydrogenase I chain G
NeoB-6	N	3267242	806	T	C		269	L269S	b3121	yhaC	orf, hypothetical protein
	N	3469576	1961	A	T		654	I654N	b3340	fusA	GTP-binding protein chain elongation factorEF-G
	N	1166579	1272	C	G		424	N424K	b1109	ndh	respiratory NADH dehydrogenase
	N	4024838	289	T	A		97	W97R	b3844	fre	ferrisiderophore reductase; flavin reductase(NADPH:flavin oxidoreductase)
NeoB-7	N	3469708	1829	G	A		610	P610L	b3340	fusA	GTP-binding protein chain elongation factorEF-G
	N	396194	332	G	A		111	W111*	b0377	sbmA	sensitivity to microcin B17, possibly envelopprotein
	N	449021	845	C	T		282	W282*	b0431	cyoB	cytochrome o ubiquinol oxidase subunit I
	N	770907	230	A	G		77	G77R	b0733	cydA	cytochrome d terminal oxidase, polypeptidesubunit I
NeoB-8	N	3469576	1961	A	T		654	I654N	b3340	fusA	GTP-binding protein chain elongation factorEF-G
	B	1165303		T	G				b1109	ndh	395-b1108, -5-b1109
	D	2396385	1809	C	-A		603		b2283	nuoG	NADH dehydrogenase I chain G



**Table S2.1 (Continued). All mutations found in final (Day 17) evolved strains from genomic sequencing<sup>1</sup>.**

	I	3052649	214	G	+T		72		b2908	pepP	proline aminopeptidase P II
NeoB-9	N	2413888	1120	A	T		374	I374F	b2297	pta	phosphotransacetylase
NeoB-10	N	252943	235	G	A		79	D79N	b0234	yafP	orf, hypothetical protein
	I	2395576	2618	A	+GATGCGGCCAG		873		b2283	nuoG	NADH dehydrogenase I chain G
EqM-1	D	2337193	250	C	-CGA		84		b2231	gyrA	DNA gyrase, subunit A, type II topoisomerase
	N	1058647	169	T	G		57	S57A	b0997	torA	trimethylamine N-oxide reductase subunit
	N	1587604	422	A	C		141	V141G	b1505	ydeT	putative outer membrane protein
	N	2658952	602	G	A		201	S201F	b2530	iscS	cysteine desulfurase
EqM-2	B	3575661		G	A				b3437	gntK	-85-b3437 , 93-b3438
	D	2337193	250	C	-CGA		84		b2231	gyrA	DNA gyrase, subunit A, type II topoisomerase
	D	1617501	301	C	-ACCAAGAAATTAACAAAAA		101		b1530	marR	multiple antibiotic resistance protein; repressor of mar operon
	D	1938990	607	G	-GA		203		b1856	yebA	orf, hypothetical protein
	N	2504594	61	G	A		21	L21F	b2385	ypdF	putative peptidase
	N	3439771	350	G	A		117	P117L	b3297	rpsK	30S ribosomal subunit protein S11
EqM-3	D	4106425	851	G	-T		284		b3916	pfkA	6-phosphofructokinase I
	D	2337193	250	C	-CGA		84		b2231	gyrA	DNA gyrase, subunit A, type II topoisomerase
	I	1029705	244	T	+C		82		b0969	yccK	putative sulfite reductase (EC 1.8.-.-)
	I	1617563	363	G	+A		121		b1530	marR	multiple antibiotic resistance protein; repressor of mar operon
EqM-4	D	3090996	110	C	-TCT		37		b2948	yqgE	orf, hypothetical protein
	D	485056	72	C	-TCACA		24		b0464	acrR	acrAB operon repressor
	D	1617249	49	C	-TGGAT		17		b1530	marR	multiple antibiotic resistance protein; repressor of mar operon
	N	2337198	245	T	C		82	D82G	b2231	gyrA	DNA gyrase, subunit A, type II topoisomerase
	D	2659433	121	G	-A		41		b2530	iscS	cysteine desulfurase

**Table S2.1 (Continued). All mutations found in final (Day 17) evolved strains from genomic sequencing<sup>1</sup>.**

	N	4628215	331	A	G		111	Y111H	b4391	yjK	putative ATP-binding component of a transportsystem
EqM-5	D	2337193	250	C	-CGA		84		b2231	gyrA	DNA gyrase, subunit A, type II topoisomerase
	D	1617409	209	A	-CCCGAATGACAAGC		70		b1530	marR	multiple antibiotic resistance protein; repressor of mar operon
	D	4133699	1842	C	-GGCAT		614		b3942	katG	catalase; hydroperoxidase HPI(I)
	D	4466520	873	G	-CTGATT		291		b4242	mgTA	Mg2+ transport ATPase, P-type 1
	N	2337183	260	T	C		87	D87G	b2231	gyrA	DNA gyrase, subunit A, type II topoisomerase
EqM-6	D	446216	714	C	-GCG		238		b0428	cyoE	protoheme IX farnesyltransferase (haeme Obiosynthesis)
	N	485202	218	T	C		73	L73P	b0464	acrR	acrAB operon repressor
	I	1617423	223	C	+GCG		75		b1530	marR	multiple antibiotic resistance protein; repressor of mar operon
	D	4104125	283	G	-T		95		b4484	cpxP	periplasmic repressor of cpx regulon byinteraction with CpxA
	D	2337193	250	C	-CGA		84		b2231	gyrA	DNA gyrase, subunit A, type II topoisomerase
EqM-7	D	1617552	352	T	-ATTGCTTAA		118		b1530	marR	multiple antibiotic resistance protein; repressor of mar operon
	I	2658801	753	T	+CCGA		251		b2530	iscS	cysteine desulfurase
	I	779732		G	+C				b0743	lysT	tRNA-Lys
EqM-8	D	1617452	252	C	-GGCGGGCAATAT		84		b1530	marR	multiple antibiotic resistance protein; repressor of mar operon
	R	3421668	10	C	T		4		b3273	thrV	tRNA-Thr
	I	3780316	270	G	+GTACGC		90		b3607	cysE	serine acetyltransferase
EqM-9	N	1617277	77	T	A		26	V26E	b1530	marR	multiple antibiotic resistance protein; repressor of mar operon
	N	485082	98	C	A		33	S33*	b0464	acrR	acrAB operon repressor
	N	2485724	3329	A	T		1110	Q1110L	b2370	evgS	putative sensor for regulator EvgA
EqM-10	I	3275279	256	C	+CATTCAA		86		b3129	sohA	putative protease; htrA suppressor protein
	D	2337193	250	C	-CGA		84		b2231	gyrA	DNA gyrase, subunit A, type II topoisomerase



**Table S2.1 (Continued). All mutations found in final (Day 17) evolved strains from genomic sequencing<sup>1</sup>.**

EqP-5	D	2532171	84	G	-A		28	b2416	ptsI	PEP-protein phosphotransferase system enzyme I
	D	3090995	109	G	-CTCT		37	b2948	yqgE	orf, hypothetical protein
EqP-6	N	3469847	1690	C	A		564	G564C	fusA	GTP-binding protein chain elongation factorEF-G
	N	2533858	3	G	C		1	M11	crr	PTS system, glucose-specific IIA component
	N	3469622	1915	G	T		639	R639S	fusA	GTP-binding protein chain elongation factorEF-G
	N	3469837	1700	G	A		567	A567V	fusA	GTP-binding protein chain elongation factorEF-G
	D	3877306	837	A	-CCG		279	b3699	gyrB	DNA gyrase subunit B, type II topoisomerase,ATPase activity
	N	4025072	523	T	A		175	W175R	fre	ferrisiderophore reductase; flavin reductase(NADPH:flavin oxidoreductase)
	N	236356	290	T	C		97	I97T	dnaQ	DNA polymerase III, epsilon subunit
	N	798286	478	G	T		160	G160C	ybhE	putative isomerase
	S	1155527	543	A	G		181	b1099	holB	DNA polymerase III, delta prime subunit
	N	1422280	475	G	A		159	G159S	trkG	trk system potassium uptake protein
EqP-7	N	1617394	194	T	A		65	V65E	marR	multiple antibiotic resistance protein; repressor of mar operon
	N	2675494	890	A	T		297	L297Q	yphE	putative ATP-binding component of a transportsystem
	S	2988986	411	T	C		137	b2850	ygeF	orf, hypothetical protein
	D	3066607	224	C	-CCCAGGTGACCAGCG		75	b2923	yggA	orf, hypothetical protein suppresses inhibitory activity of CsrA
	S	3388695	1356	A	T		452	b3244	tlpD	
	D	4024540		G	-AGAAAAGCGCAT			b3844	fre	36-b3843, -10-b3844
	N	3469576	1961	A	T		654	I654N	fusA	GTP-binding protein chain elongation factorEF-G
EqP-8	N	485061	77	A	C		26	Q26P	acrR	acrAB operon repressor
	D	4024853	304	G	-AAGAGCGTCCGATGA		102	b3844	fre	ferrisiderophore reductase; flavin

**Table S2.1 (Continued). All mutations found in final (Day 17) evolved strains from genomic sequencing<sup>1</sup>.**

EqP-9	N	396689	827	A	G		276	E276G	b0377	sbmA	reductase(NADPH:flavin oxidoreductase)	
	N	460141	2030	G	C		677	G677A	b0439	lon	sensitivity to microcin B17, possibly envelopprotein	
	B	1020179		A	G				b0958	suiA	DNA-binding, ATP-dependent protease La; heatshock K-protein	
	D	1331242	2171	G	-TT		724		b1274	topA	-37-b0958, -182-b0959	
	N	2658836	718	G	A		240	R240C	b2530	iscS	DNA topoisomerase type I, omega protein	
	N	4102632	367	A	G		123	Y123H	b3911	cpxA	cysteine desulfurase	
	I	485122	138	T	+G		46		b0464	acrR	probable sensor protein (histidine proteinkinase), acting on arcA	
	N	1549213	729	T	A		243	D243E	b1475	fdnH	acrAB operon repressor	
	I	2336499	944	A	+CTTCACCGACCG		315		b2231	gyrA	formate dehydrogenase-N, nitrate-inducible, iron-sulfur beta subunit	
	N	2391864	1205	A	T		402	I402N	b2278	nuoL	DNA gyrase, subunit A, type II topoisomerase	
EqP-10	N	3469561	1976	G	T		659	P659Q	b3340	fusA	NADH dehydrogenase I chain L	
	N	4102266	733	C	A		245	D245Y	b3911	cpxA	GTP-binding protein chain elongation factorEF-G	
	D	2337193	250	C	-CGA		84		b2231	gyrA	probable sensor protein (histidine proteinkinase), acting on arcA	
	B	988229		T	C				b0930	asnS	DNA gyrase, subunit A, type II topoisomerase	
	D	1211382		G	-T				b1160	iraM	-21-b0930, 148-b0931	
	I	2863507	385	A	+TTTTAC		129		b2740	ygbN	-156-b1160, 544-b1161	
	N	3375172	271	C	A		91	V91F	b3229	sspA	putative transport protein	
	R	1989967	45	T	C		15		b1910	cysT	regulator of transcription; stringent starvationprotein A	
	I	3326631	92	G	+C		31		b3181	greA	tRNA-Cys	
	D	3805456	666	C	-TCATCTACACAA		222		b3632	rfaQ	transcription elongation factor: cleaves 3'nucleotide of paused mRNA	
Hyb-1	D	3805456	666	C	-TCATCTACACAA		222		b3632	rfaQ	lipopolysaccharide core	
	Hyb-2											

**Table S2.1 (Continued). All mutations found in final (Day 17) evolved strains from genomic sequencing<sup>1</sup>.**

	N	4255457	320	C	A		107	P107Q	b4043	lexA	biosynthesis
Hyb-3	D	2337193	250	C	-CGA		84		b2231	gyrA	regulator for SOS(lexA) regulon DNA gyrase, subunit A, type II topoisomerase
	N	3473296	59	T	C		20	E20G	b3344	yheM	orf, hypothetical protein
	D	3806034	88	G	-CAGCATATC		30		b3632	rfaQ	lipopolysaccharide core biosynthesis
Hyb-4	D	2337193	250	C	-CGA		84		b2231	gyrA	DNA gyrase, subunit A, type II topoisomerase
	N	3211802	734	C	A		245	A245D	b3067	rpoD	RNA polymerase, sigma(70) factor; regulation of proteins induced at high temperatures
Hyb-5	N	1406218	145	C	T		49	H49Y	b1342	ydaN	orf, hypothetical protein
	D	2335733	1710	T	-GCG		570		b2231	gyrA	DNA gyrase, subunit A, type II topoisomerase
	D	3473427	314	T	-G		105		b3345	yheN	orf, hypothetical protein
	D	4522096	22	C	-A		8		b4297	yjhG	putative dehydratase
Hyb-6	D	2337193	250	C	-CGA		84		b2231	gyrA	DNA gyrase, subunit A, type II topoisomerase
	N	987463	746	A	G		249	M249T	b0930	asnS	tRNA-Asn
	D	2534192	337	C	-GCGTGAAGTTG		113		b2417	crr	PTS system, glucose-specific IIA component
Hyb-7	N	1799046	1549	A	C		517	S517A	b1719	thrS	threonine tRNA synthetase
	N	2335077	2366	A	T		789	V789E	b2231	gyrA	DNA gyrase, subunit A, type II topoisomerase
Hyb-8	D	2337193	250	C	-CGA		84		b2231	gyrA	DNA gyrase, subunit A, type II topoisomerase
	N	1329292	221	A	G		74	D74G	b1274	topA	DNA topoisomerase type I, omega protein
	I	3210928		A	+GAGGCAG				b3066	dnaG	54-b3066, -141-b3067
Hyb-9	N	485010	26	C	A		9	A9E	b0464	acrR	acrAB operon repressor
	N	2337171	272	C	T		91	R91H	b2231	gyrA	DNA gyrase, subunit A, type II topoisomerase
	D	3335400	514	T	-G		172		b3192	yrbC	orf, hypothetical protein

**Table S2.1 (Continued). All mutations found in final (Day 17) evolved strains from genomic sequencing<sup>1</sup>.**

	D	3421650	28	T	-G	10	b3273	thrV	tRNA-Thr
	N	4066483	817	C	T	273	D273N	yihQ	putative glycosidase
	I	3275279	256	C	+CATTCAA	86	b3129	sohA	putative protease; htrA suppressor protein
Hyb-10	N	961896	679	C	T	227	R227C	rpsA	30S ribosomal subunit protein S1
	N	2335587	1856	A	T	619	I619N	gyrA	DNA gyrase, subunit A, type II topoisomerase
	N	4094390	1082	G	A	361	P361L	rhaB	rhamnulokinase
Ctrl-1	N	1900180	109	G	C	37	V37L	manX	PTS enzyme IIAB, mannose-specific

<sup>1</sup> No differences were found between the ancestral strain, controls 2-4, and the reference MG1655 genome.

\* N indicates amino acid changing (non-synonymous); S indicates amino acid preserving (synonymous); D indicates small deletion; I indicates small insertion; B indicates intergenic SNPs (between genes); R indicates a SNP in a noncoding gene

\*\* Annotations provided in U00096.2. When intergenic, the nearest genes and distances to those genes are indicated (negative numbers indicate upstream, positive numbers indicate downstream)